Semi-Inclusive electroproduction of pions with CLAS

M. Osipenko

14th Lomonosov conference,

August 21,

Moscow State University

Jefferson Lab

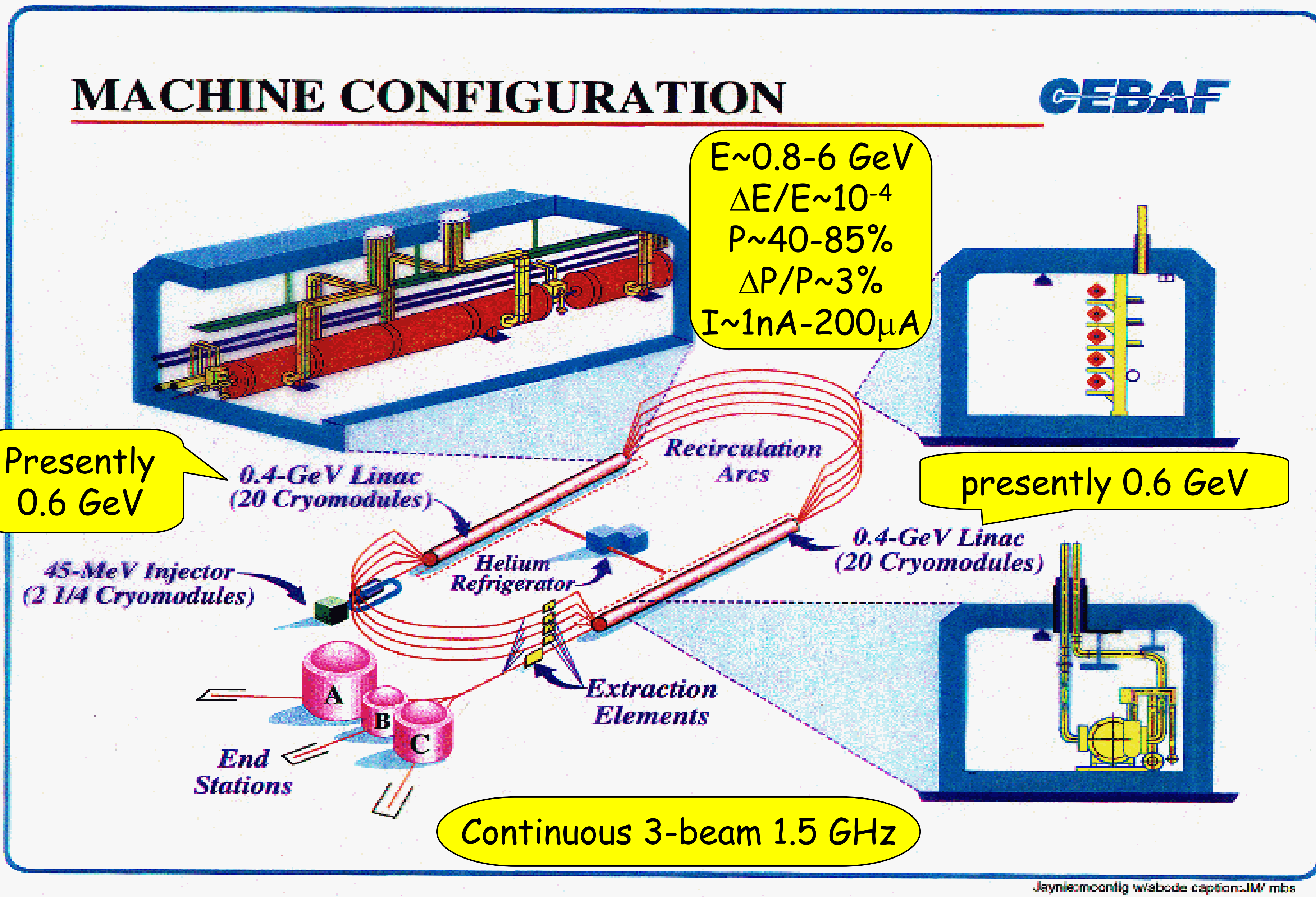

CLAS detector

- 4π detector operating at luminosity $L \sim 10^{34}\ cm^{-2}s^{-1}$
- Charged particles detection $\Delta p/p \sim 0.5\text{-}1\%$, $\Delta\theta/\theta \sim 1$ mrad, $\theta_e \sim 15\text{-}50°$
- Neutral particles detection γ ($\Delta E/E \sim 10\%$), n ($0.5 < p_n < 2$ GeV)
- Particle identification e/π separation, TOF ($\sigma \sim 200$ ns)

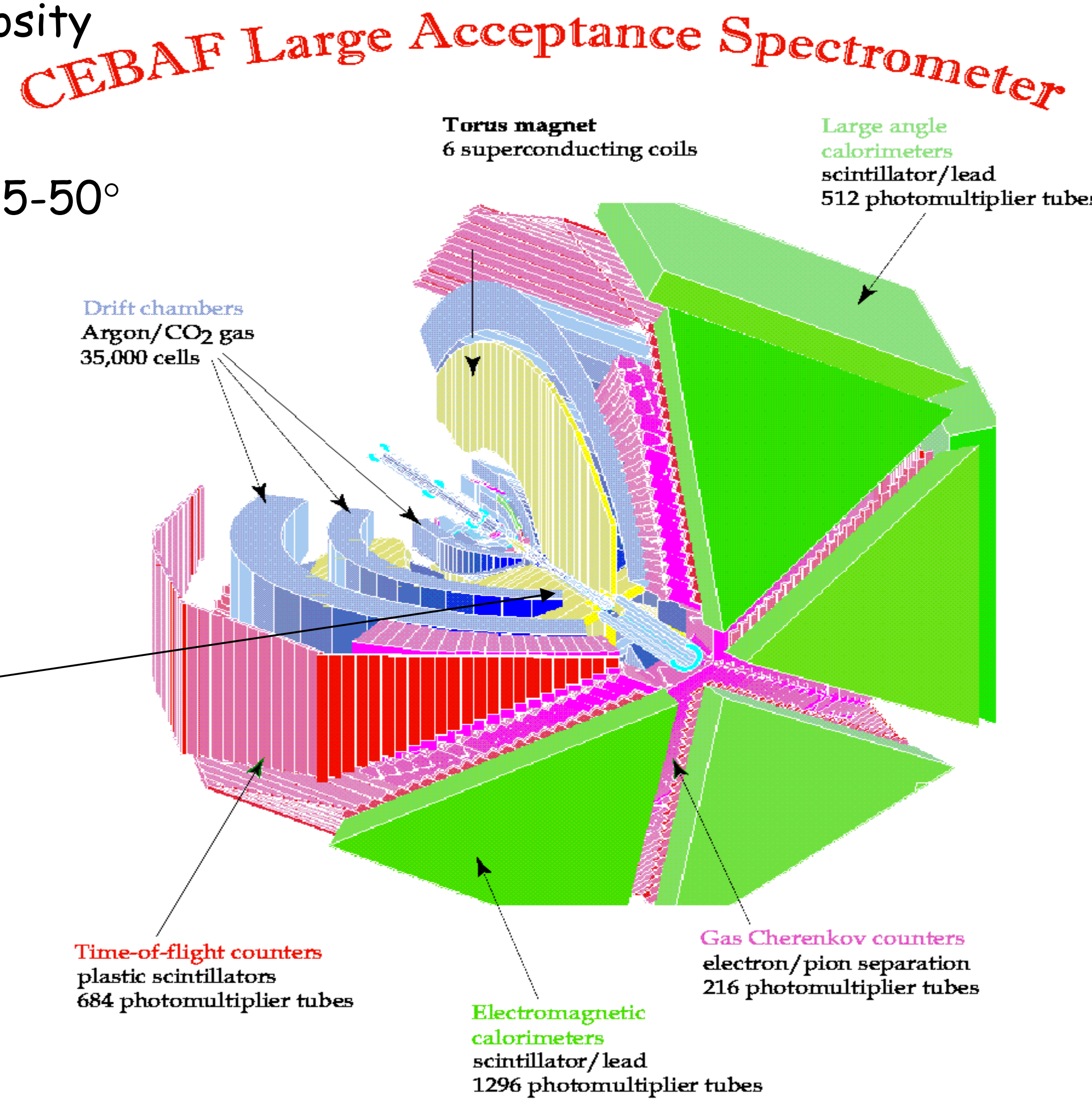

New inner calorimeter

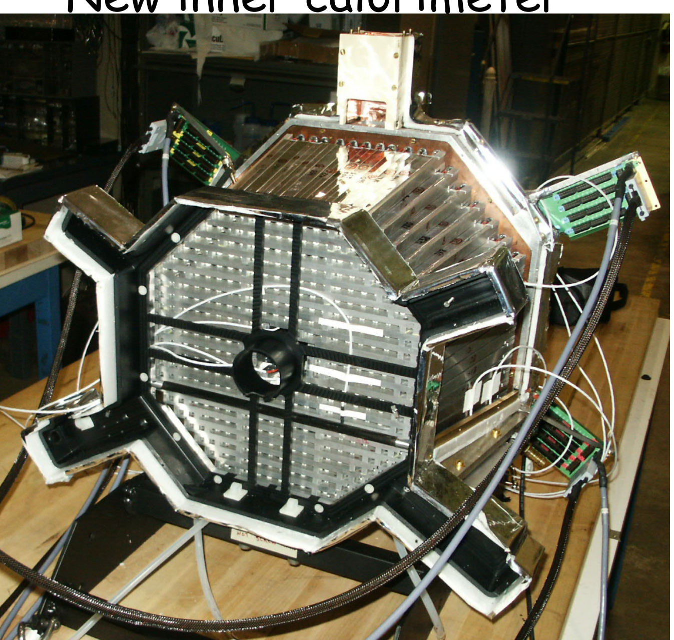

Semi-inclusive Kinematics

Detect the scattered electron in coincidence with hadron h: $e+p \to e'+h+X$

In OPE approximation: $\gamma_V(q) + p(P) \to h(p_h) + X$

Four-momenta in Lab: $q = (k - k') = (\nu, \vec{q}) \quad P = (M, 0) \quad p_h = (E_h, \vec{p}_h)$

5 independent variables

Initial state: $Q^2 = -q^2 \qquad x = \dfrac{-q^2}{2qP} = \dfrac{Q^2}{2M\nu}$

Final state: $z = \dfrac{Pp_h}{Pq} = \dfrac{E_h}{\nu} \qquad p_T = \left|\vec{p}_T\right| = \left|\vec{p}_h - \vec{p}_h \vec{q}\right| \qquad \varphi = \varphi_{\gamma h} - \varphi_{\gamma e'}$

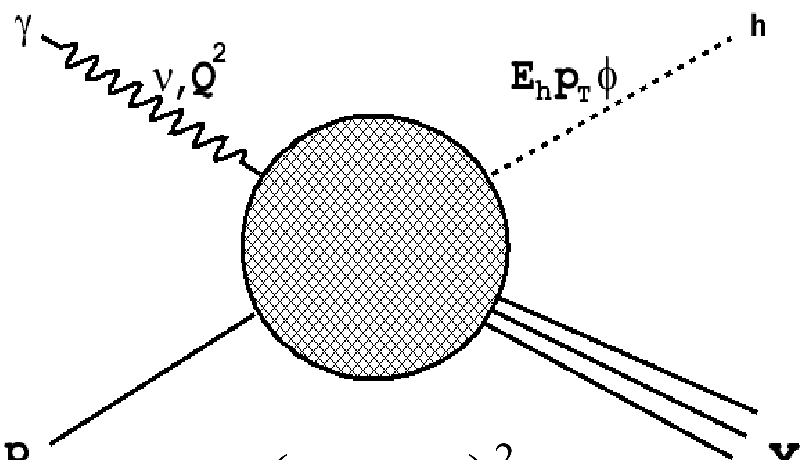

$$t = (q - p_h)^2$$

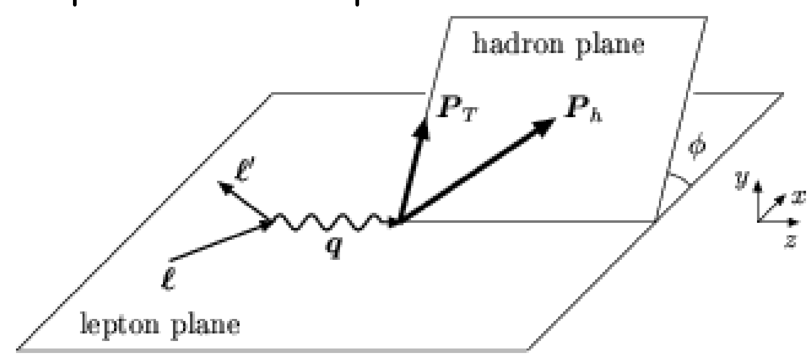

undetected hadronic final state of mass squared

$$M_X^2 = M^2 + 2M\nu(1-z) + t$$

Observables

- Cross section is described by 4 functions of 4 variables: $\mathcal{H}_i = \mathcal{H}_i(x, Q^2, z, t)$

$$\frac{d^5\sigma}{dx\,dQ^2\,dz\,dp_T^2\,d\varphi} = N\frac{E_h}{|p_{\parallel}|}\zeta\left[\varepsilon\mathcal{H}_1 + \mathcal{H}_2 + (2-y)\sqrt{\frac{\kappa}{\zeta}}\cos\varphi\mathcal{H}_3 + \kappa\cos 2\varphi\mathcal{H}_4\right]$$

J.Levelt & P.Mulders, PRD49

where

$$N = \frac{2\pi\alpha^2}{xQ^4} \quad y = \frac{\nu}{E_{beam}} \quad \gamma = \frac{2Mx}{\sqrt{Q^2}} \quad \zeta = 1 - y - \frac{1}{4}\gamma^2 y^2 \quad \varepsilon = \frac{xy^2}{\zeta} \quad \kappa = \frac{1}{1+\gamma^2}$$

- Azimuthal asymmetries (moments): $$\langle\cos n\phi\rangle = \frac{\int \sigma\cos n\varphi\, d\varphi}{\int \sigma\, d\varphi}$$

$$\langle\cos\phi\rangle = \frac{(2-y)}{2}\sqrt{\frac{\kappa}{\zeta}}\frac{\mathcal{H}_3}{\varepsilon\mathcal{H}_1 + \mathcal{H}_2} \qquad \langle\cos 2\phi\rangle = \frac{\kappa}{2}\frac{\mathcal{H}_4}{\varepsilon\mathcal{H}_1 + \mathcal{H}_2}$$

- p_T-integrated cross section:

$$H_2 = \pi E_h \int_0^{p_T^{2\max}} dp_T^2 \frac{\mathcal{H}_2(p_T^2)}{\sqrt{E_h^2 - m_h^2 - p_T^2}}$$

SIDIS: constant in ϕ

Current fragmentation

L.Trentadue & G.Veneziano, PLB323

Target fragmentation

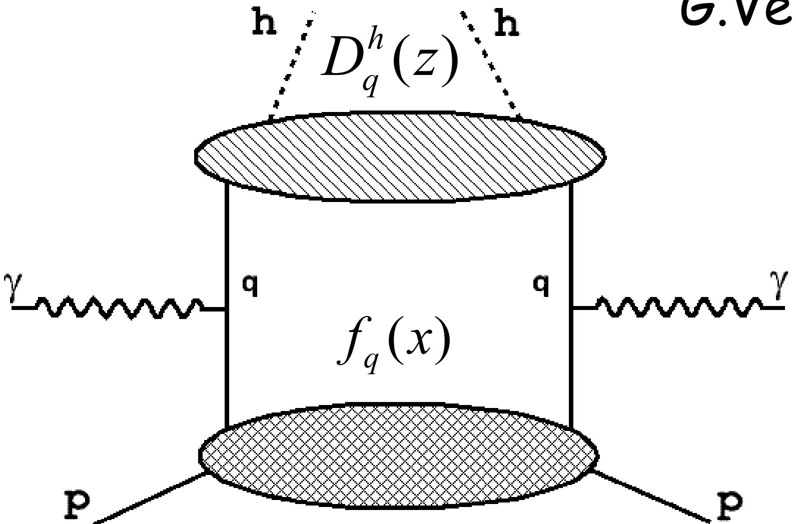

$$H_1 = 2xH_2$$

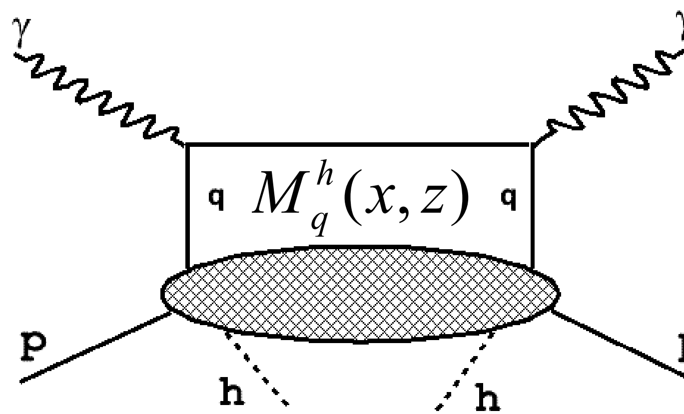

X.Ji et al., PRD71

Factorization proved

J.C.Collins, PRD57

$$H_2 = \sum_q e_q^2 f_q(x) D_q^h(z)$$

$$H_2 = \sum_q e_q^2 M_q^h(x,z)$$

$$f(x) = \frac{d\sigma}{dx}$$

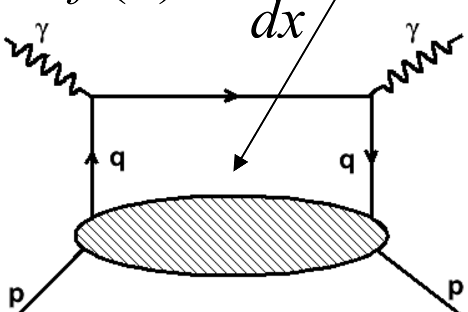

$$D^h(z) = \frac{d\sigma^h}{dz}$$

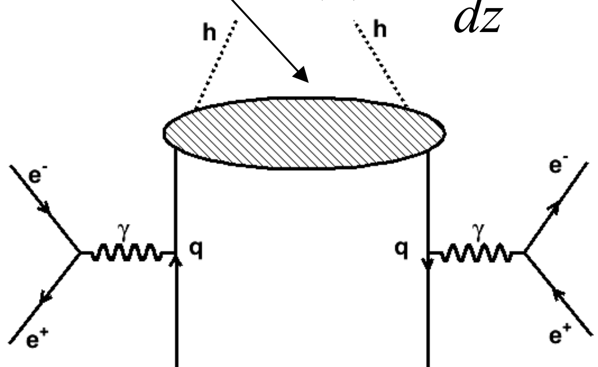

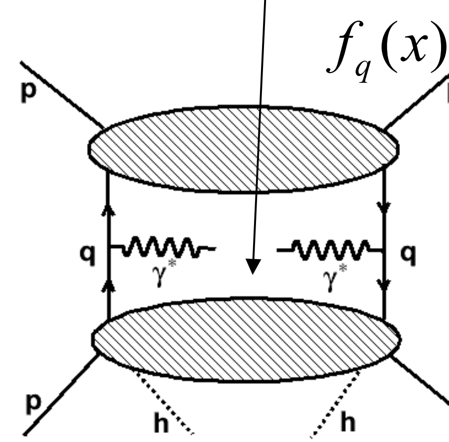

SIDIS: ϕ-dependence

R.N.Cahn, PRD40

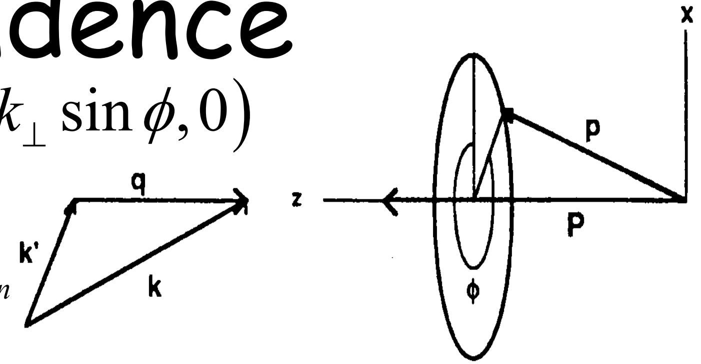

1.Cahn effect: $p = xP + k_\perp \quad k_\perp = (0, k_\perp \cos\phi, k_\perp \sin\phi, 0)$

$$\langle p_T^2 \rangle = p_\perp^2 + k_\perp^2 z^2$$

$$\langle \cos n\varphi \rangle \sim \frac{\mathcal{H}_{2+n}}{\mathcal{H}_2 + \varepsilon \mathcal{H}_1} = (-1)^n \, 4 \frac{1-y}{1+(1-y)^2} \left[\frac{k_\perp^2 z}{\langle p_T^2 \rangle} \sqrt{\frac{p_T^2}{Q^2}} \right]^n$$

E.Berger, ZPC4

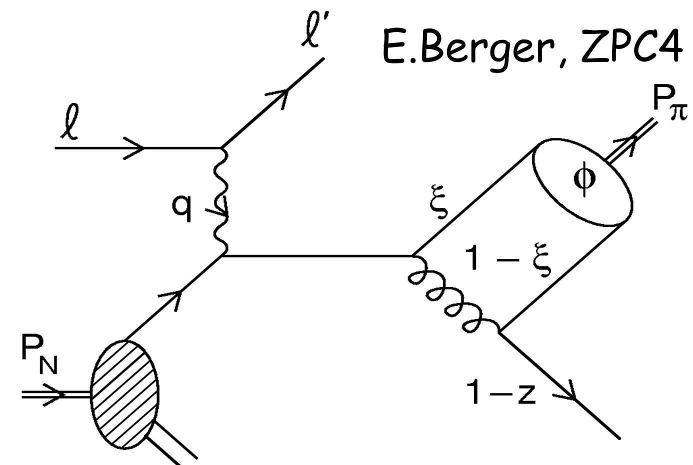

2.Berger effect (Collins fragmentation):

$$\langle \cos n\varphi \rangle \sim \int \frac{\psi^h(\xi)}{g_n(\xi, z, p_T^2)} d\xi$$

$\psi^h(\xi)$ hadron wave function

3.Boer-Mulders function $h_1^\perp$ (TMD) contribution:

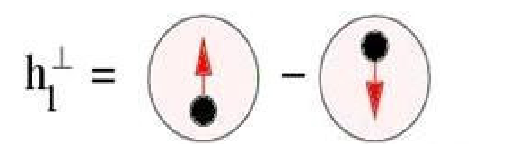

$$\langle \cos 2\varphi \rangle^{BM} \sim \frac{h_1^\perp(x, p_T^2) H_1^\perp(z, p_T^2)}{f(x) D(z)}$$

D.Boer&P.Mulders, PRD57

$H_1^\perp$ from e^+e^- collisions

4.Higher Order pQCD corrections:

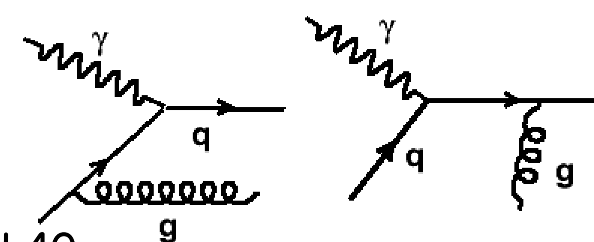

$$\langle \cos\varphi \rangle = -\frac{\alpha_S(Q^2)}{2} \sqrt{1-z} \, \frac{(2-y)\sqrt{1-y}}{1+(1-y)^2}$$

H.Georgi&H.Politzer, PRL40

Data & pQCD

Calculations contain current fragmentation only:

$$H_2 = \sum_q e_q^2 q(x) \otimes D(z)$$

CTEQ 5, Kretzer π^+

1. Except for low-x, the difference between data and pQCD is of the order of scale dependence,
2. NLO reproduces better data at low-z,
3. Leaves room for target fragmentation,
4. Calculations depend on the assumption about favored fragmentation (20% effect).

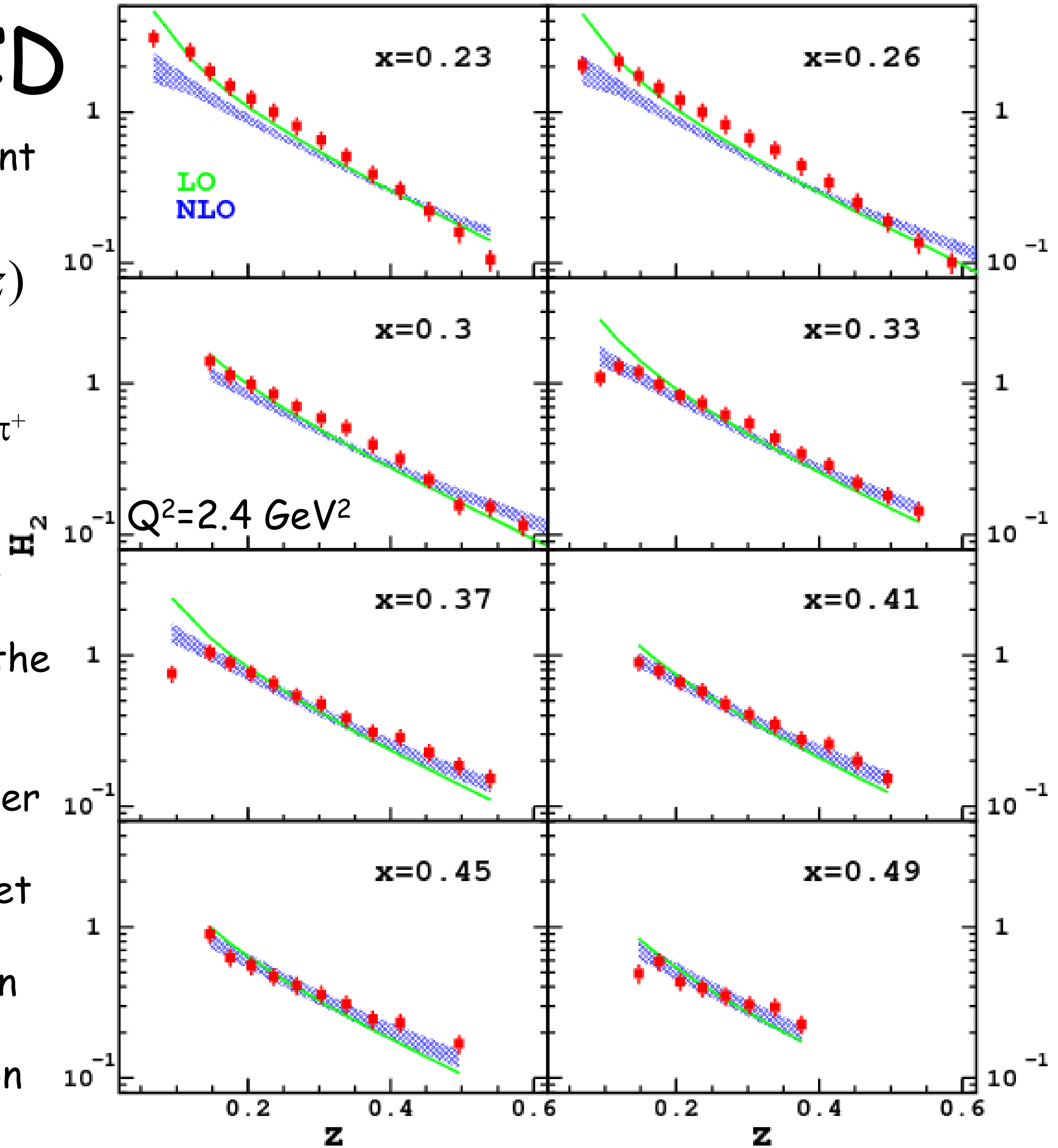

<cosφ> vs. p_T

Cahn effect calculations (using $k_\perp^2$=0.20 GeV² and $p_\perp^2$=0.25 GeV² from M.Anselmino et al., PRD71) do not reproduce measured <cosϕ> and the inclusion of Berger effect contribution does not improve the agreement significantly.

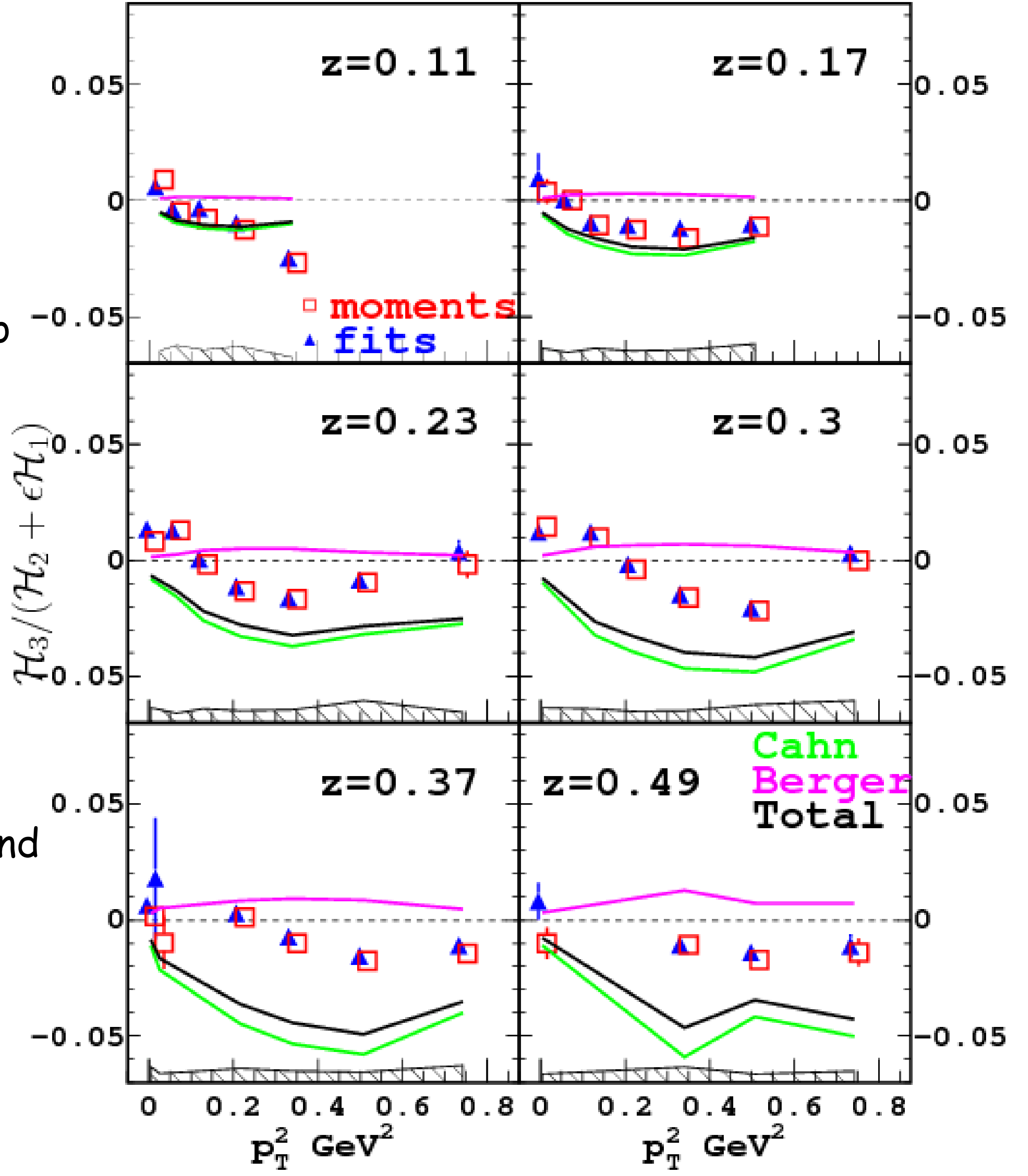

Data are integrated over x and Q^2 in DIS region.

<Q^2>=2.2 GeV²

$\langle\cos 2\varphi\rangle$ vs. p_T

Cahn and Berger effect compensate each other to give zero $\langle\cos 2\phi\rangle$ moment. Within systematic errors the data are also compatible with zero, except for low-z.

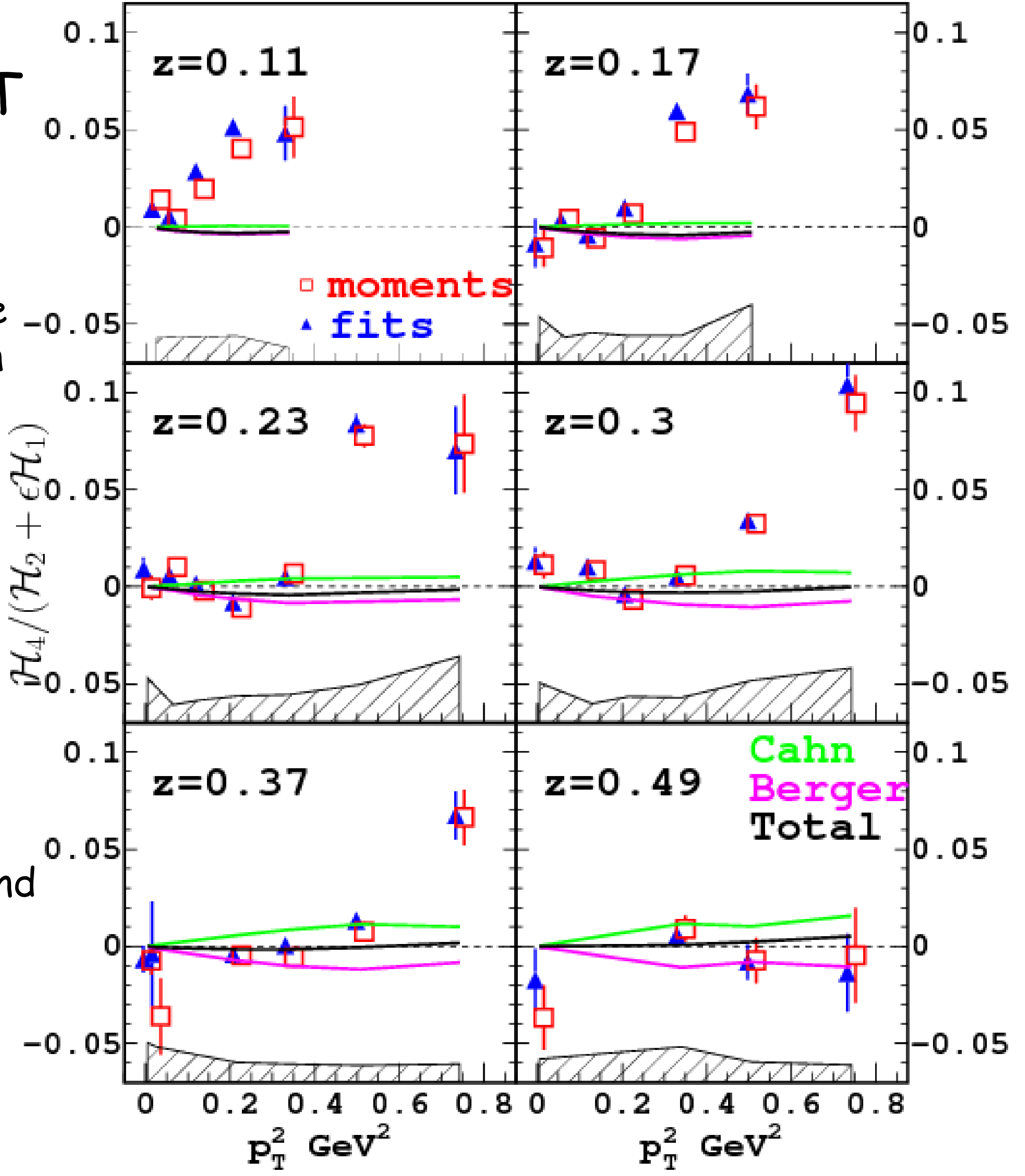

Data are integrated over x and Q^2 in DIS region.

$\langle Q^2\rangle = 2.2\ \mathrm{GeV}^2$

Q^2-dependence

We compared our data on φ-dependent terms with EMC measurement (J.Aubert et al., PLB130) performed at significantly higher Q^2:
curves show Cahn effect prediction corrected for threshold effect:

$$f_n(\nu, z) = \frac{\int_{p_T^{2\,\min}}^{p_T^{2\,\max}} p_T^n e^{-p_T^2/\langle p_T^2 \rangle} dp_T^2}{\int_{p_T^{2\,\min}}^{p_T^{2\,\max}} e^{-p_T^2/\langle p_T^2 \rangle} dp_T^2}$$

$$p_T^{2\,\max} \approx (z\nu)^2$$

and n=1,2

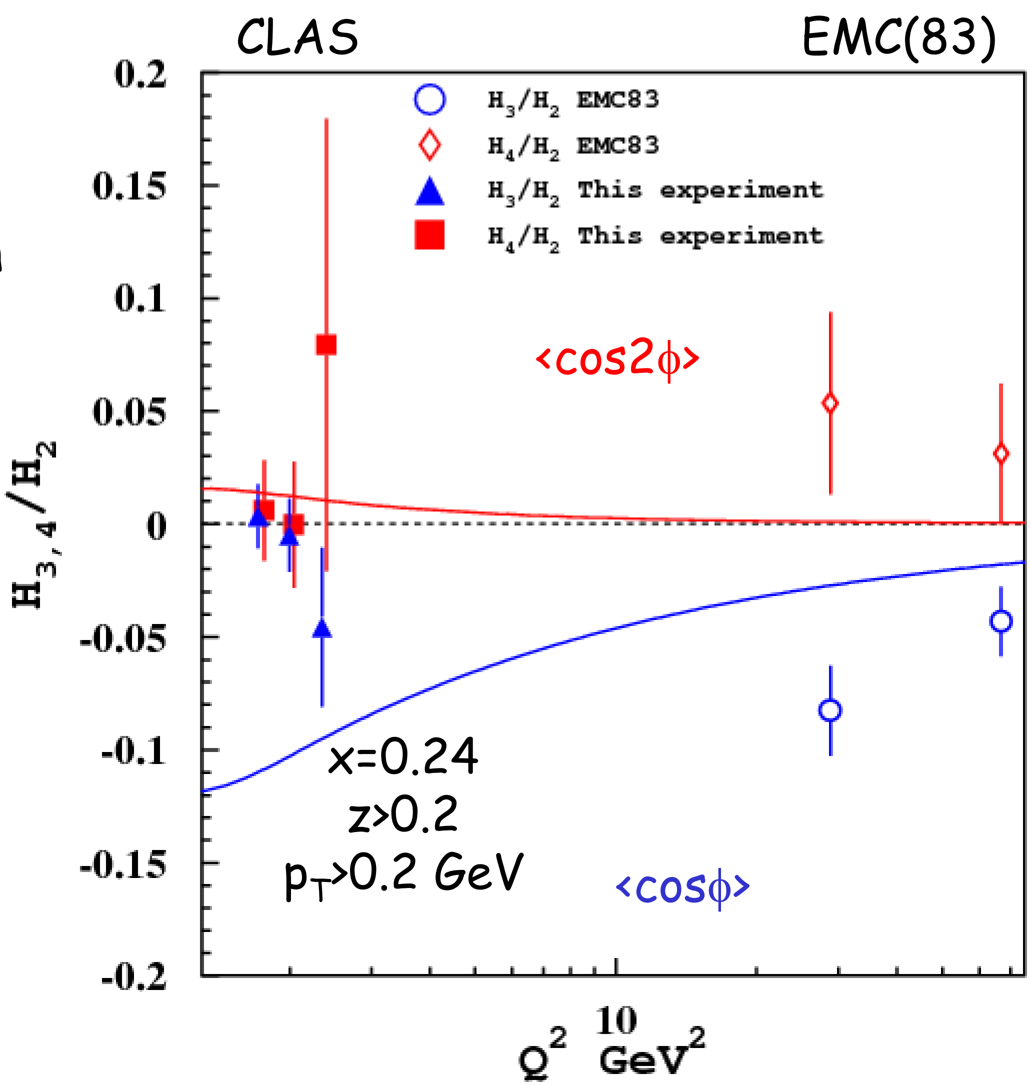

Summary

1. We measured 5-fold differential π^+ semi-inclusive electro-production cross sections in a wide kinematical range in all 5 independent variables,
2. Data are in reasonable agreement with naïve current fragmentation pQCD calculations (difference is of the order of systematic errors ~20%),
3. At low-z there is room for the target fragmentation contribution,
4. Measured $\langle \cos\phi \rangle$ moment is incompatible with Cahn and Berger effects and in striking disagreement with high Q^2 data, while $\langle \cos 2\phi \rangle$ is compatible with zero in agreement with theory except for low-z region.

BACKUP SLIDES

Graudenz variable

Struck quark light cone momentum fraction carried by the detected hadron, used in pQCD calculation, is commonly approximated:

$$z = \frac{p_h^-}{k^-} \approx \frac{p_h P}{qP} \equiv z_H$$

$$z_H \xrightarrow{Lab} \frac{E_h}{\nu}$$

$$z_H \xrightarrow{CM} \frac{E_h^{CM}(1+\cos\theta^{CM})}{\nu + M}$$

In e^+e^- function D(z) is measured as a function of:

$$z \equiv \frac{2E_h^{CM}}{\sqrt{s}} = \frac{2p_h q}{s}$$

D.Graudenz,Fortsch.Phys.45

$$z_G = \frac{E_h^{CM}}{E_p^{CM}(1-x)}$$

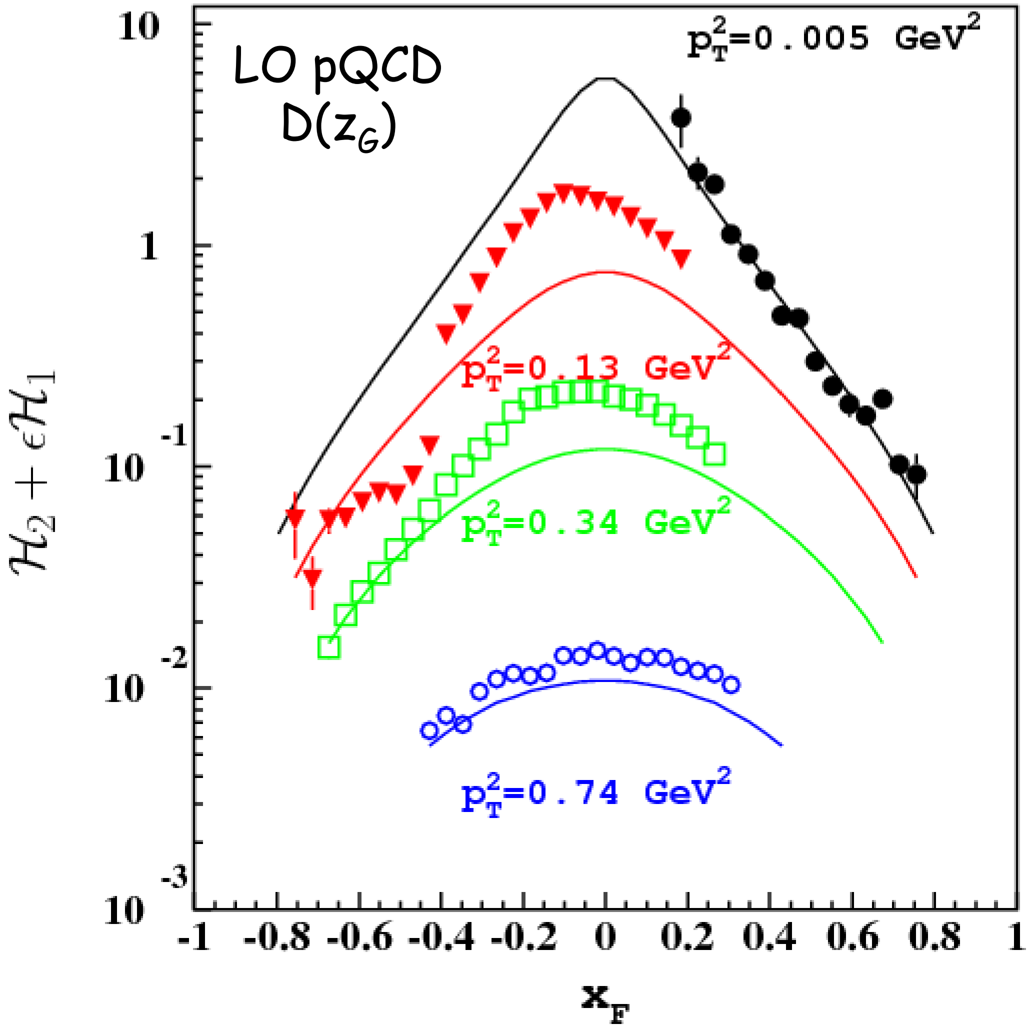

Machine Upgrade

- Beam energy increase up to 12 GeV (11 for Halls A,B,C):
- 5 new cryomodules to each LINAC
- gain increase up to 1.1 GeV/LINAC
- one new recirculation arc for Hall-D
- 85 μA maximum beam current
- maximal beam power 1 MWatt

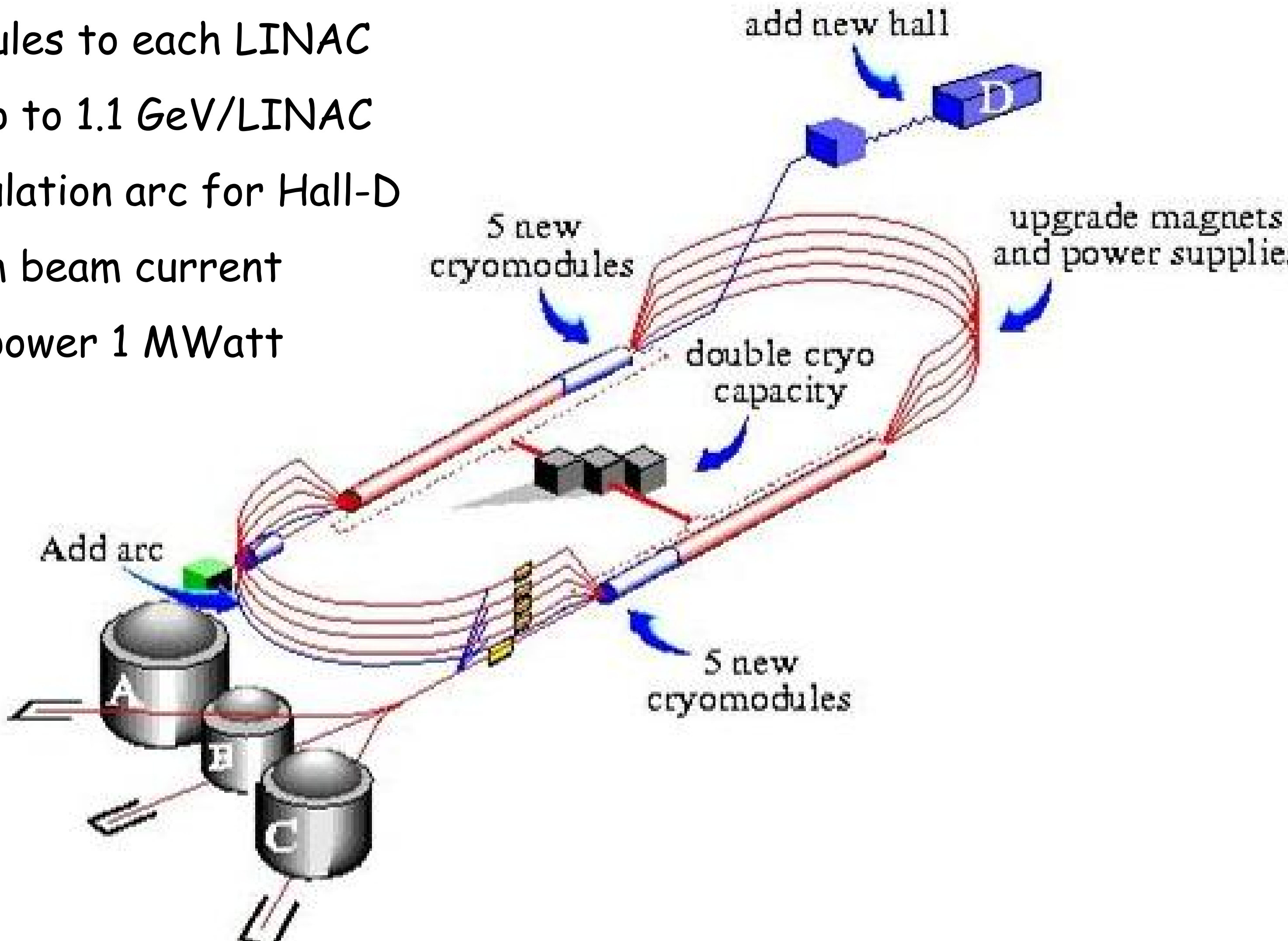

CLAS Upgrade

- Luminosity up to 10^{35} $cm^{-2}s^{-1}$
- Preshower calorimeter
- New drift chamber
- Improved TOF σ~50-60 ps
- High threshold Cherenkov
- Central detector 40-130°
  Electromagnetic calorimeter
  TOF
  Tracking detector
- Vertex detector
- No photon tagger

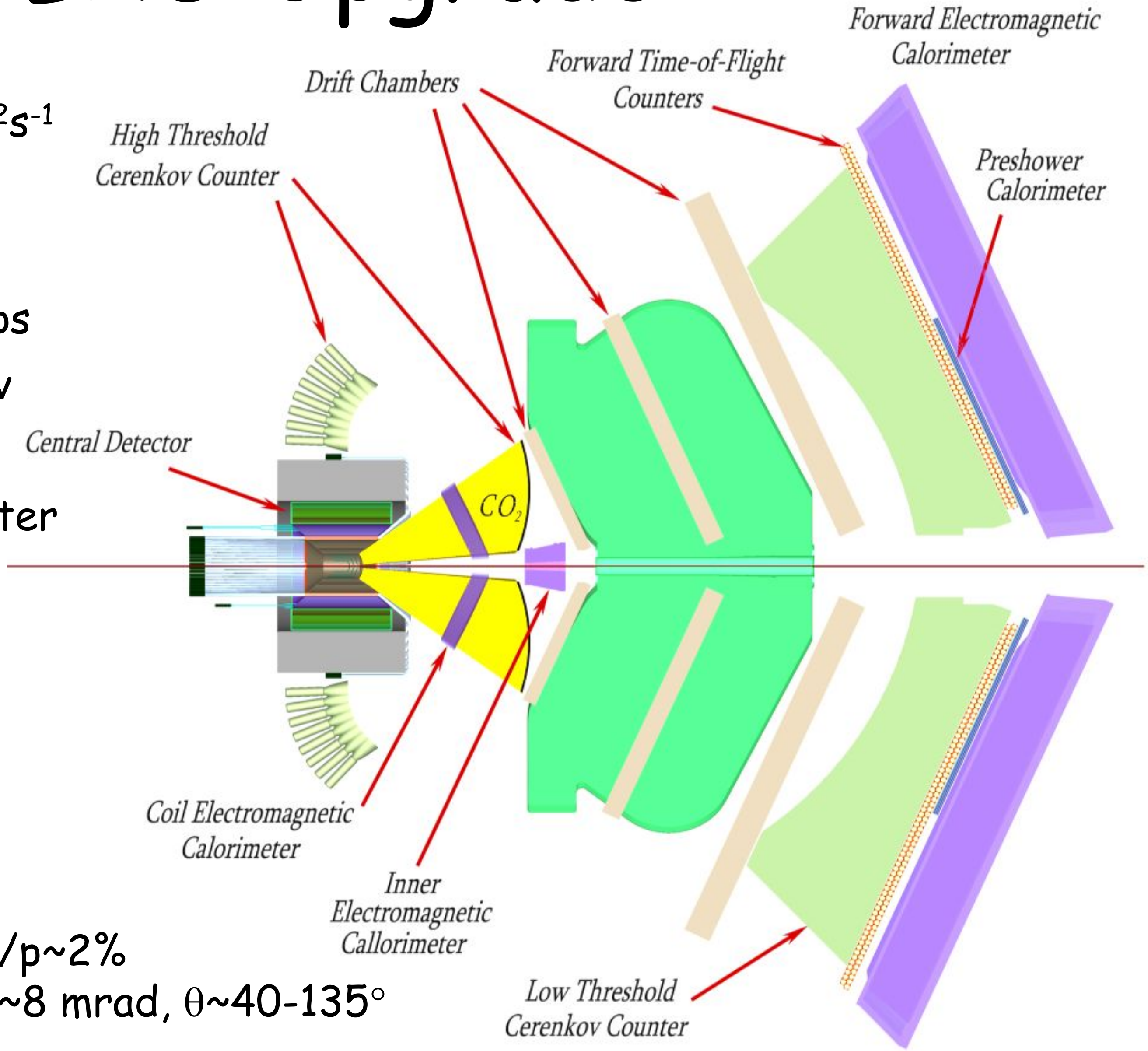

$\Delta p/p$~0.3%+0.1%p
$\Delta\theta$~1mrad, θ~5-40°
$e/\pi > 10^3$ (p<4.8 GeV)

$\Delta p/p$~2%
$\Delta\theta$~8 mrad, θ~40-135°

Central detector

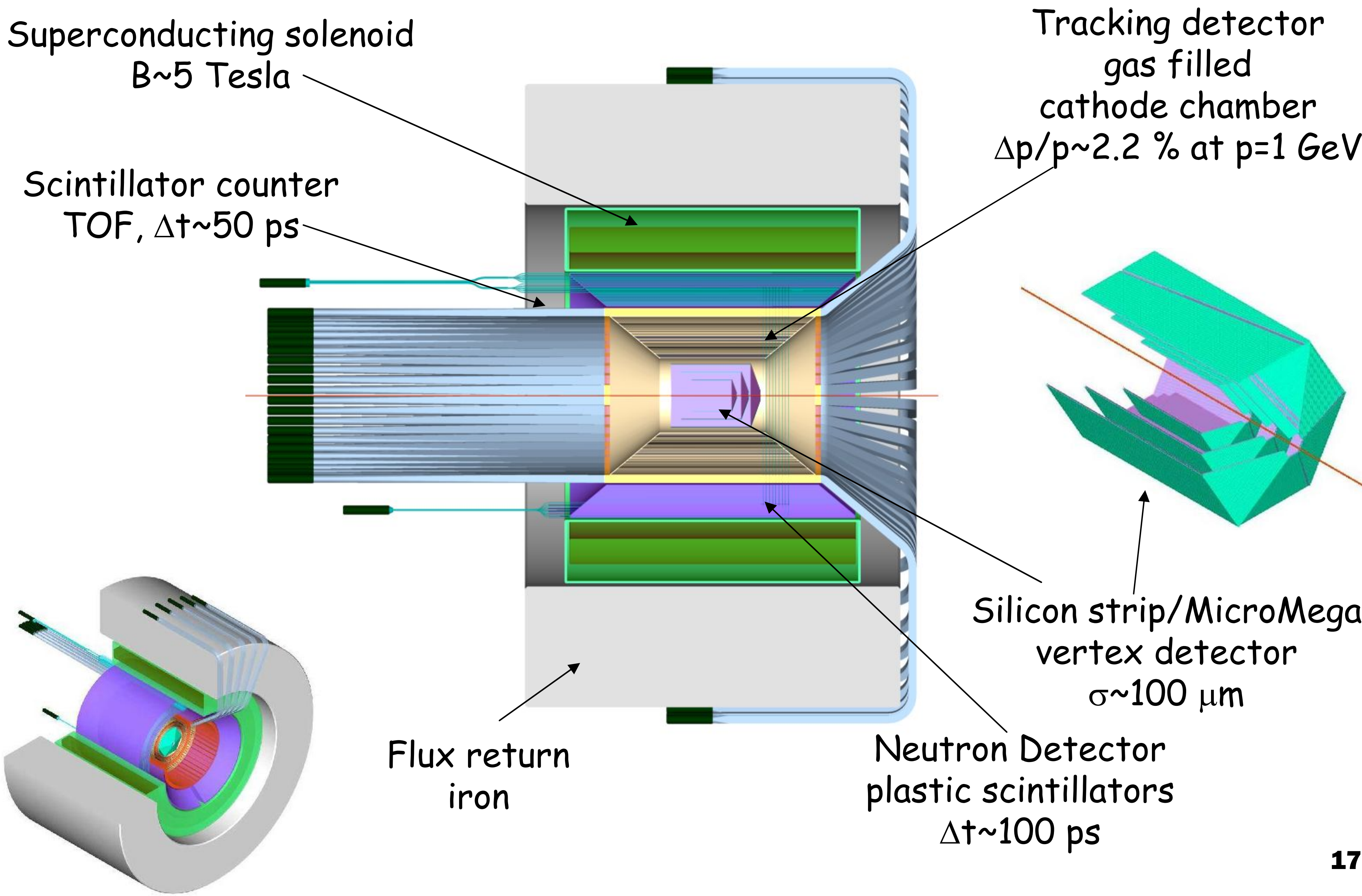

CLAS12 - Expected Performance

	Forward Detector	Central Detector
Angular coverage:		
Tracks (inbending)	8^o - 37^o	40^o - 135^o
Tracks (outbending)	5^o - 37^o	40^o - 135^o
Photons	3^o - 37^o	40^o - 135^o
Track resolution:		
δp (GeV/c)	$0.003p + 0.001p^2$	$\delta p_T = 0.02 p_T$
$\delta\theta$ (mr)	1	5
$\delta\phi$ (mr)	2 - 5	2
Photon detection:		
Energy range	> 150 MeV	> 60 MeV
$\delta E/E$	0.09 (1 GeV)	0.06 (1 GeV)
$\delta\theta$ (mr)	3 (1 GeV)	15 (1 GeV)
Neutron detection:		
η_{eff}	0.5 (p > 1.5 GeV/c)	
Particle id:		
e/π	>>1000 (< 5 GeV/c) >100 (> 5 GeV/c)	
π/K (4σ)	< 3 GeV/c	0.6 GeV/c
π/p (4σ)	< 5 GeV/c	1.3 GeV/c

12 GeV upgrade kinematical reach

- High luminosity gives access to large x
  - Valence quarks only
  - No explicit hard gluons (if observable couples to valence quarks)
  - Hadronic fluctuations of the virtual photon are suppressed
  - x→1 limit, sensitive test for spin-flavor symmetry breaking
  - x>1 region for nuclear targets to probe high density quark matter
- Polarization: beam, target, recoil
  - Distribution of the spin in the nucleon

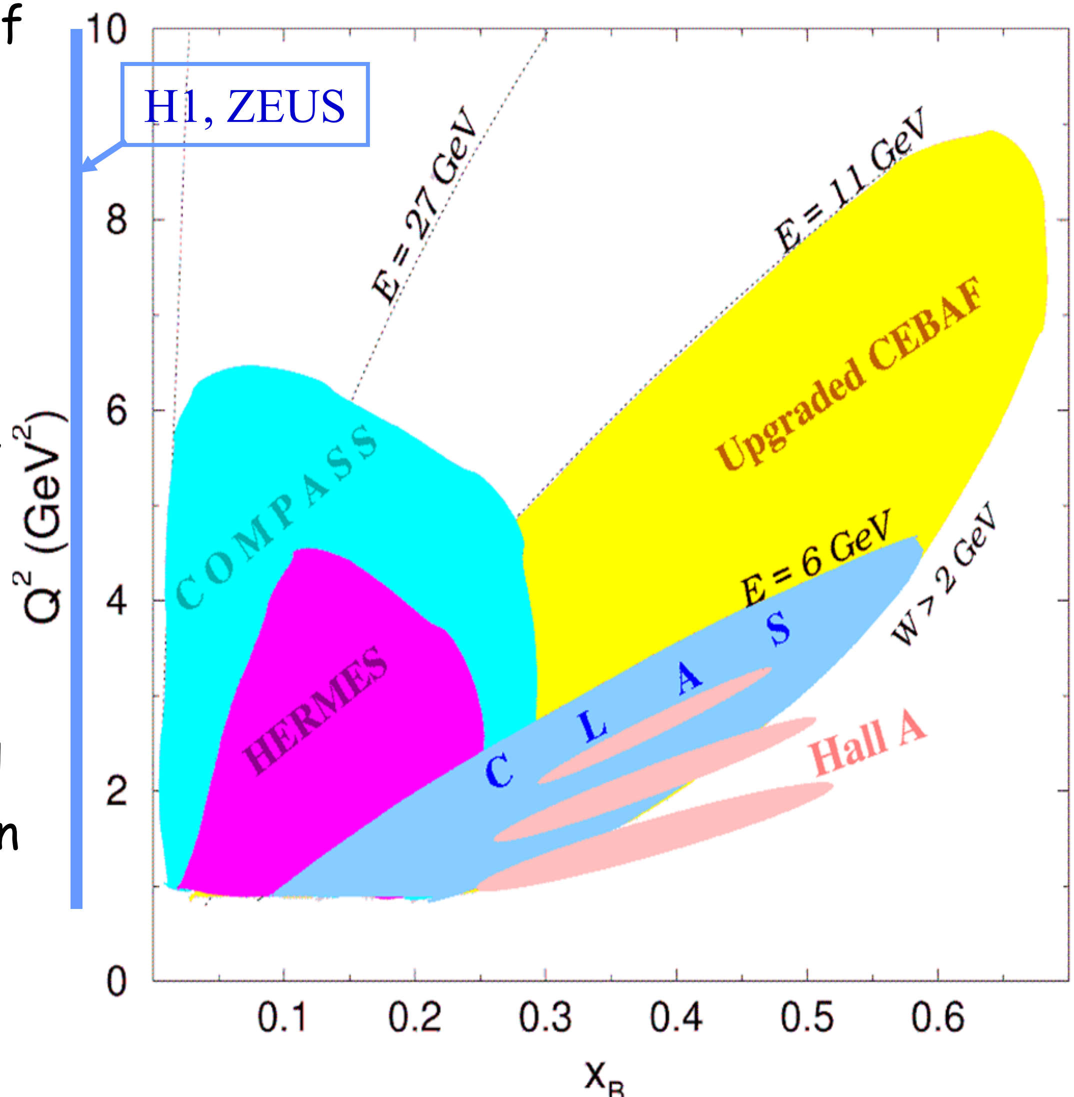

k_T- Dependent Parton Distributions

f_1, g_1 studied for decades:
h_1 essentially unknown

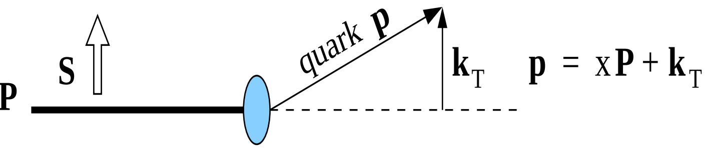

$$f_1(x) = \int d^2k_T f_1(x, k_T)$$

N \ q	U	L	T
U	f_1		$h_1^\perp$
L		g_1	$h_{1L}^\perp$
T	$f_{1T}^\perp$	g_{1T}	h_1 $h_{1T}^\perp$

In standard notations $f_1^u(x) \equiv u(x),\ g_1^u(x) \equiv \Delta u(x),\ h_1^u(x) \equiv \delta u(x)$

Study pQCD evolution in k_T:

Hadronization model is necessary to obtain information on distributions in quark transverse momentum k_T.

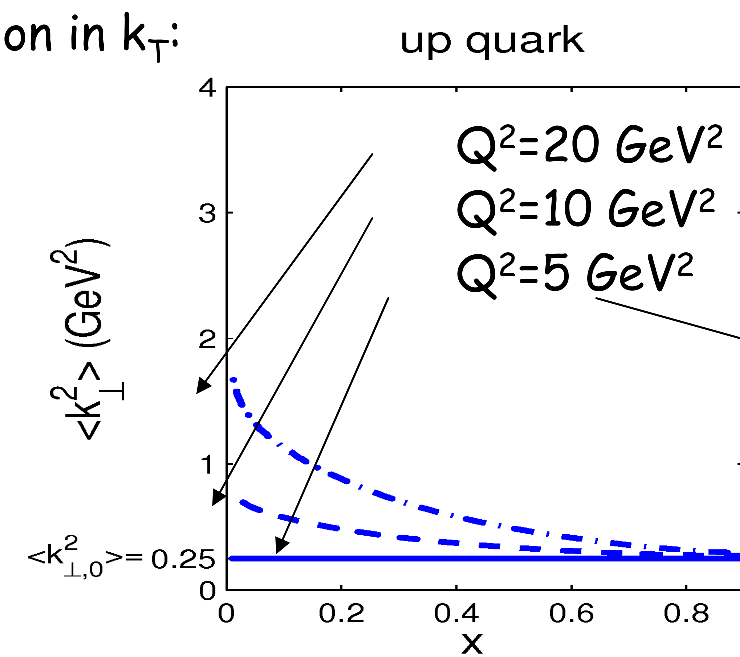

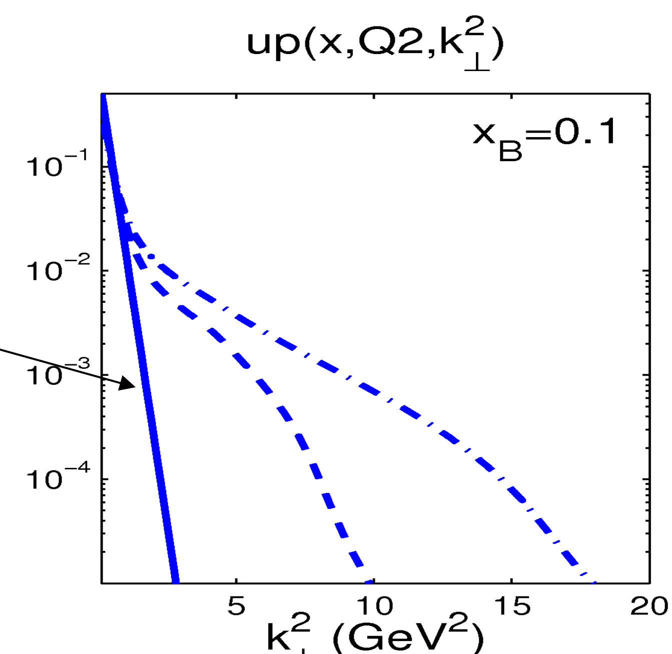

Q^2-dependence at x=0.34

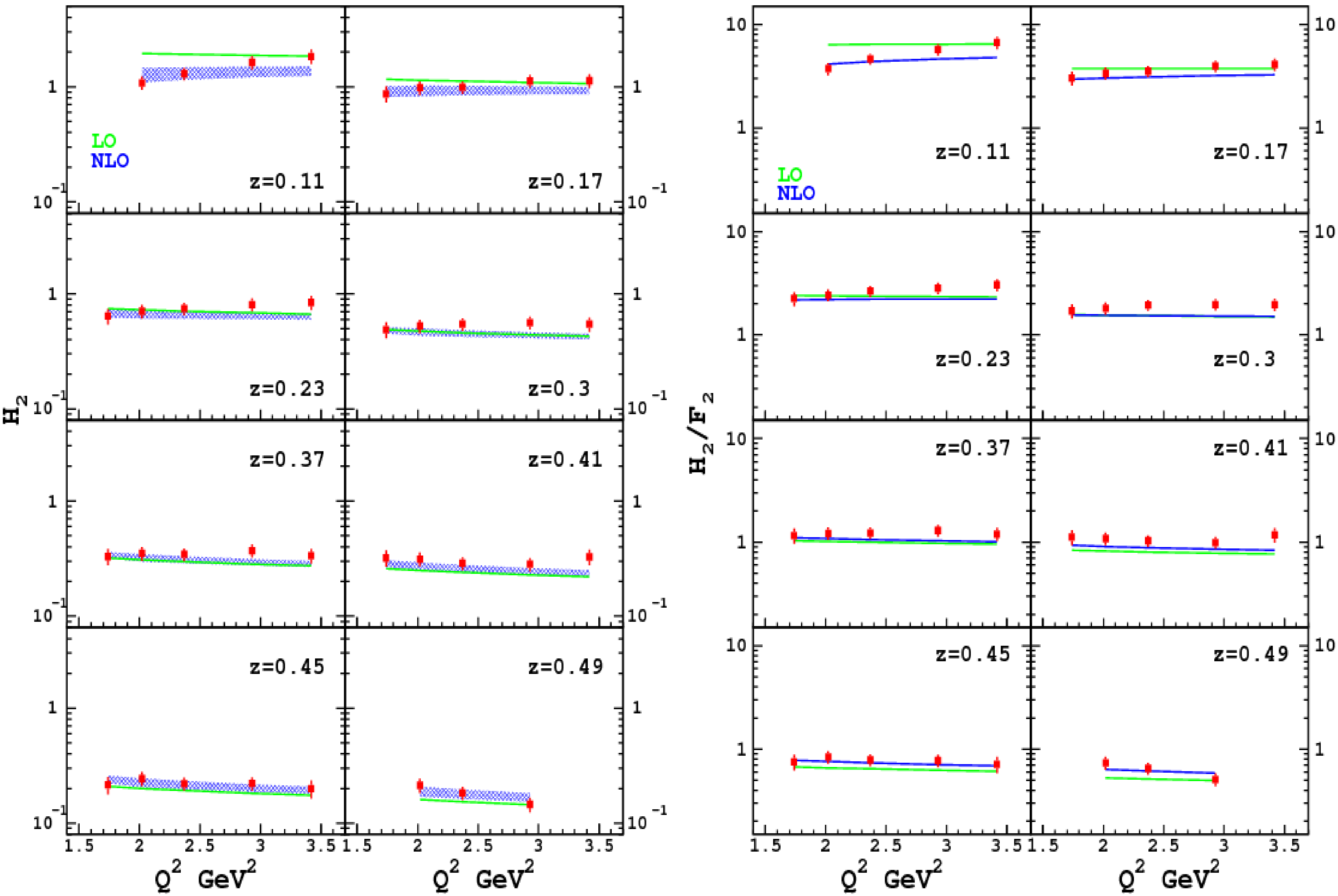

x-dependence at Q^2=2.4 GeV^2

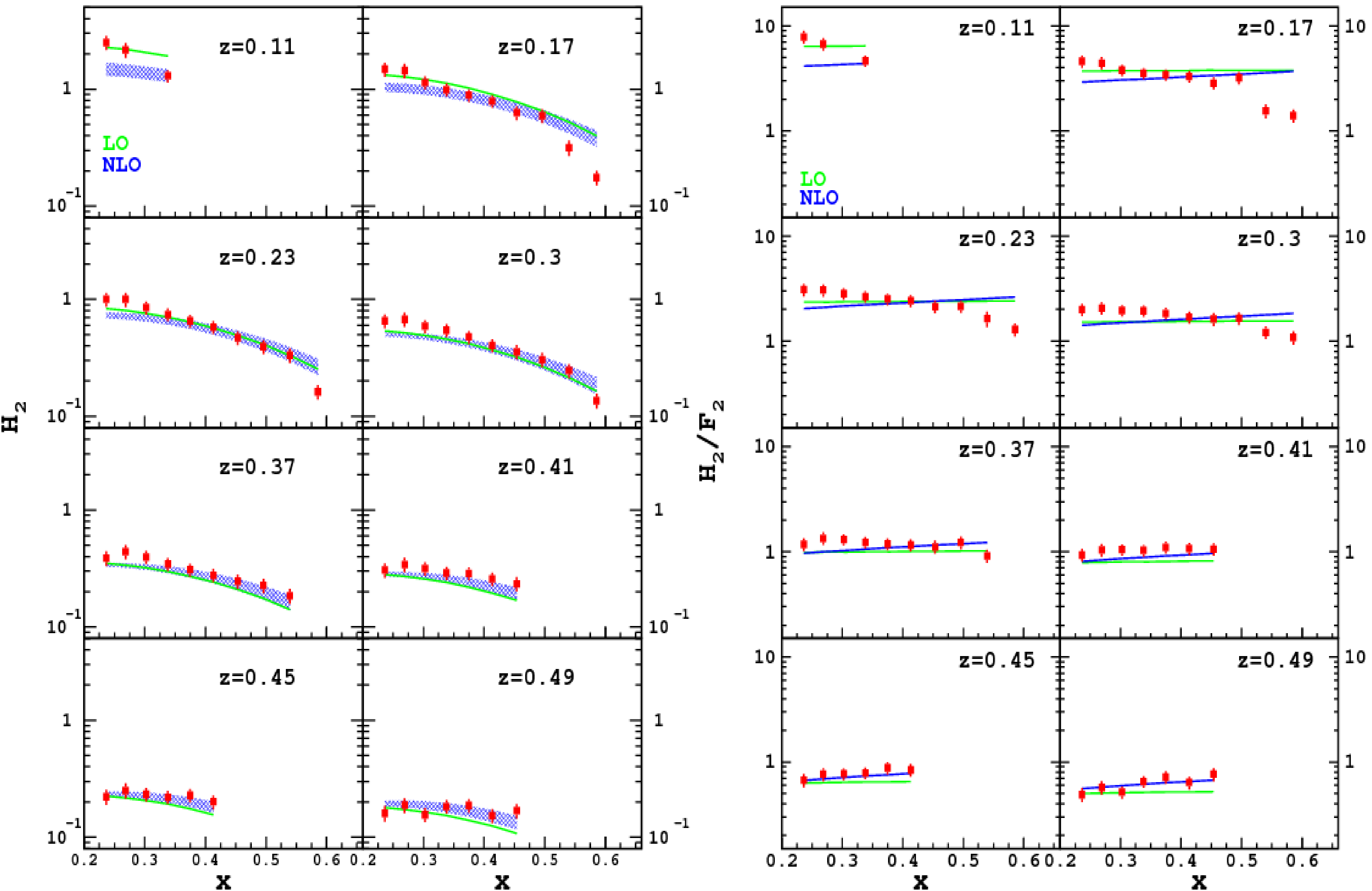

z-dependence at Q^2=2.4 GeV^2

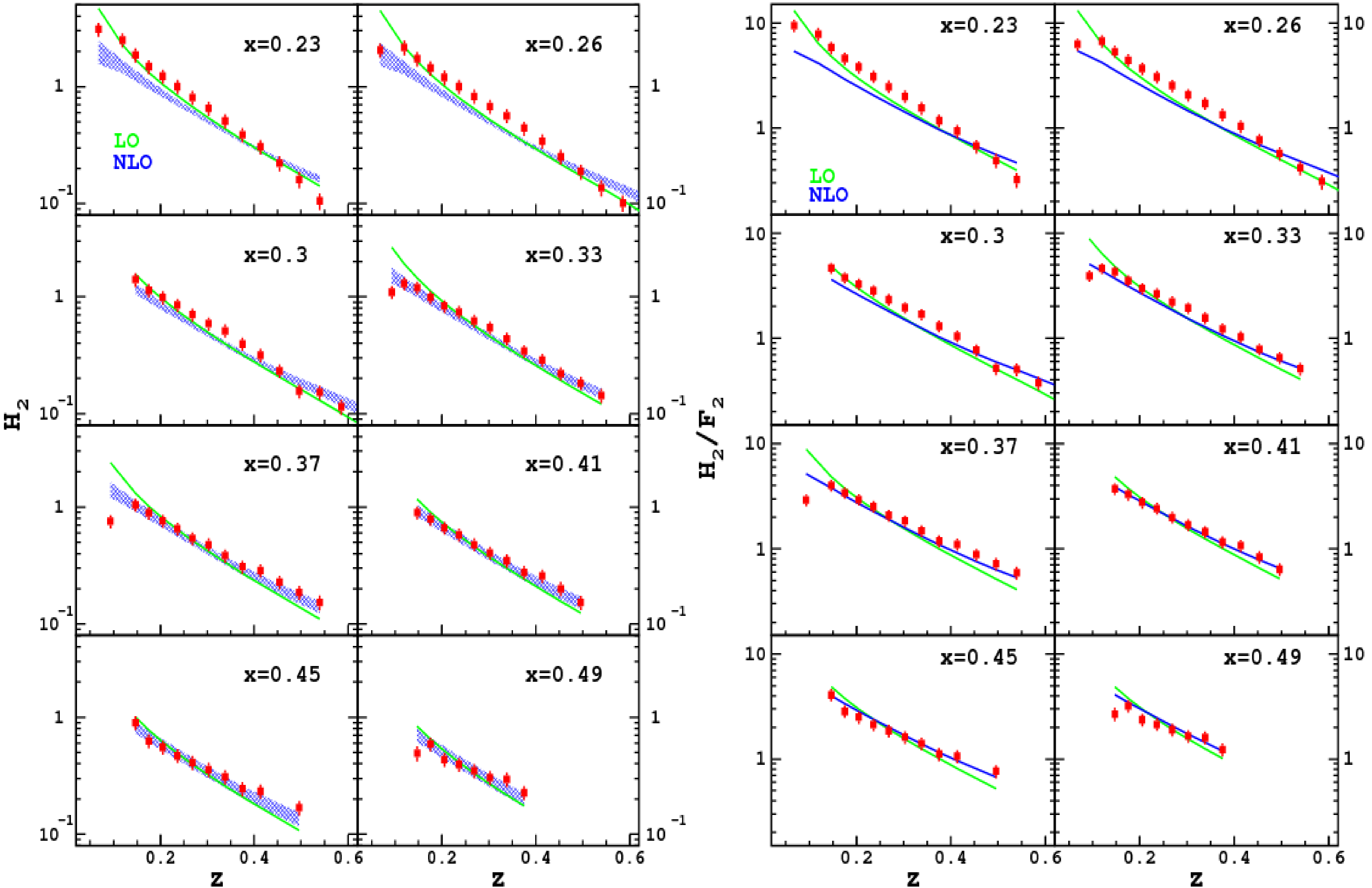

z-dependence at fixed p_T

At large p_T the suppression of z-distribution is clearly seen, but its contribution to the integral is small (low p_T dominates) and modeled by phenomenological transverse momentum distribution:

$$H_2\left(p_T^2\right) = H_2 \frac{1}{\pi\left\langle p_T^2\right\rangle} e^{-\frac{p_T^2}{\left\langle p_T^2\right\rangle}}$$

$$\left\langle p_T^2\right\rangle = a^2 + b^2 z^2$$

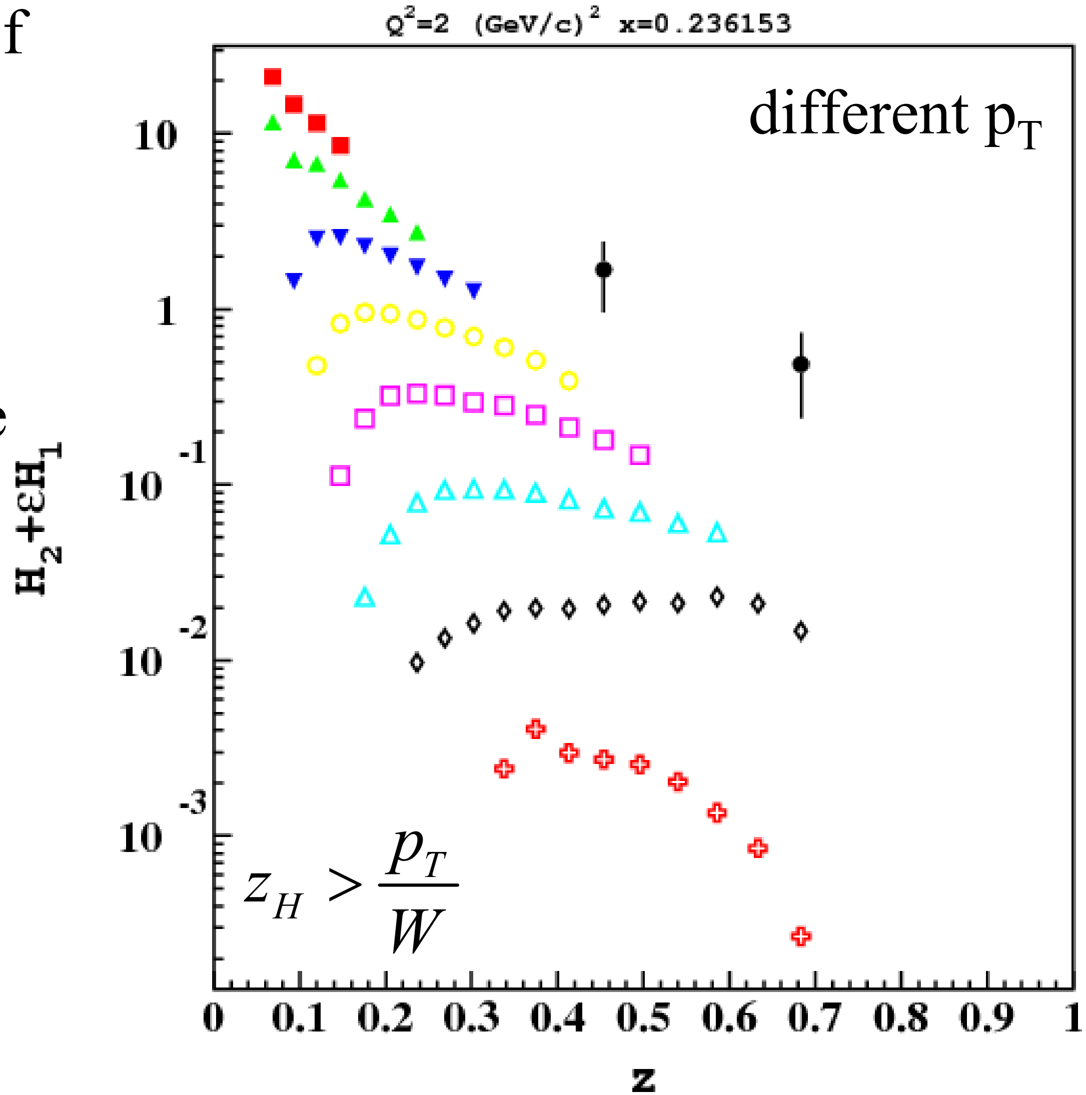

Normalization

Hadron multiplicity: $z = \frac{2E_h^{CM}}{\sqrt{s}}$ $D(z) \equiv \frac{1}{\sigma_{tot}} \frac{d\sigma}{dz}$

In e^+e^- collisions

$$\langle n_h(s) \rangle^{e^+e^-} = \sum_q \int_0^1 \left\{ D_q^h(z) + D_{\bar{q}}^h(z) \right\} dz$$

In SIDIS, neglecting target fragmentation contribution

$$\langle n_h(s) \rangle^{ep} = \frac{1}{\sum_{q,\bar{q}} f_q(x)} \sum_q \int_0^1 \left\{ f_q(x) D_q^h(z) + f_{\bar{q}}(x) D_{\bar{q}}^h(z) \right\} dz$$

$x_F > 0$ => $z_H > \frac{p_T}{W}$ => $p_T < z_H W < z_H \nu$

Cut on x_F removes part of the p_T region breaking normalization of transverse momentum distribution.

<cosφ> vs z

The same situation.

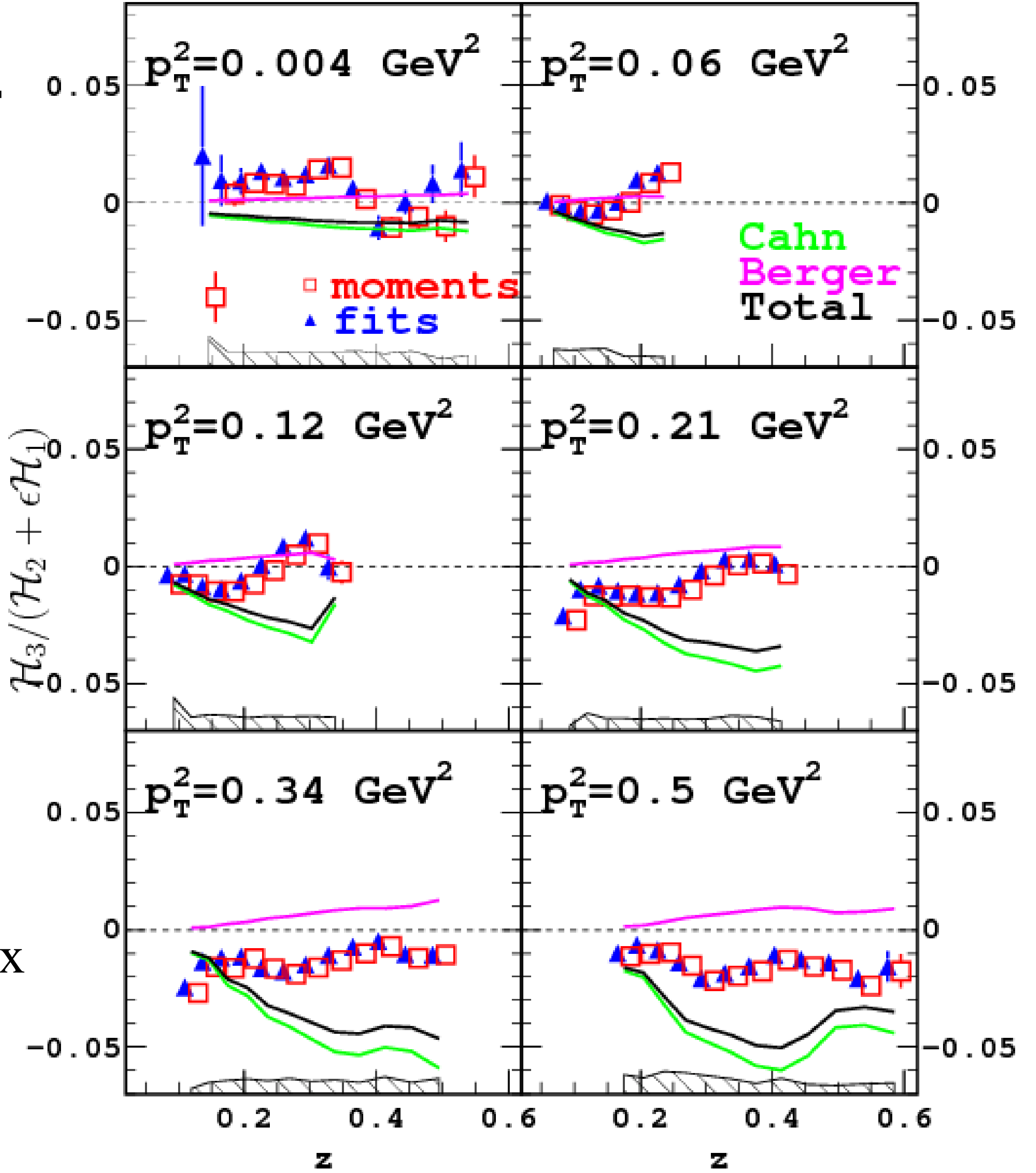

Data are integrated over x and Q^2 in DIS region.

<cos2φ> vs z

The same situation.

$\langle Q^2 \rangle = 2.3$ GeV^2

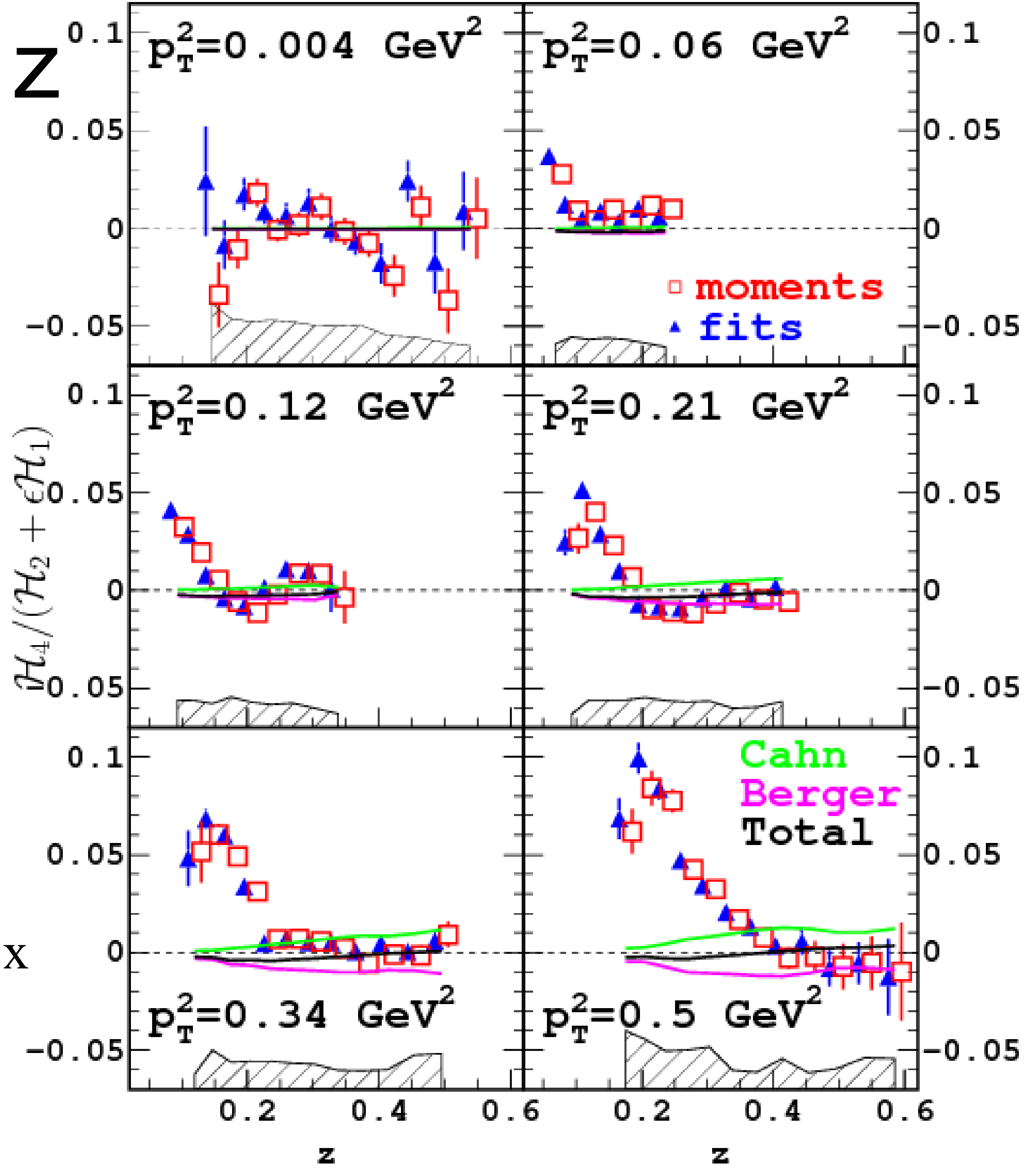

Data are integrated over x and Q^2 in DIS region.

Azimuthal angle definition

$$\langle\cos\varphi\rangle \equiv \frac{\left(\left[\vec{k}\times\vec{q}\right],\left[\vec{p}_h\times\vec{q}\right]\right)}{\left|\vec{k}\times\vec{q}\right|\left|\vec{p}_h\times\vec{q}\right|}$$

k – initial electron 3-momentum,
p_h – hadron 3-momentum,
q – virtual photon 3-momentum

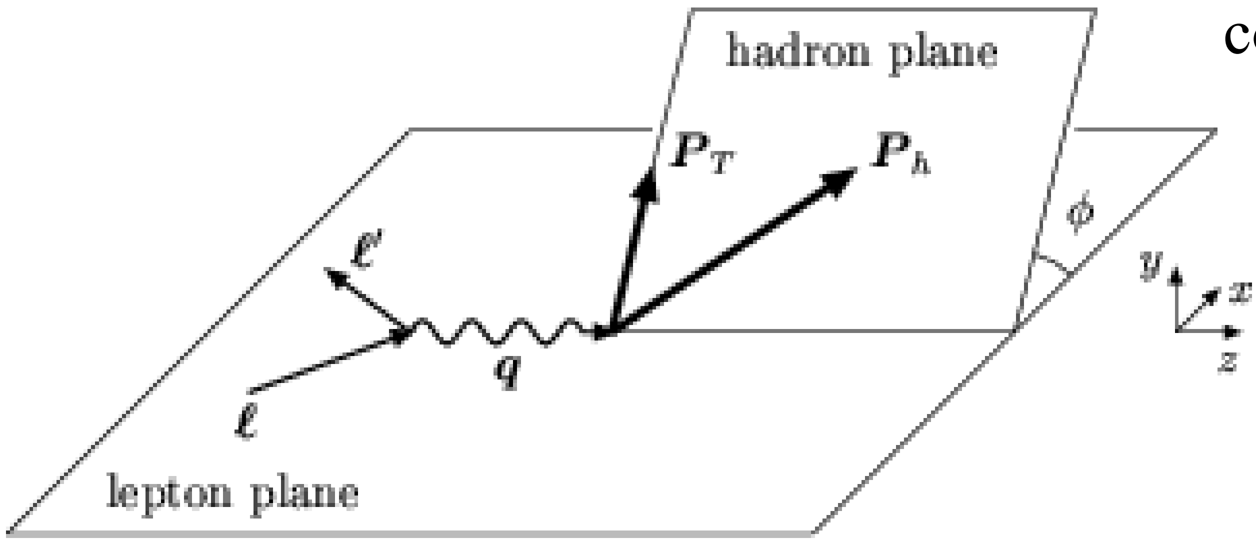

Trento convention

p_T-dependence

- Structure functions were separated by fitting ϕ dependences in each separate kinematical bin.
- Only bins with complete ϕ-coverage were considered.

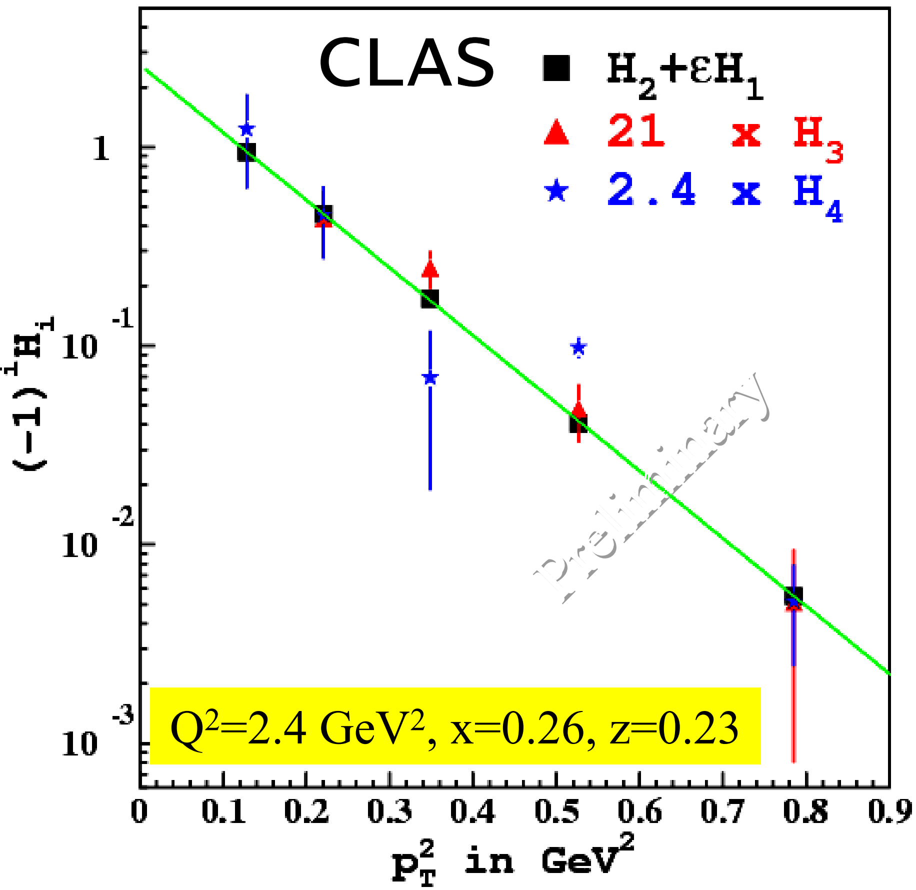

✓The same p_T behavior for all structure functions => trivial kinematical factors for azimuthal asymmetries <cosϕ> and <cos2ϕ>

✓H_3 contribution is negative

✓H_4 is mostly positive

✓Suggest only internal transverse motion of quarks (Cahn)?

$$\langle \cos\varphi \rangle \sim p_T \quad \langle \cos 2\phi \rangle \sim p_T^2$$

up to p_T~1 GeV

e^- measurement

1. Cherenkov Counter (CC) uniquely identify electrons up to P~3 GeV
2. Electromagnetic Calorimeter (EC) separates high energy electrons

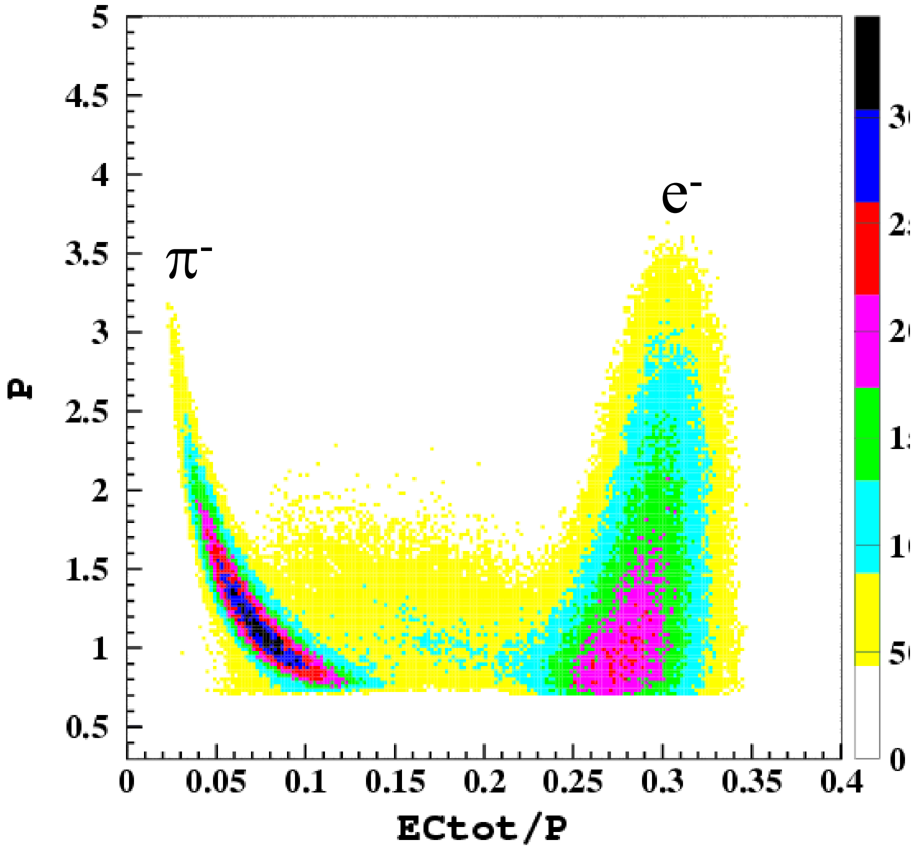

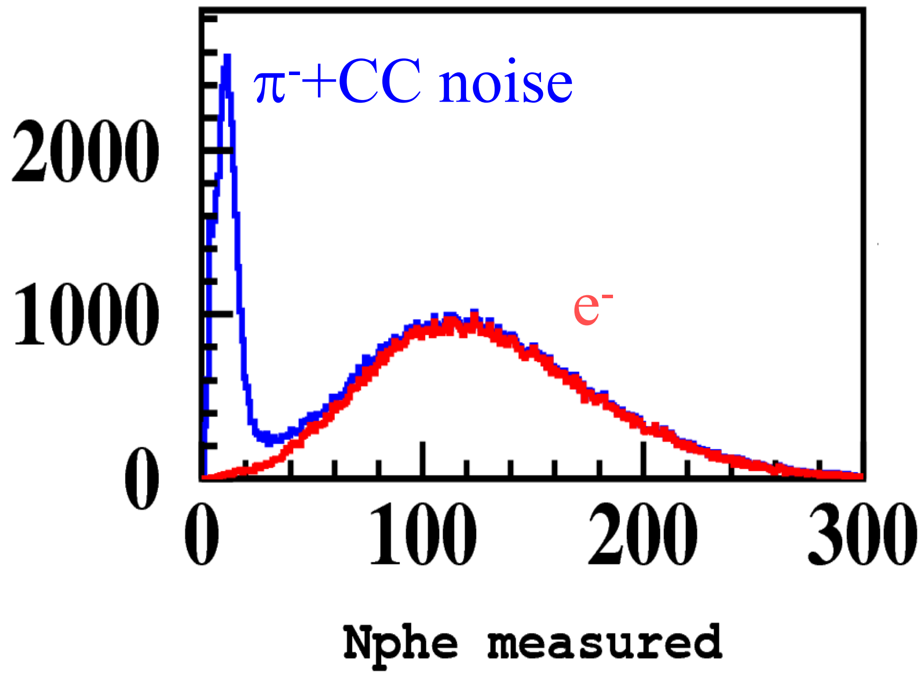

e^- inclusive

1. Inclusive cross sections obtained with the same data are in good agreement with world data.
2. Little effort needed to complete the inclusive data analysis at 6 GeV

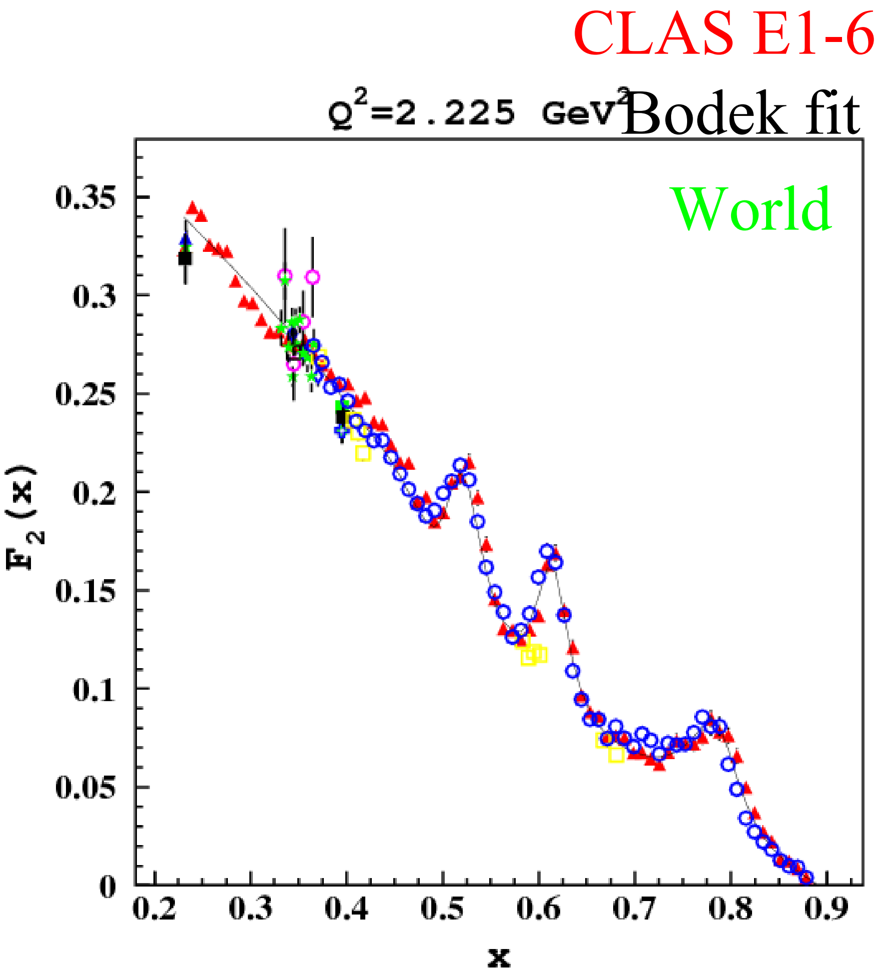

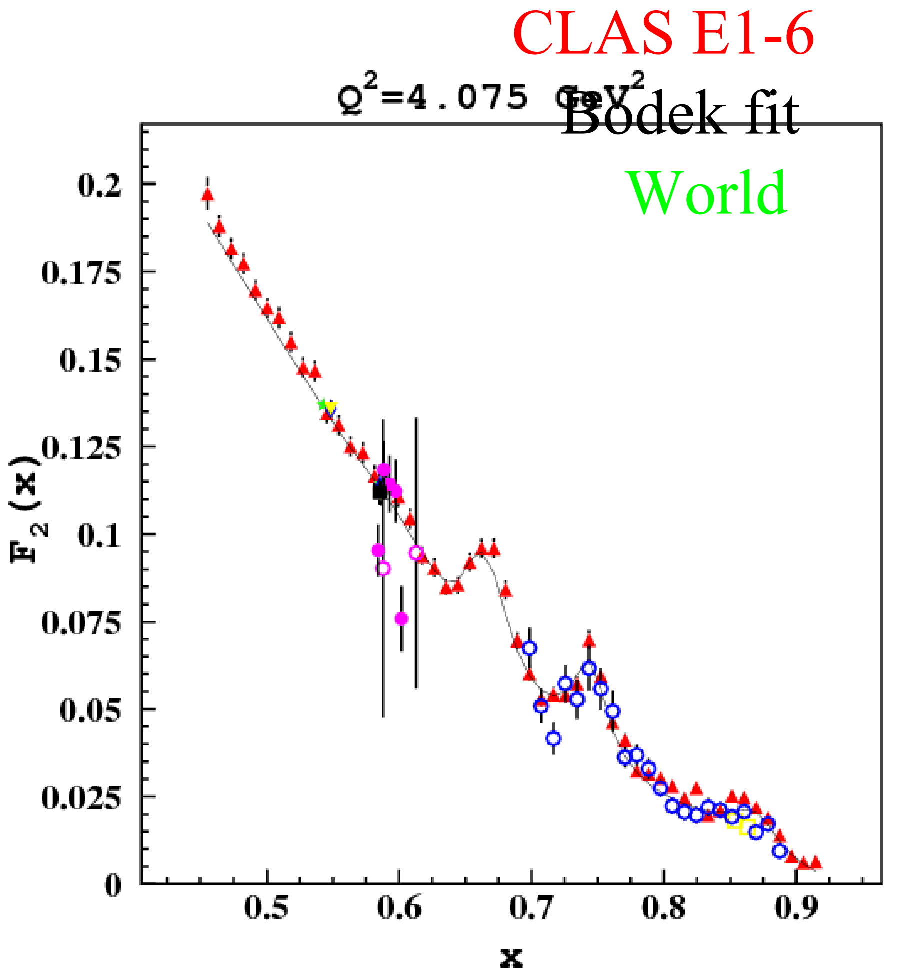

Ep-elastic

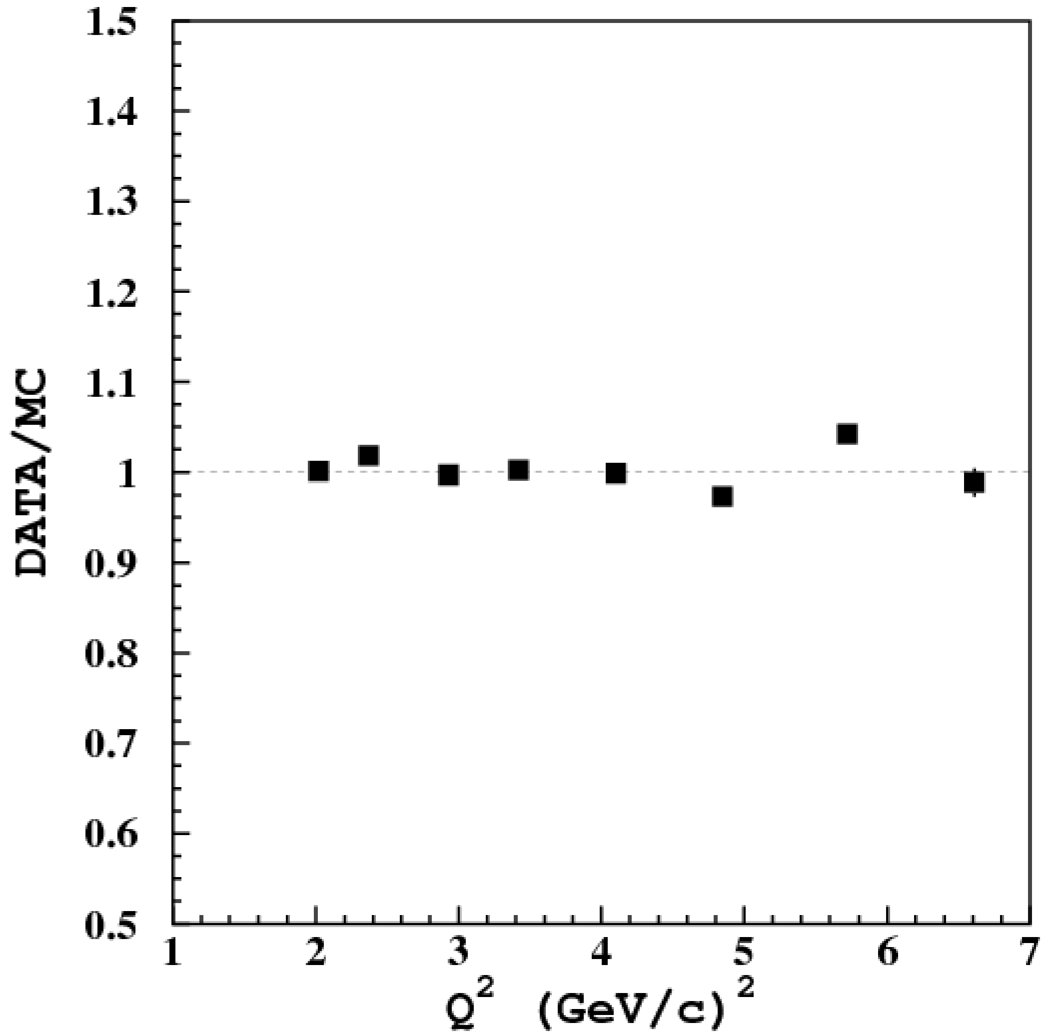

π^+ measurement

1. Pions are well identified by Time Of Flight (TOF) measurement in all accessible kinematical range
2. Loss of events in data and Monte Carlo (MC) simulations due to PID cuts was checked in π^+n peak

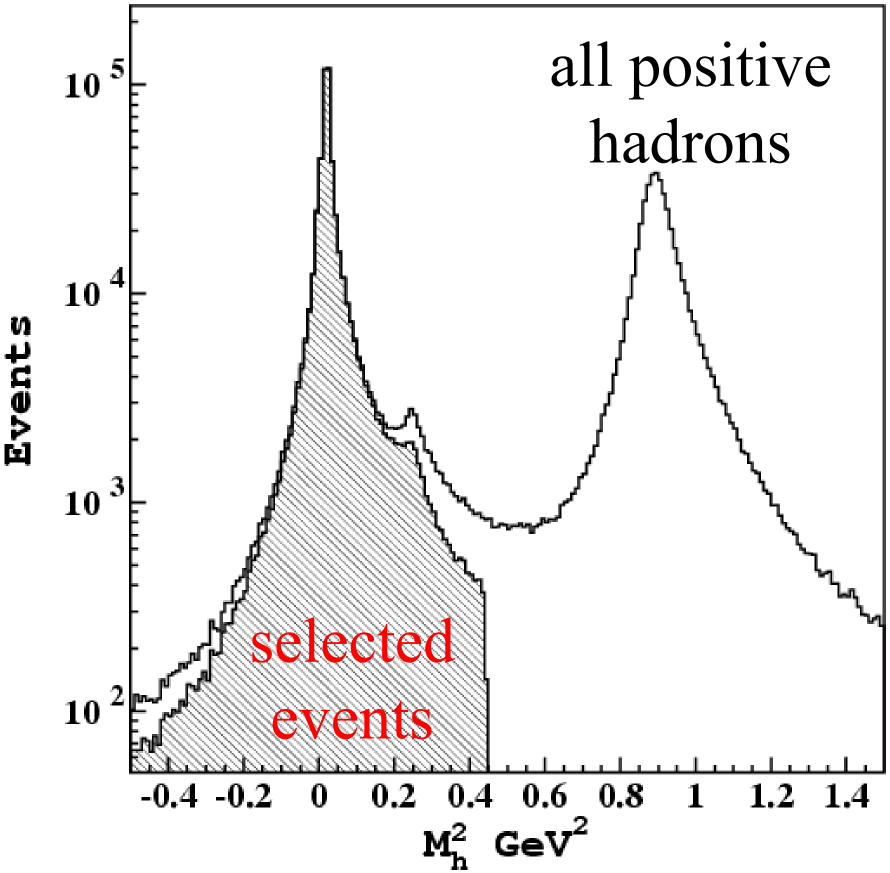

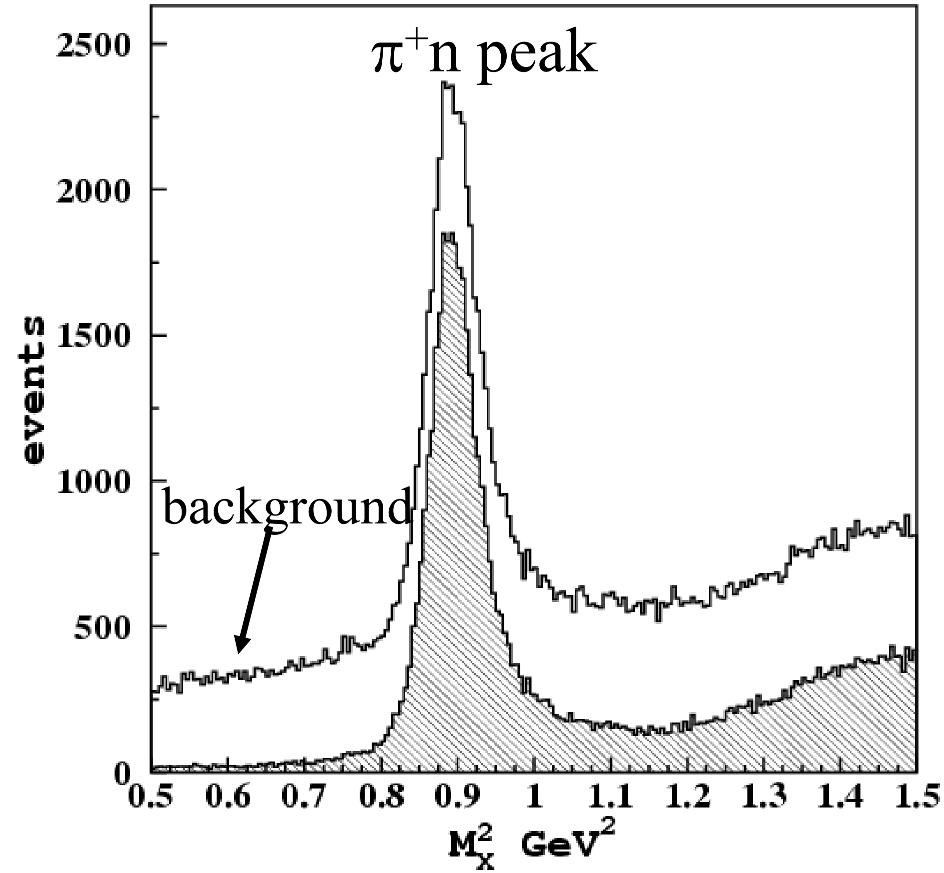

π^+ semi-inclusive

1. New CLAS data are in agreement with previously published measurements within given uncertainties
2. Comparison also shows non-trivial p_T-behavior

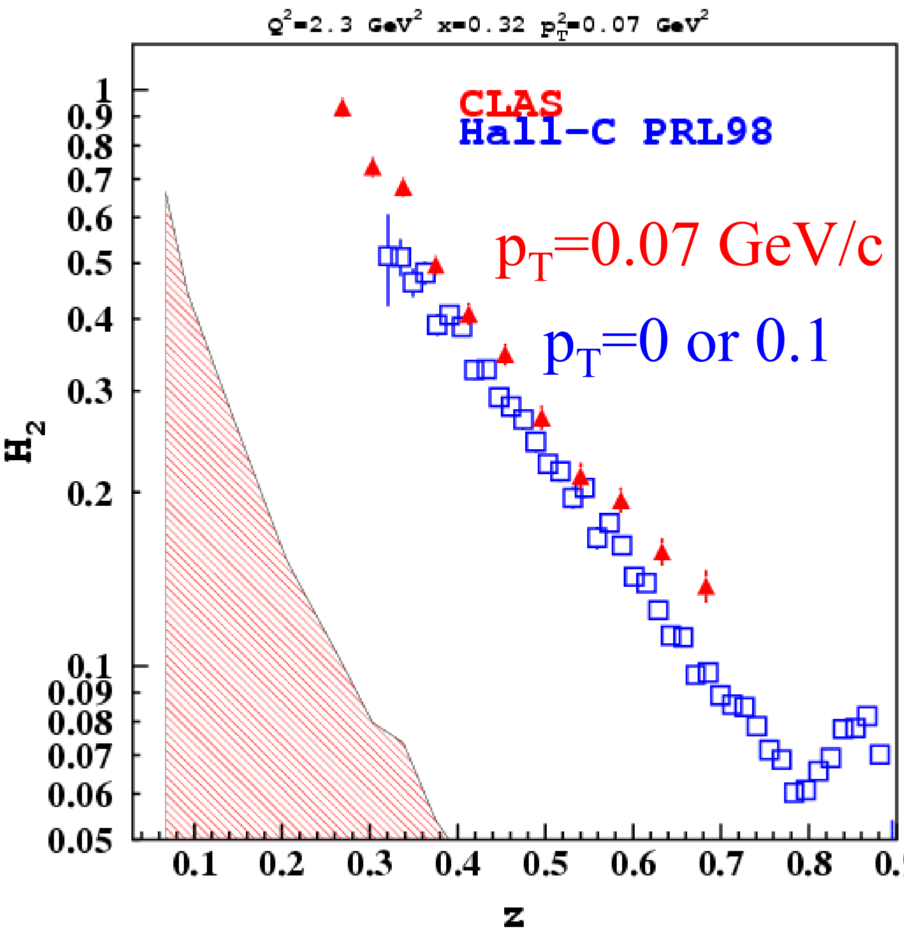

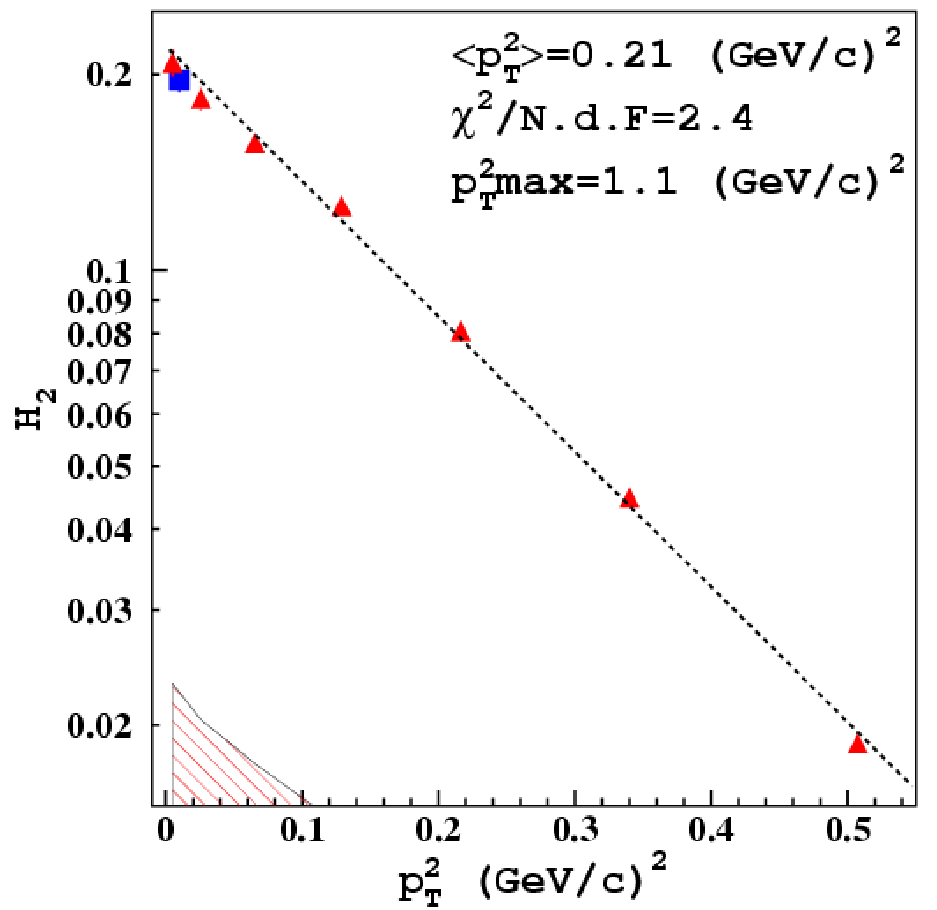

π^+ semi-inclusive

Kinematics does not match perfectly, some extrapolations have been performed in CLAS data.

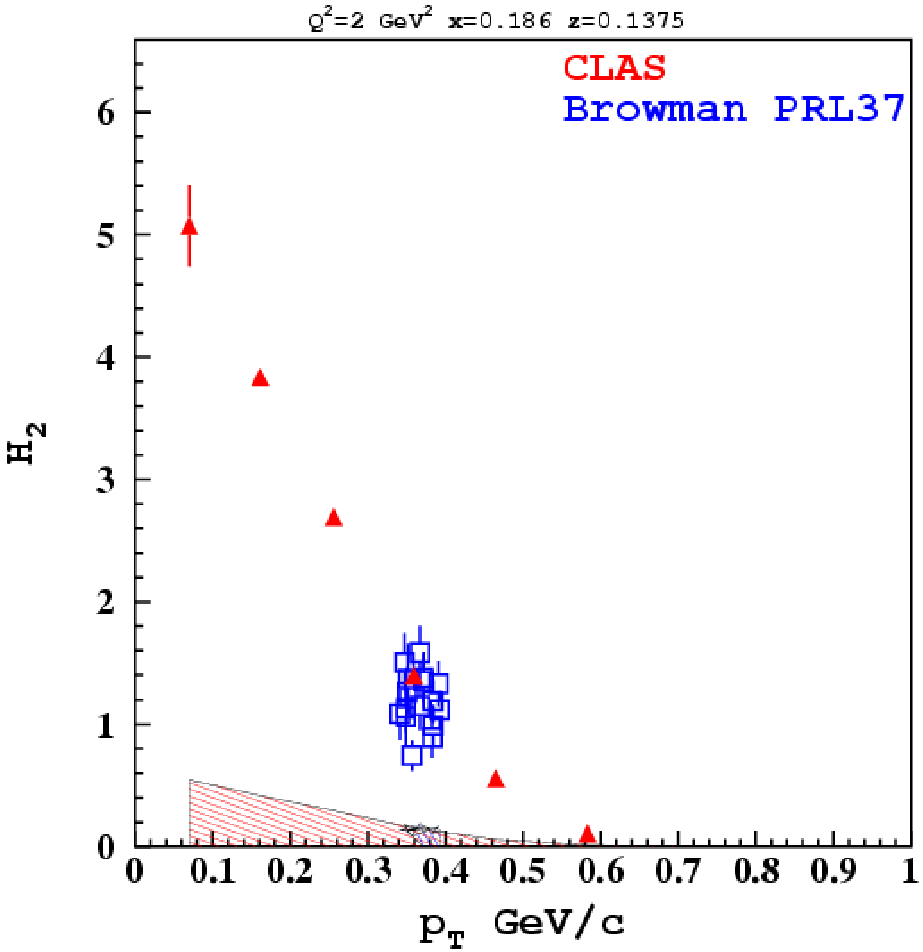

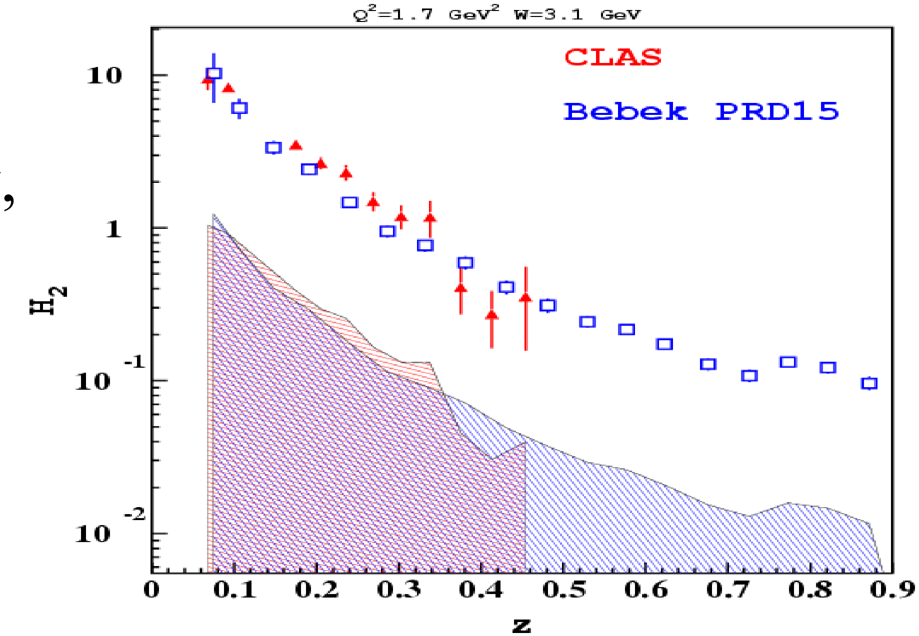

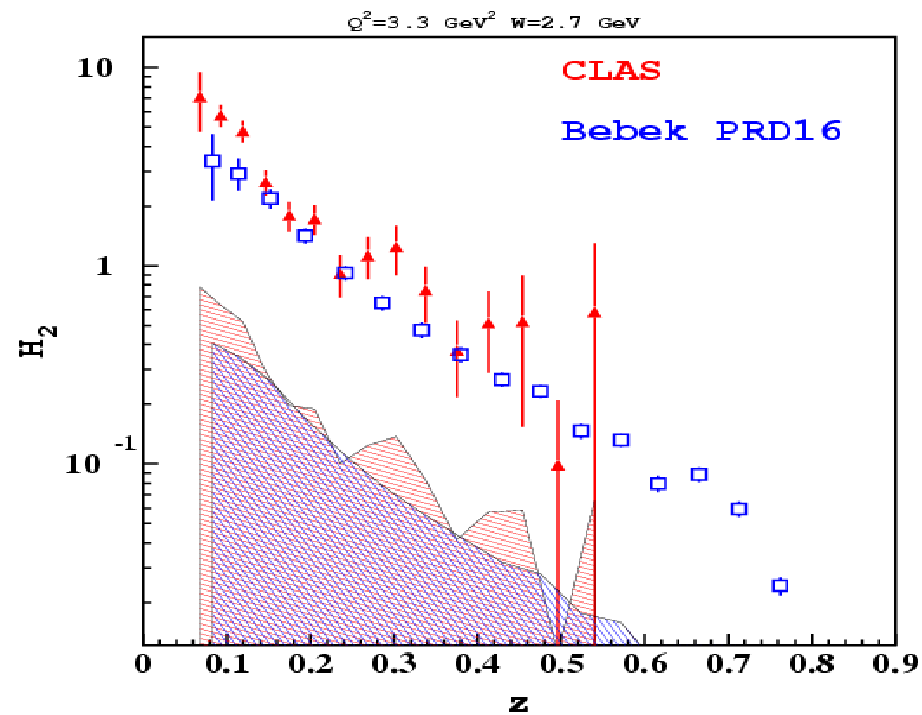

EMC data

Much larger $<p_T^2>$ values measured by EMC, but seen to increase rapidly with W.

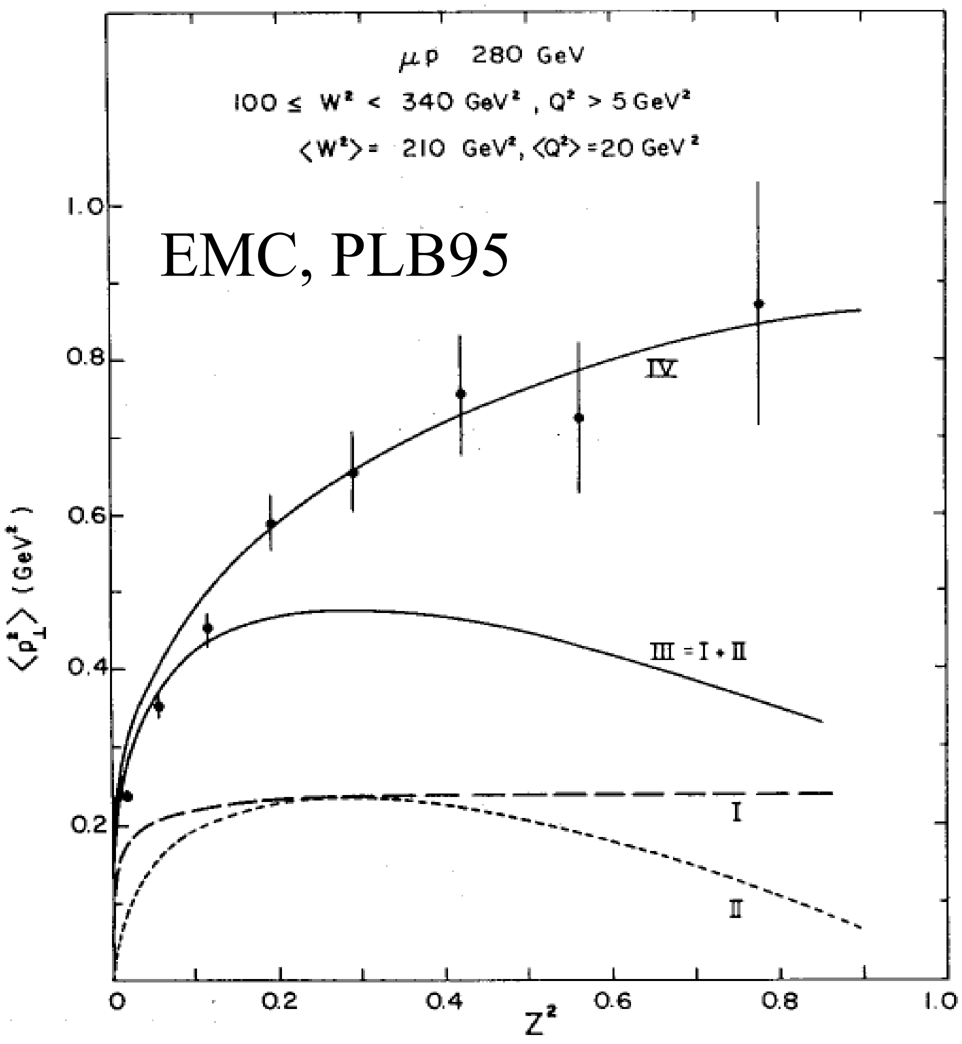

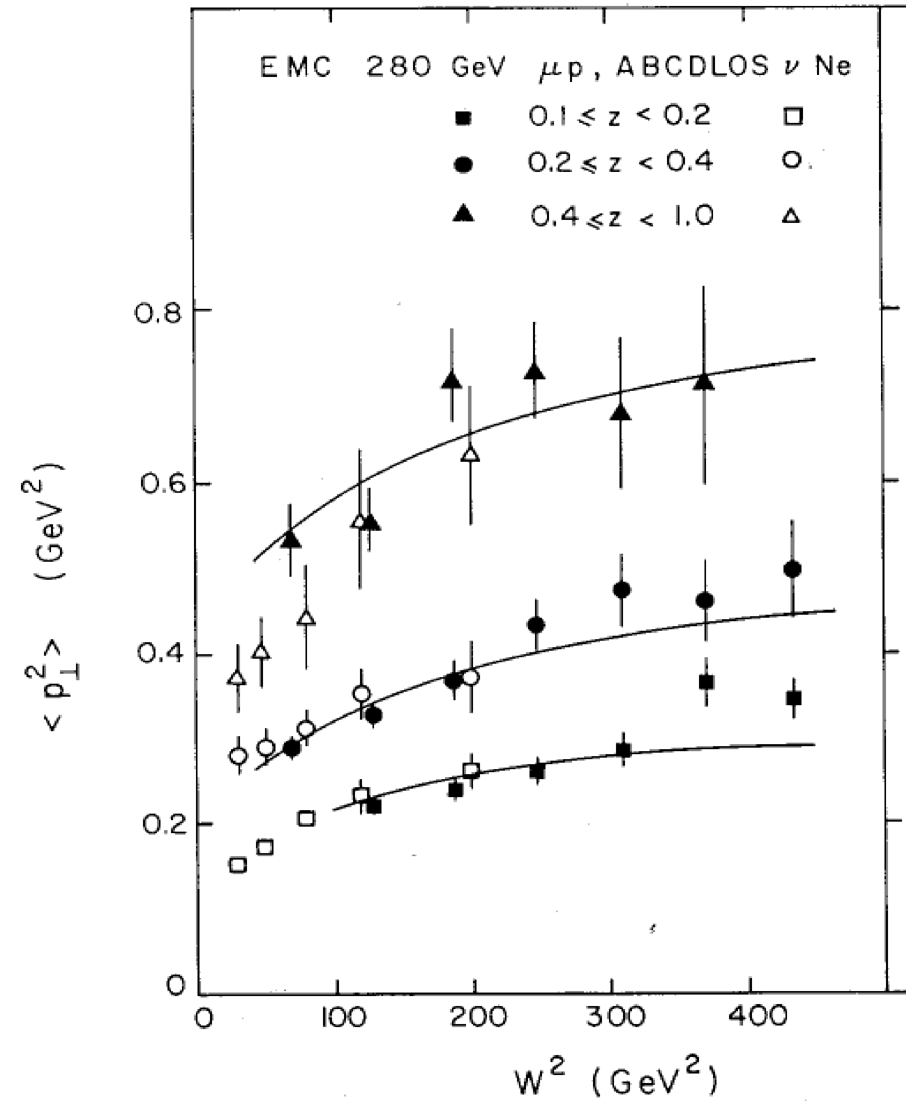

Mass Corrections

At low energies masses are not negligible, one has to use correct variables (Mulders, PRD49):

$$x' = -\frac{q^+}{P^+} = \frac{2x}{1+\sqrt{1+\frac{4M^2x^2}{Q^2}}} \qquad z' = \frac{p_h^-}{q^-} = \frac{z\left(1+\frac{p_{\parallel}}{E_h}\right)}{1+\sqrt{1+\frac{4M^2x^2}{Q^2}}}$$

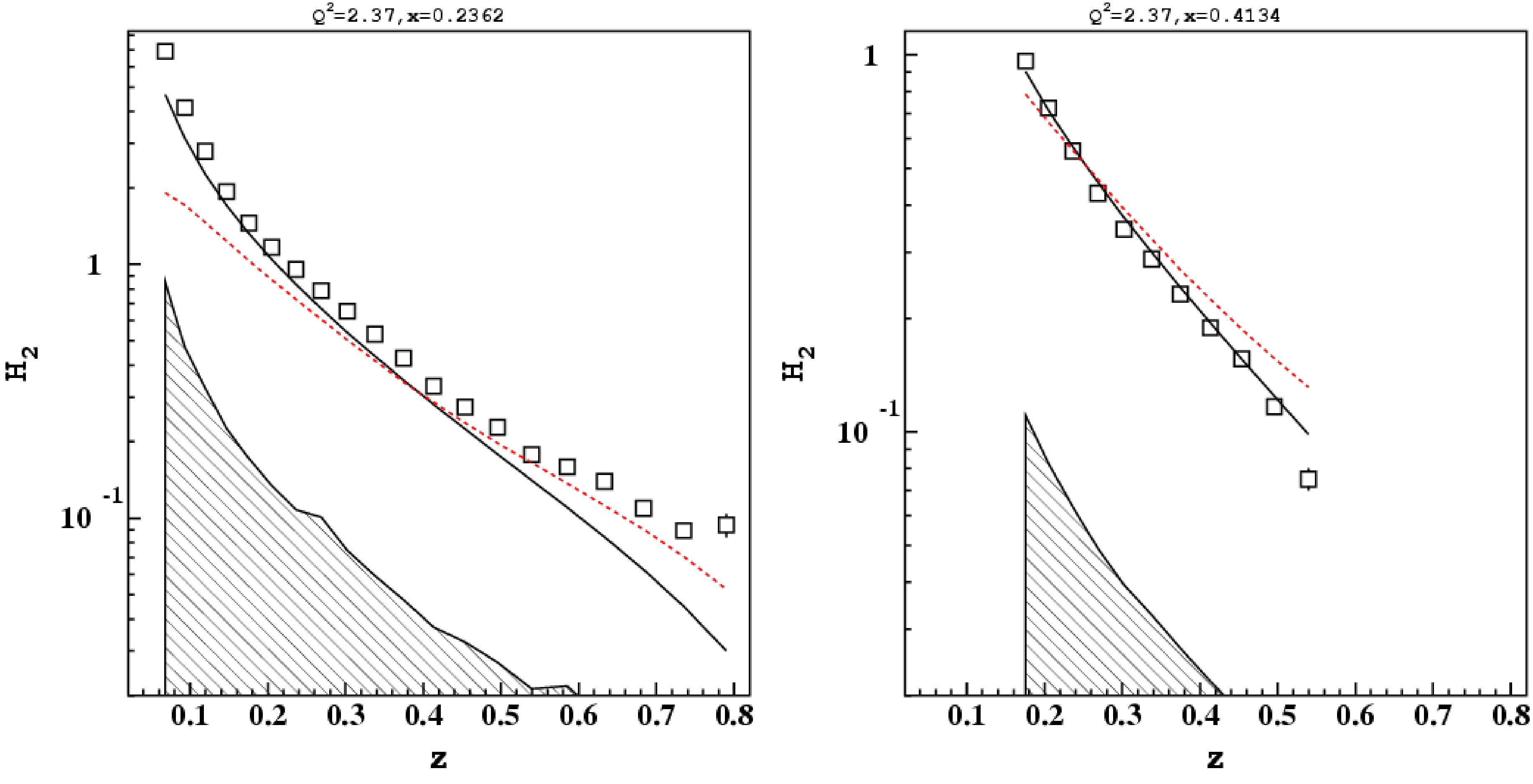

x_F cut

Cut on x_F simply remove low-z part of the spectrum. Its application always destroy the good agreement with pQCD calculations in these region.

BEBC (CERN), PLB87

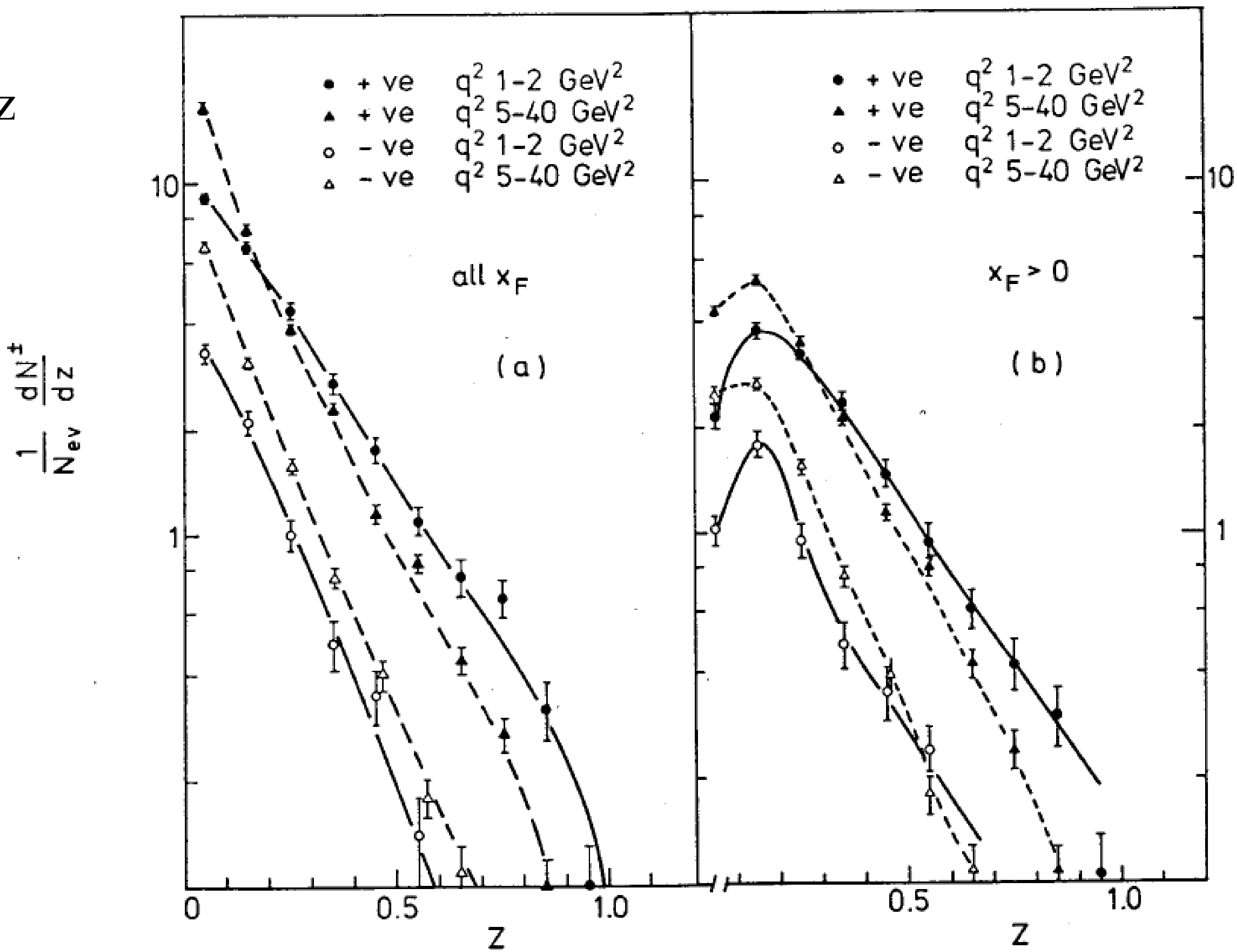

EMC data vs. pQCD

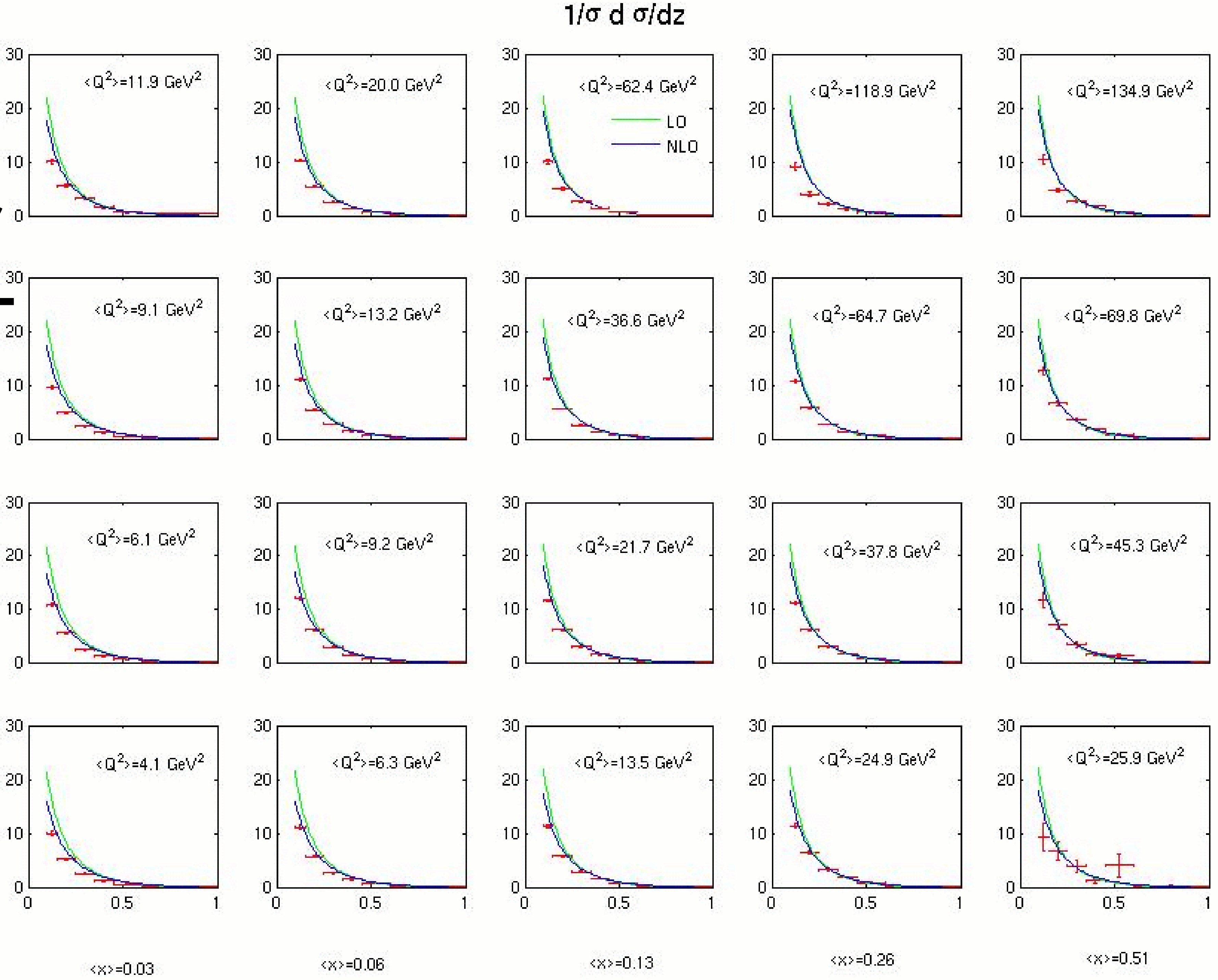

EMC data vs. pQCD

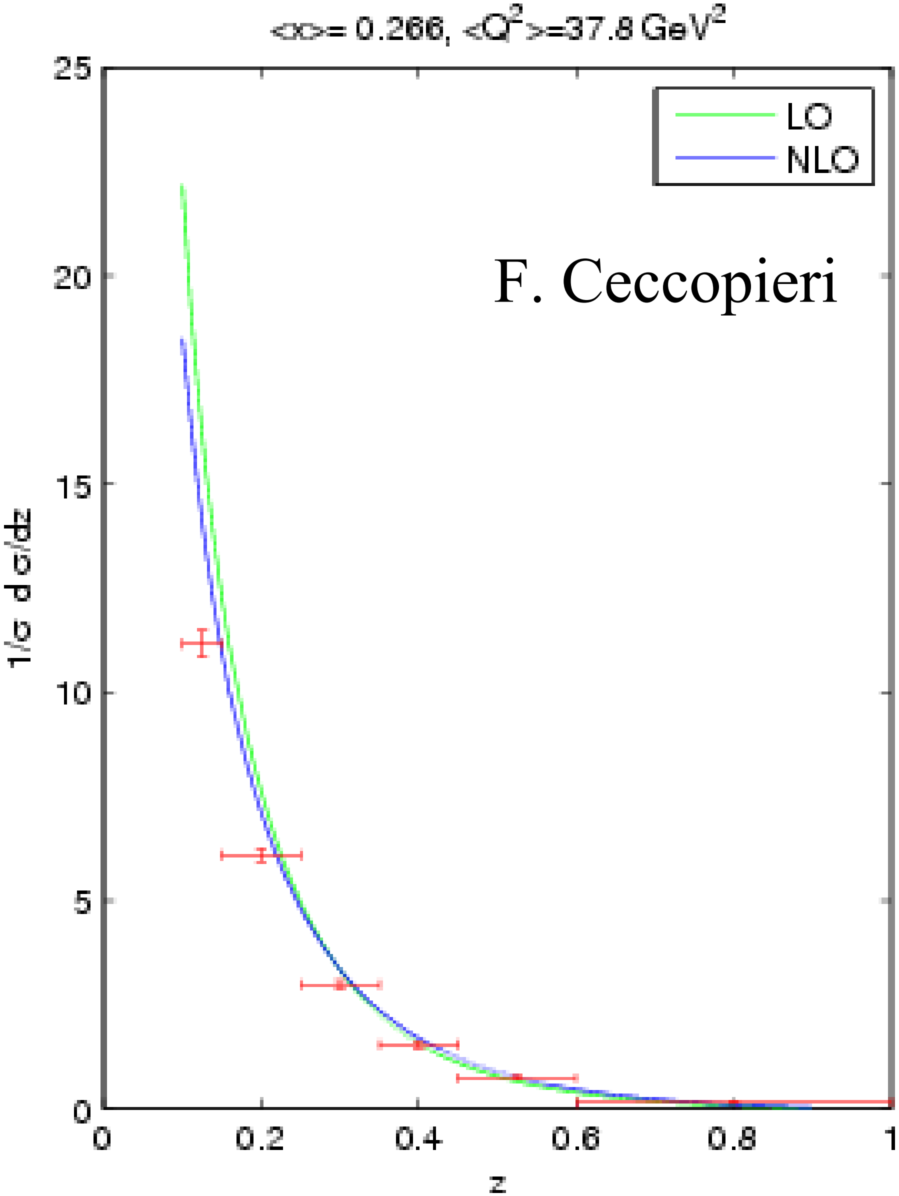

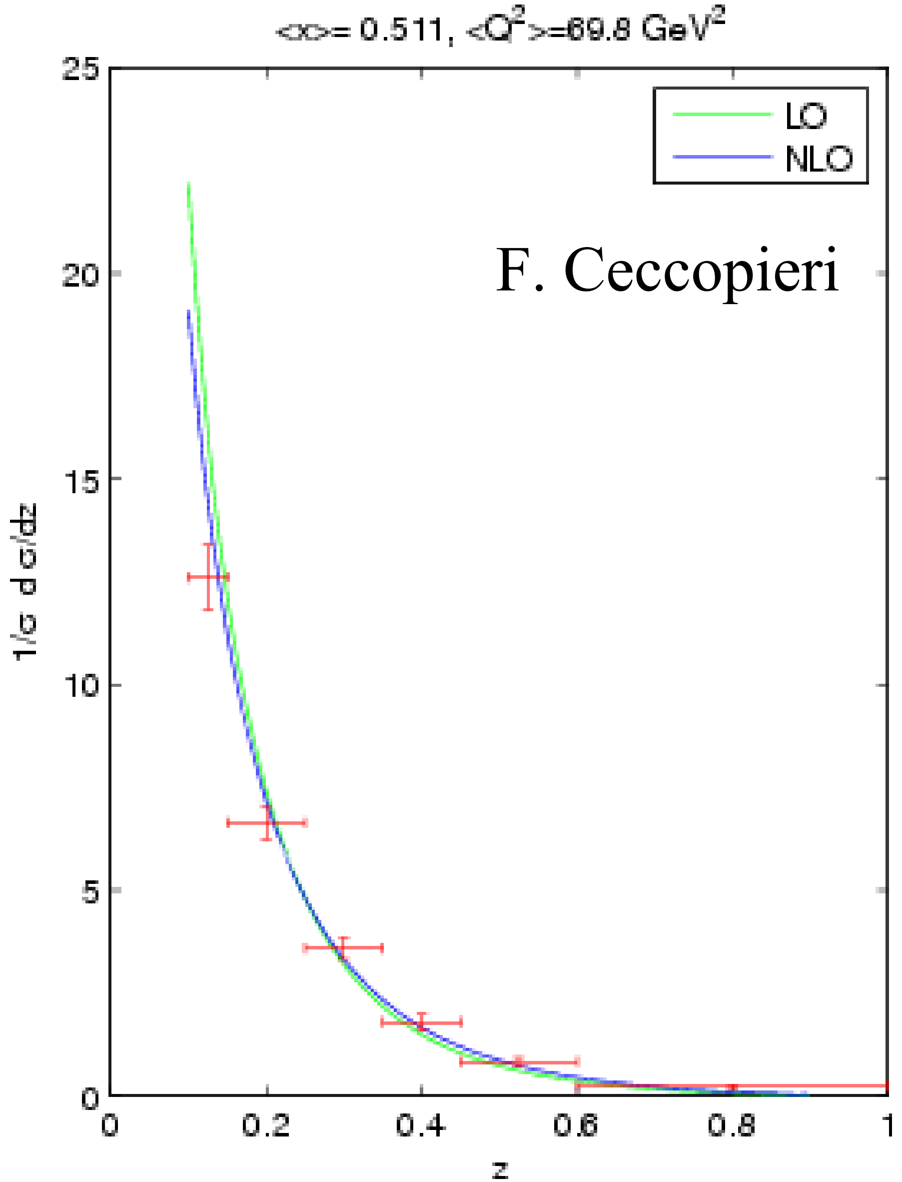

Parameterization dependence

1. Very small uncertainty due to parton distribution function
2. Larger uncertainty due to fragmentation function

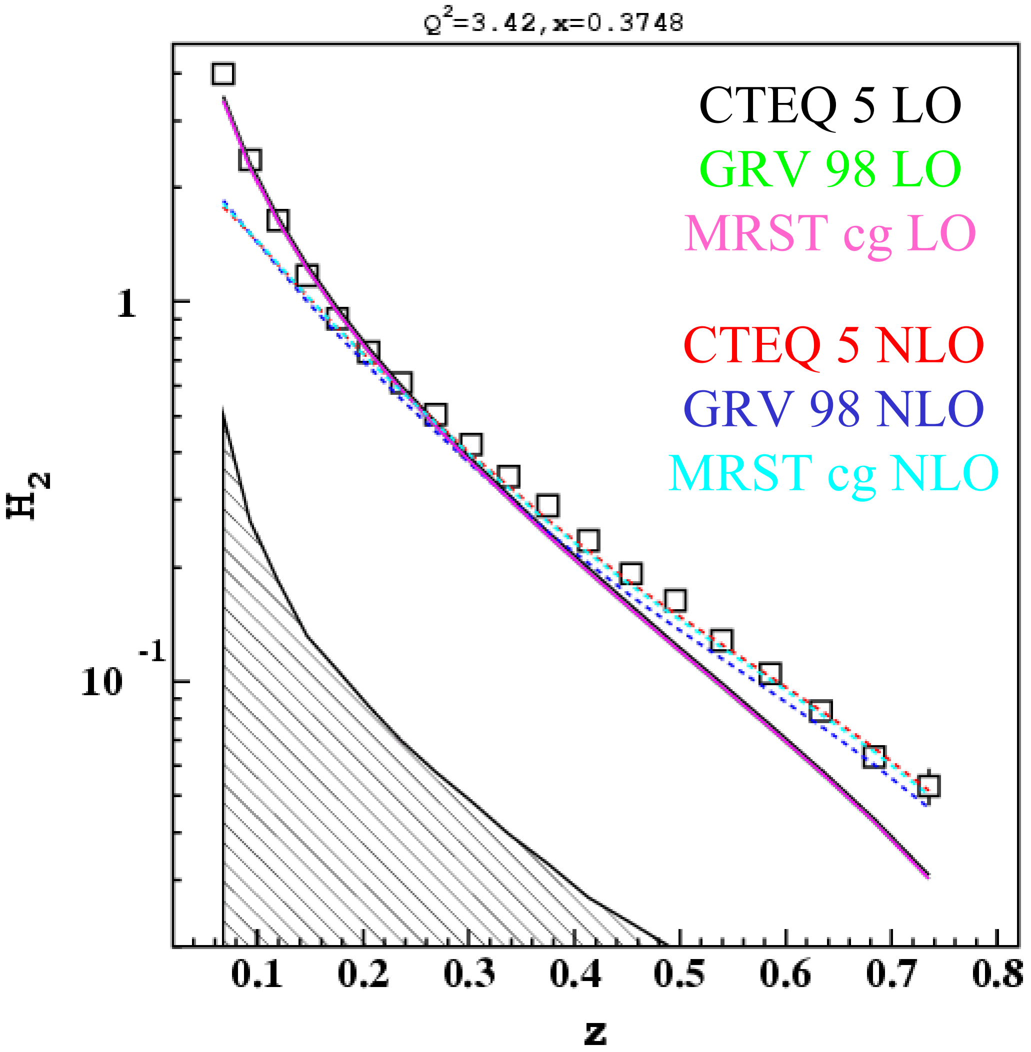

ZEUS data

1. The same limitations as for EMC and E665
2. More detailed data sample in hep-ex/0608053 represented in different variables (pseudorapidity and minimum hadronic energy in HCM) and integrated also over neutral hadrons appears hard to compare

$0.01<x<0.1$

$180<Q^2<7220\ \mathrm{GeV}^2$

$0.2<z<1$

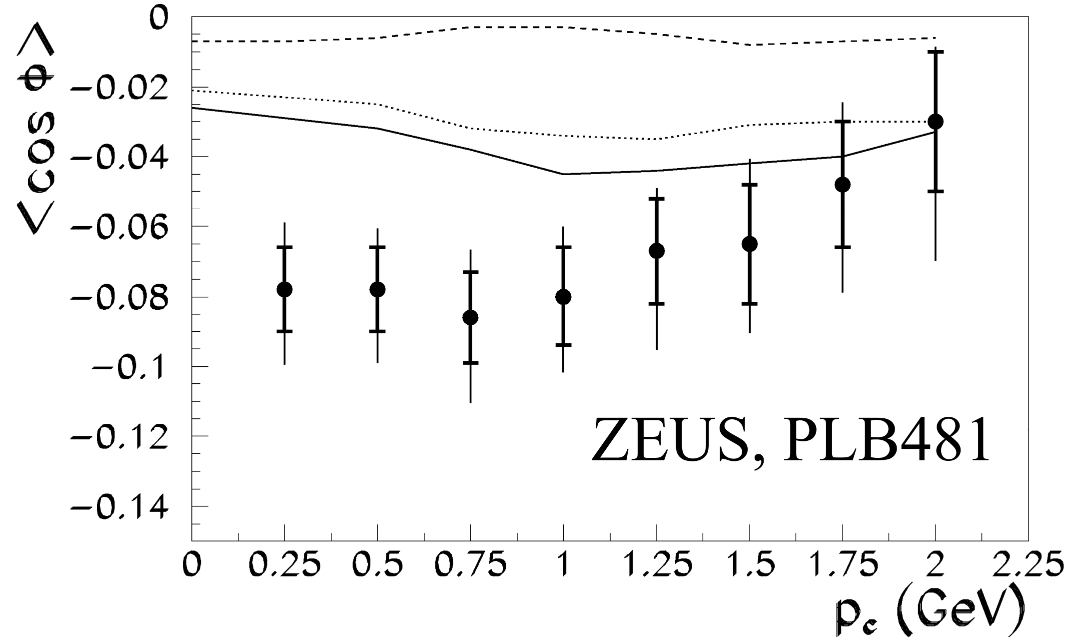

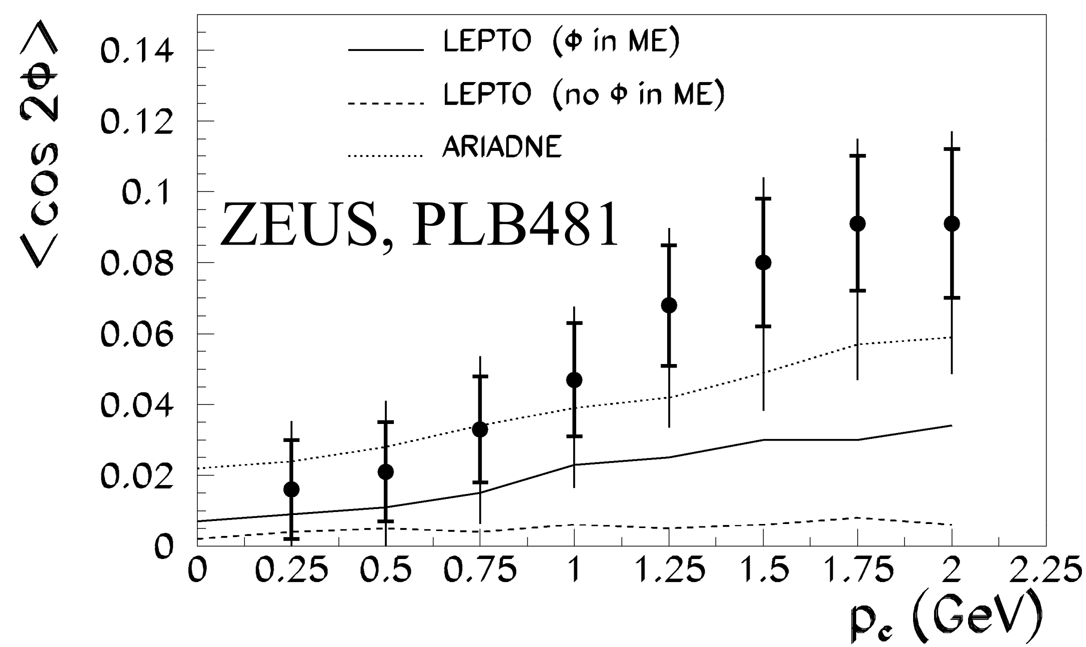

EMC and E665 data

1. The same limitations also in E665 data
2. Minimum transverse momentum of hadrons is commonly used p_T^C which can mask possible sign change at low p_T
3. Strong x_F variation is seen by EMC

$$\langle \cos n\varphi \rangle (p_T^C) = \int_{p_T^C}^{\infty} dp_T \, \langle \cos n\varphi \rangle$$

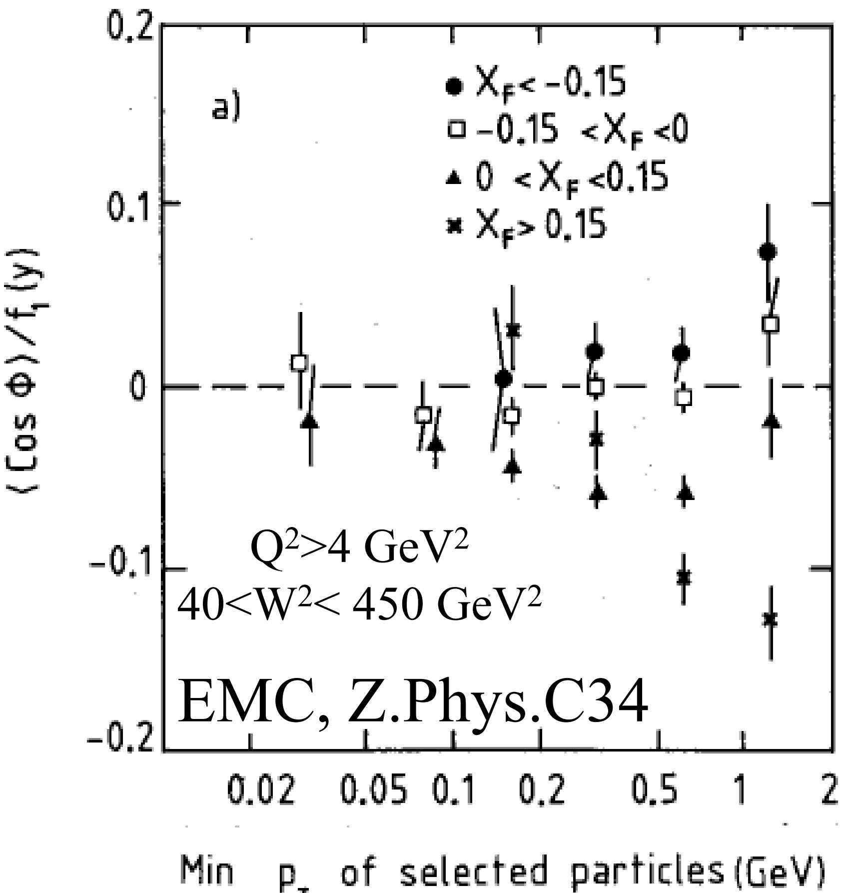

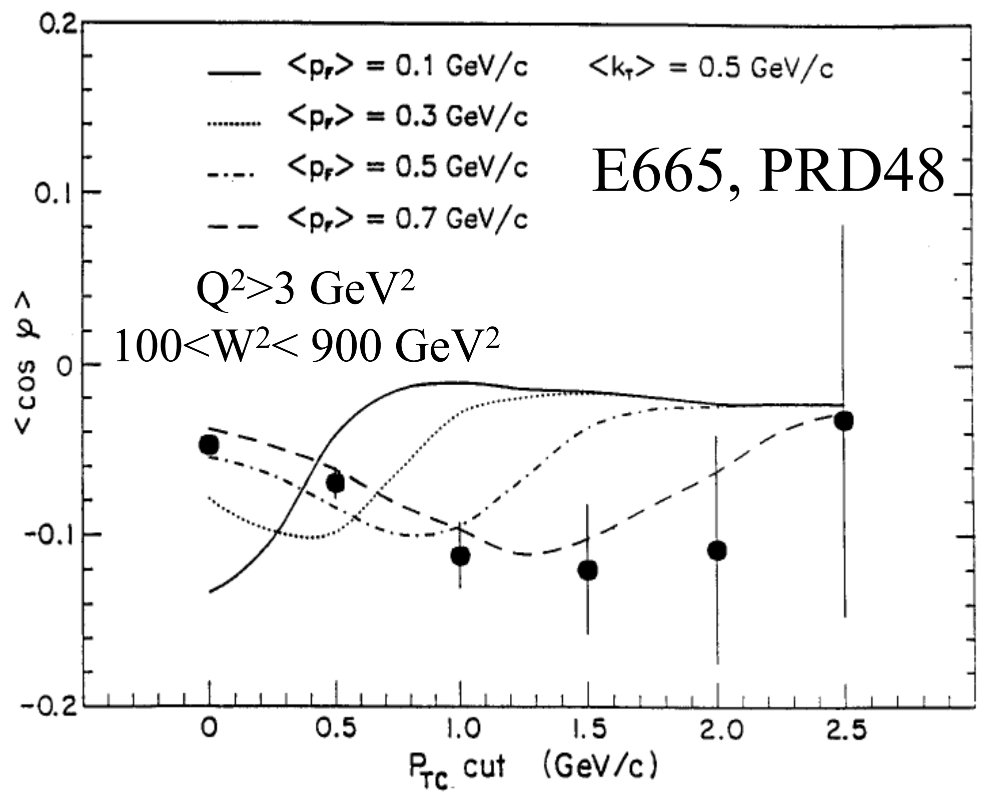

EMC data in p_T

1. Summed over all charged hadrons positive and negative, no PID
2. Integrated over all other variables: x, Q^2, z
3. Radiative corrections with Monte Carlo

$$f_1(y) = (2-y)\frac{\sqrt{1-y}}{1+(1-y)^2} \qquad f_2(y) = \frac{1-y}{1+(1-y)^2} \qquad y = \frac{\nu}{E_l}$$

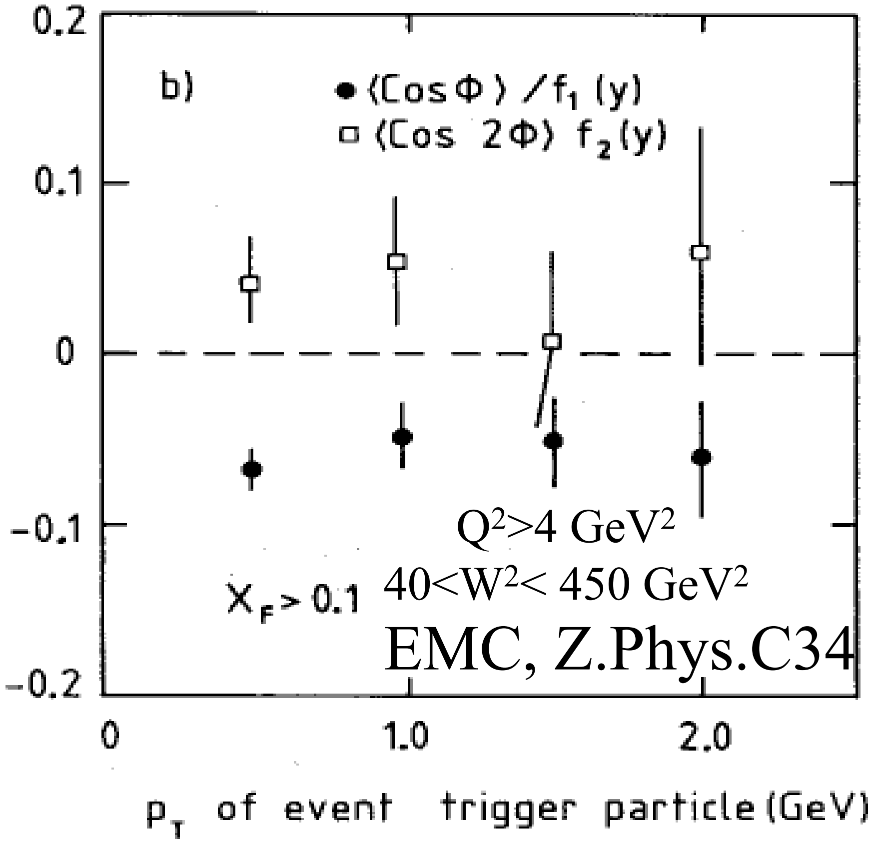

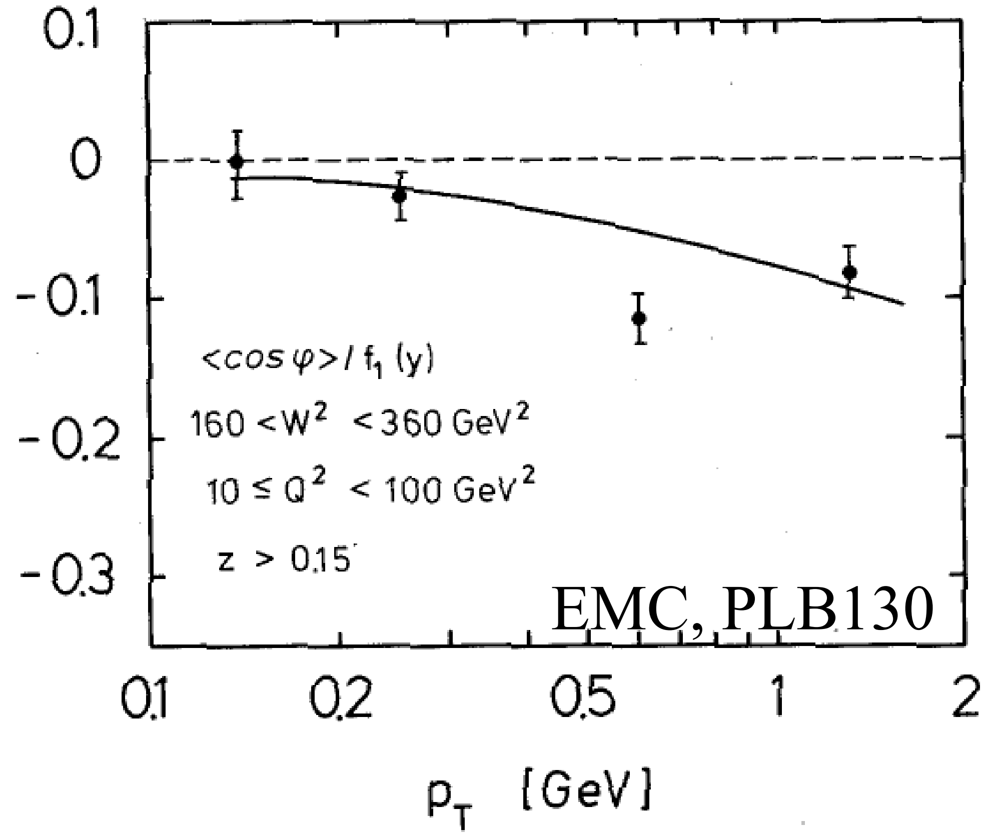

Interference term

- QCD predicts the scale dependence of M :

$$\frac{\partial}{\partial \log Q^2} M_{i,h/p}(x,z,Q^2) = \frac{\alpha_s(Q^2)}{2\pi}\int_{x/(1-z)}^{1}\frac{du}{u}P_j^i(u)M_{j,h/N}\left(\frac{x}{u},z,Q^2\right) + $$
$$+\frac{\alpha_s(Q^2)}{2\pi}\int_x^{x/(x+z)}\frac{du}{x(1-u)}\hat{P}_j^{i,l}(u)F_{j/p}\left(\frac{x}{u},Q^2\right)D_{h/l}\left(\frac{zu}{x(1-u)},Q^2\right)$$

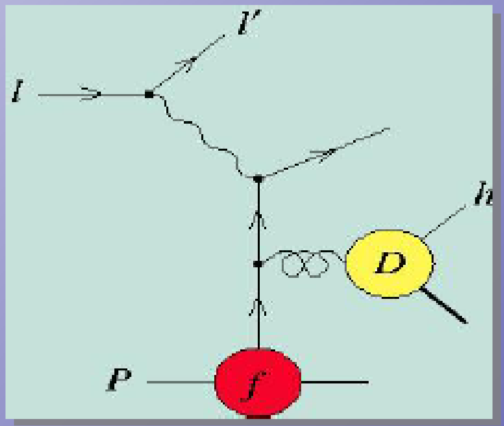

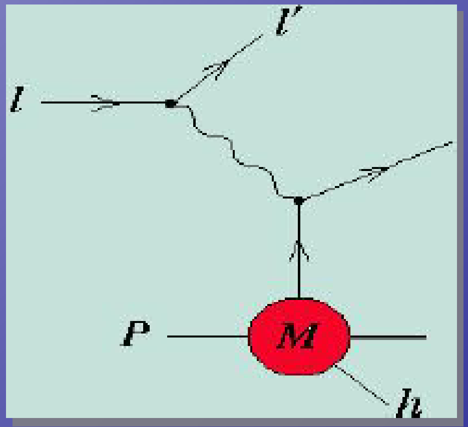

➡ Leading twist LO SIDIS cross section is thus:

$$\frac{d^3\sigma_p^h}{dx_B\, dQ^2\, dz_h} \propto \sum_{i=q,\bar{q}} e_i^2 \Big[\underbrace{F_{i/p}(x_B,Q^2)D_{h/i}(z_h,Q^2)}_{\sigma_{current}} + \underbrace{(1-x_B)M_{i,h/p}(x_B,(1-x_B)z_h,Q^2)}_{\sigma_{target}}\Big]$$

Kinematical Separation (for π)

Current fragmentation

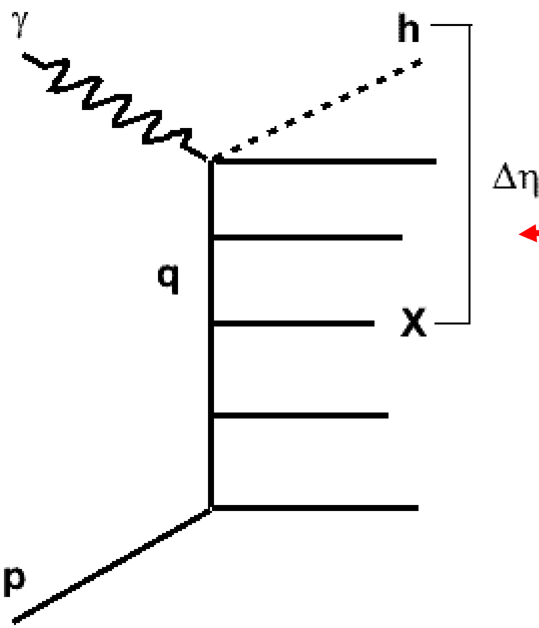

Hadron rapidity

$$\eta = \frac{1}{2}\frac{\log(E^h + p_{\parallel}^h)}{\log(E^h - p_{\parallel}^h)}$$

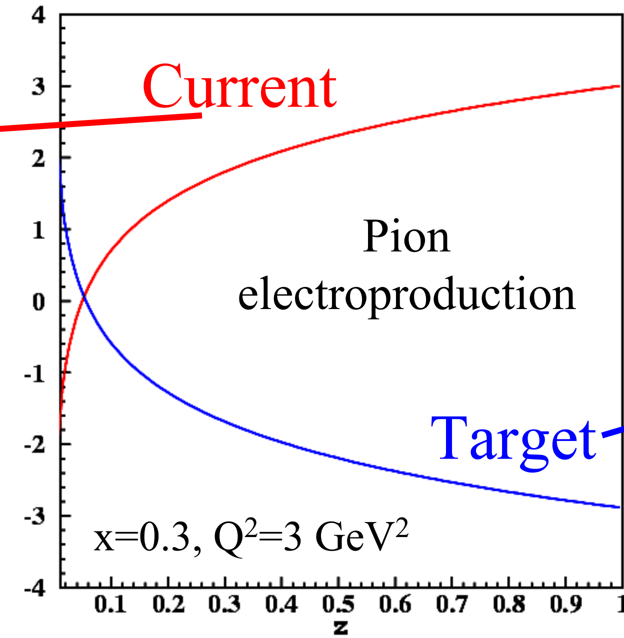

Target fragmentation

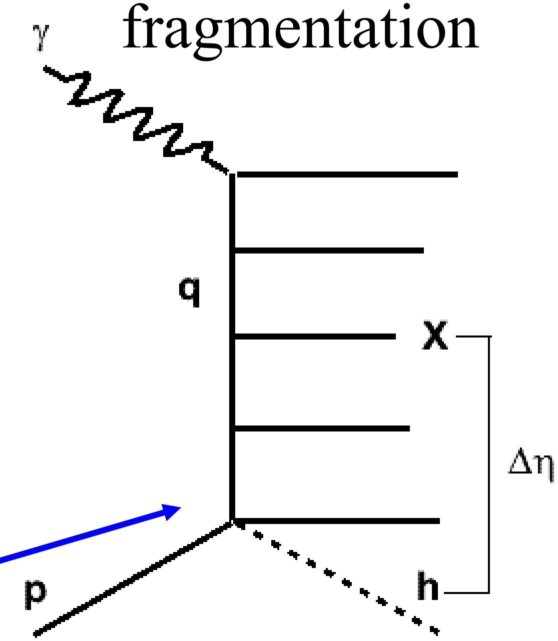

Separation is possible by means of a cut on the energy flow from the virtual photon to the measured hadron.

Mulders Rapidity Gap

$$\eta_{CM} = \frac{1}{2}\ln\left\{\frac{p_h^-}{p_h^+}\right\} = \ln\left\{\frac{\sqrt{2}p_h^-}{M_h^\perp}\right\} = -\ln\left\{\frac{\sqrt{2}p_h^+}{M_h^\perp}\right\}$$

$$p_h^\pm = E_h \mp p_h^{||}$$

$$\frac{p_h^-}{p_h^+}\frac{p_h^-}{p_h^-} = 2\left[\frac{p_h^-}{M_h^\perp}\right]^2$$

$$M_k^\perp = \sqrt{M_h^2 + p_\perp^2}$$

$$z_c = \frac{p_h^-}{q^-} \neq \frac{E_h}{\nu} \qquad z_t = \frac{p_h^+}{(1-x)P^+} \neq \frac{E_h}{\nu}$$

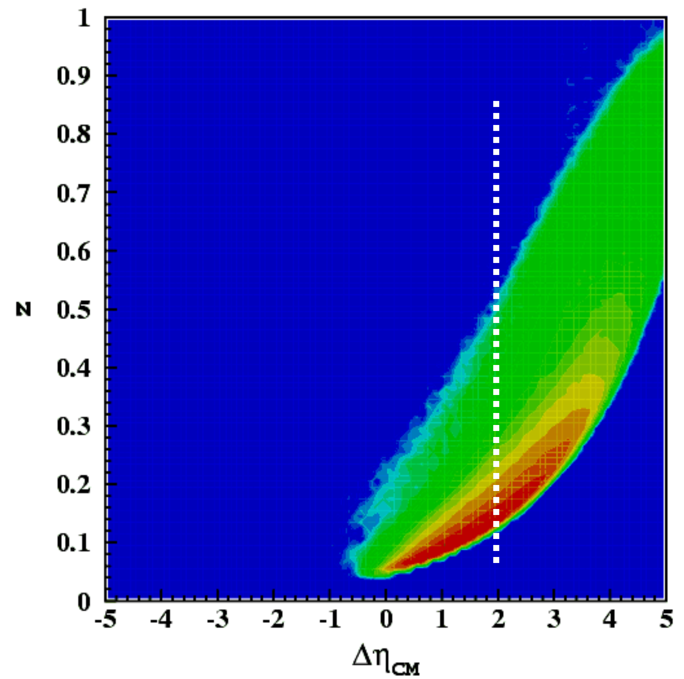

$$\eta_{CM}^{c(Mulders)} = \ln z_c + \ln\left\{\frac{\sqrt{2}q^-}{M_h^\perp}\right\} \qquad \eta_{CM}^{t(Mulders)} = -\ln z_t - \ln\left\{\frac{\sqrt{2}(1-x)P^+}{M_h^\perp}\right\}$$

$$W = (1-x)ys \neq (1-x)Mq^- \qquad y = \frac{q^-}{k^-} \neq \frac{\nu}{E}$$

$$\eta_{CM}^{Mulders} = \ln z + \ln\left\{\frac{W}{M_h^\perp}\right\}$$

Longitudinal Momentum

- CEBAF beam energy in combination with CLAS acceptance allow to explore current fragmentation for *light mesons* and target fragmentation for *baryons*.
- In DIS Feynman $x_F = \frac{2 p_{\parallel}^{h(CM)}}{W}$ permits to disentangle two regions, however, at small invariant masses W separation is ambiguous.

6 GeV beam energy

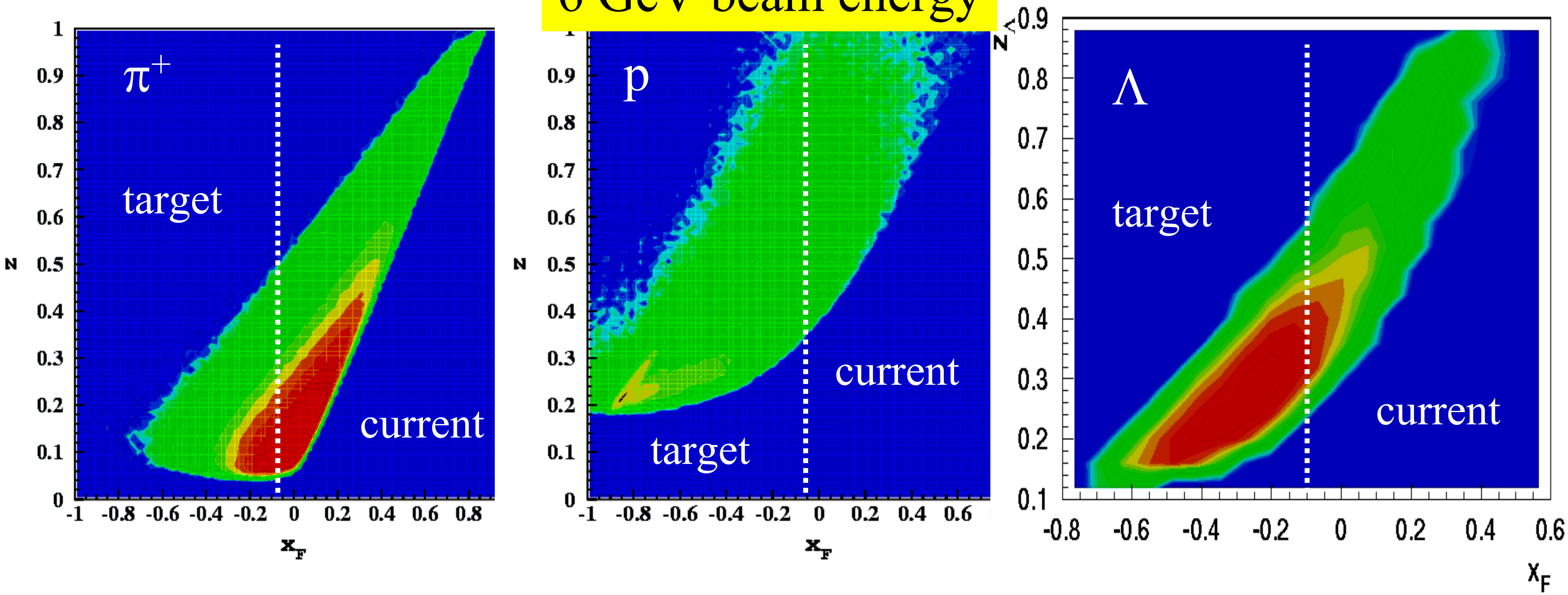

Rapidity gap at CLAS

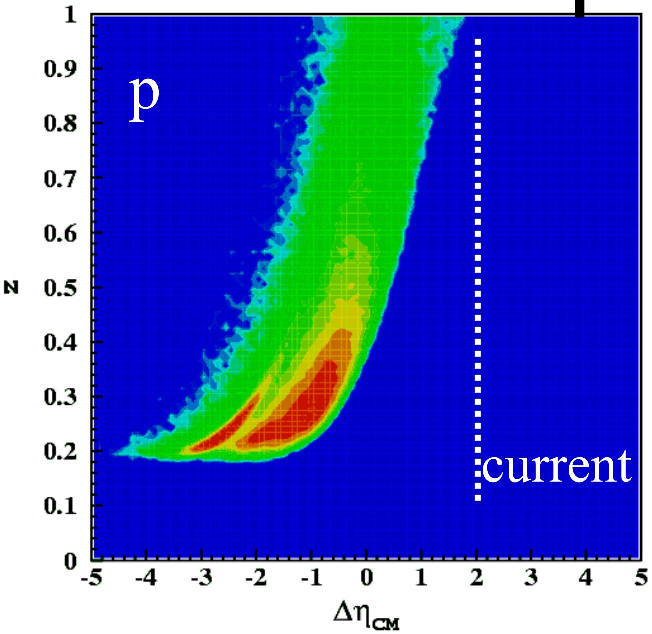

Separation of the current and target fragments:

Berger criterion $\Delta\eta_{CM} > 2$

$$\eta = \frac{1}{2}\log\left\{\frac{E^h + p_{\parallel}^h}{E^h - p_{\parallel}^h}\right\}$$

$$\Delta\eta_{CM}^{Mulders} = \ln z - \ln\left\{\frac{1}{z}\frac{m_h^2}{Q^2}\frac{x}{1-x}\right\}$$

DIS only!

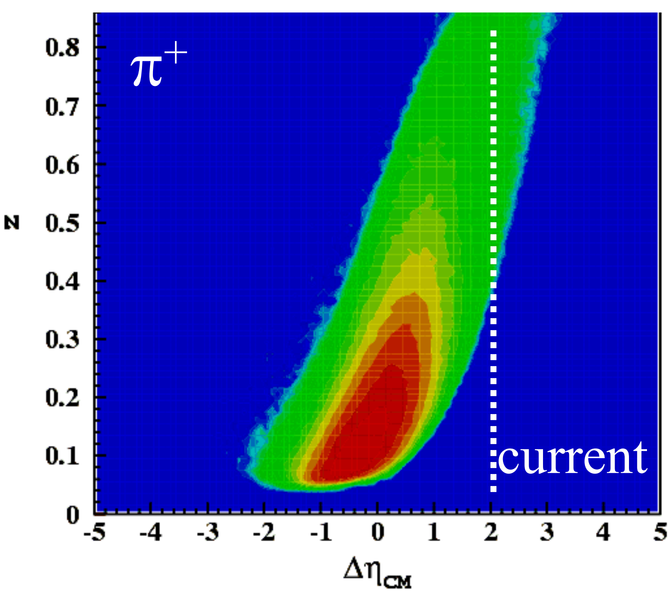

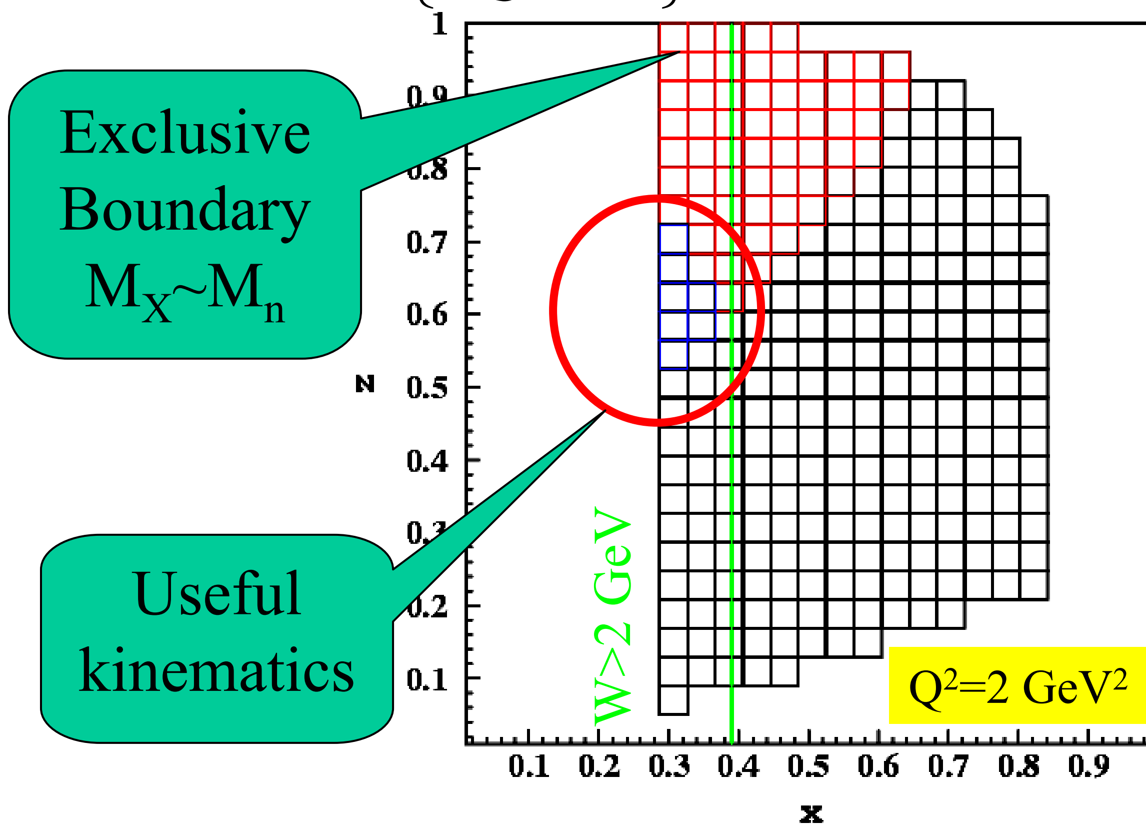

CLAS Acceptance 0

Zero-order approximation:

$$\sigma = \frac{\int N^{DATA}(\varphi)d\varphi}{\int N^{GSIM}(\varphi)d\varphi}\sigma^{GEN}$$

φ-constant term

$$\langle \cos n\varphi \rangle = \langle \cos n\varphi \rangle^{DATA} - \langle \cos n\varphi \rangle^{GSIM} + \langle \cos n\varphi \rangle^{GEN}$$

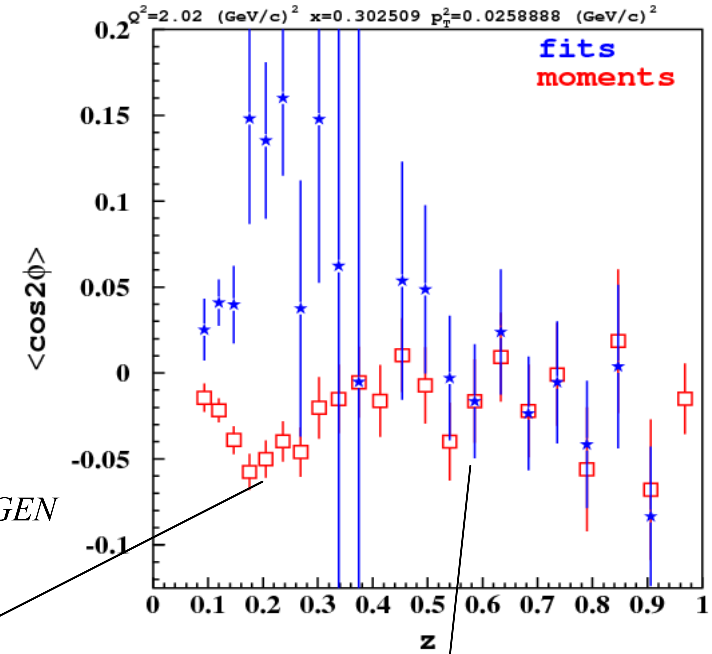

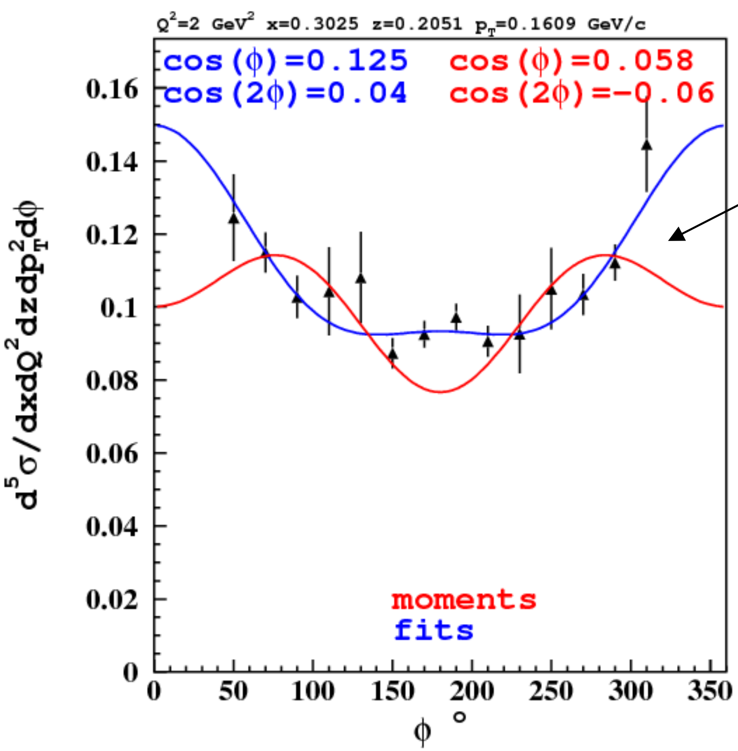

Acceptance mixes Fourier coefficients with different n.

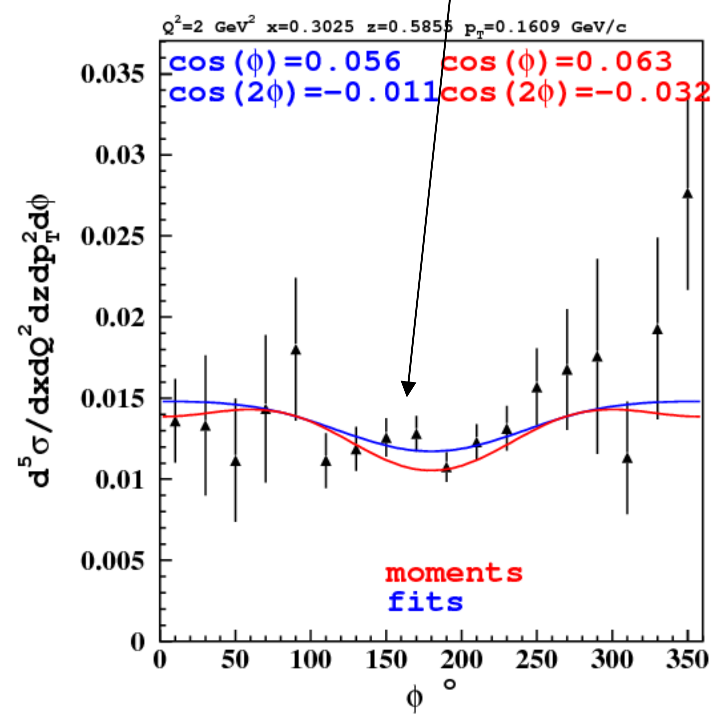

Fourier analysis of acceptance

100 harmonic expansion: CLAS acceptance is cosine-like. Even number of sectors generate mostly even functions in azimuthal distributions.

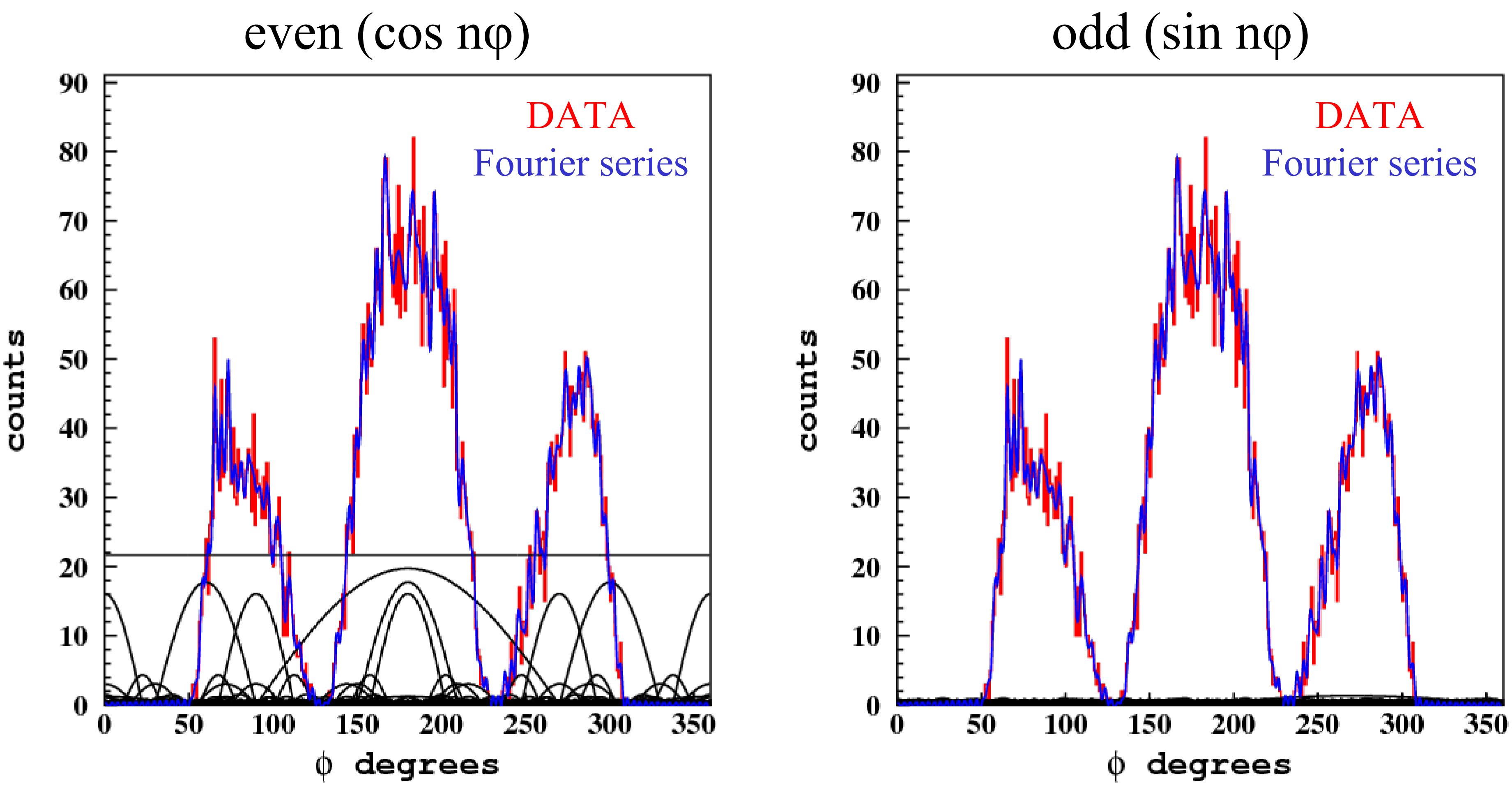

CLAS Acceptance

$$N(\varphi) = \frac{1}{L}\sigma(\varphi) A^{acc/eff}(\varphi)$$

$$\sigma(\varphi) = V_0^{DATA,GEN} + V_1^{DATA,GEN}\cos\varphi + V_2^{DATA,GEN}\cos 2\varphi$$

$$A^{eff/acc} = \frac{A_0}{2} + A_1\cos\varphi + B_1\sin\varphi + A_2\cos 2\varphi + B_2\sin 2\varphi + \dots$$

$$I_n^{DATA,GSIM} = \frac{1}{\pi}\int_0^{2\pi} LN^{DATA,GSIM}(\varphi)\cos n\varphi d\varphi \qquad \sigma(\varphi) = LN(\varphi)$$

$$I_n^{DATA,GSIM} = \frac{1}{\pi}\int_0^{2\pi} \left\{V_0^{DATA,GSIM} + V_1^{DATA,GSIM}\cos\varphi + V_2^{DATA,GSIM}\cos 2\varphi\right\}$$

$$\left[\frac{A_0}{2} + A_1\cos\varphi + A_2\cos 2\varphi + \dots\right]\cos n\varphi d\varphi$$

$$I_n^{DATA,GSIM} = A_n V_0^{DATA,GSIM} + \frac{A_{n-1} + A_{n+1}}{2} V_1^{DATA,GSIM} + \frac{A_{n-2} + A_{n+2}}{2} V_2^{DATA,GSIM}$$

$$n = 0, 1, 2, \dots \qquad A_{-n} = A_n$$

CLAS Acceptance

$$[I]^{GSIM}_{1\times N} = [A]_{N\times N}[V]^{GEN}_{N\times 1}$$

$$\downarrow$$

$$A_n$$

$$\downarrow$$

$$[I]^{DATA}_{1\times N} = [A]_{N\times N}[V]^{DATA}_{N\times 1}$$

$$\downarrow$$

$$V_0^{DATA} \sim H_2 + \varepsilon H_1$$
$$V_1^{DATA} \sim H_3$$
$$V_2^{DATA} \sim H_4$$

Only first 10 harmonics are significant, but 20 harmonics are kept in the analysis.

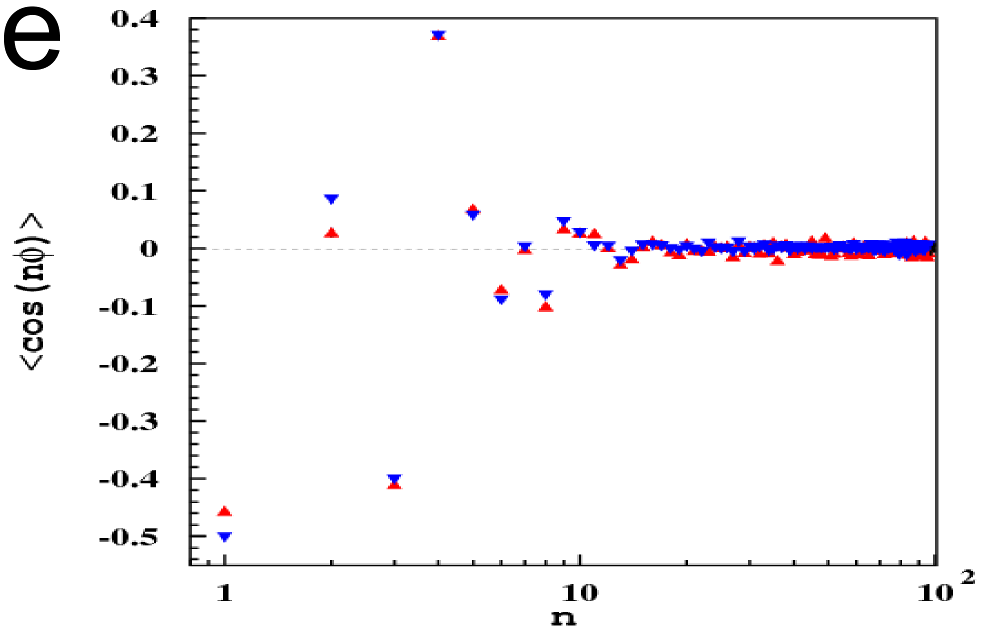

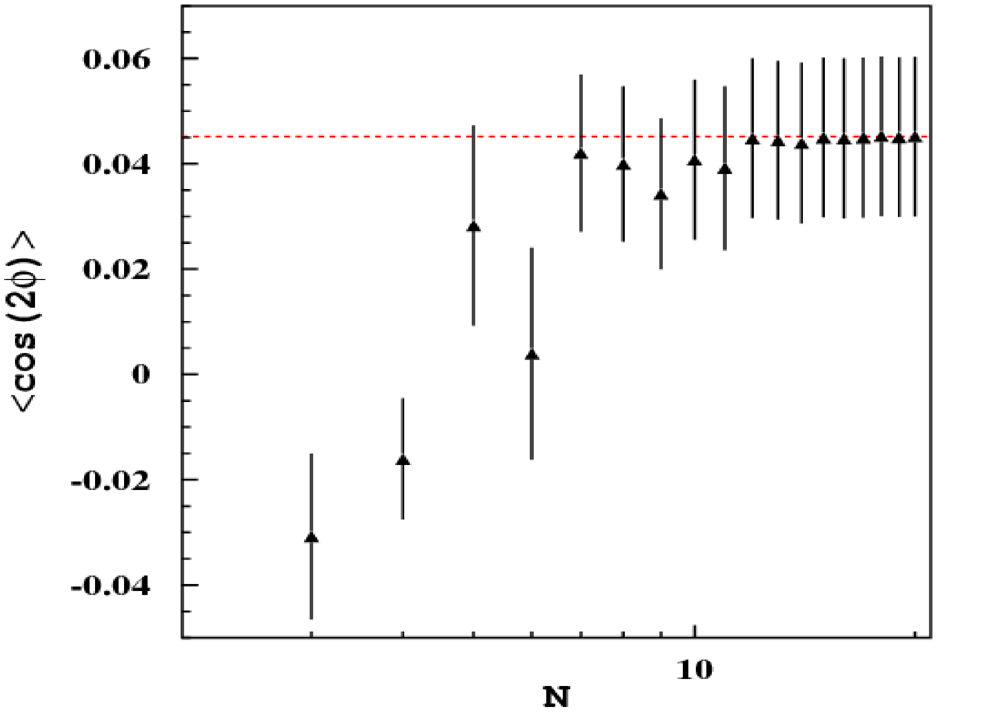

Three methods

Comparison of the three methods for structure function separation:

1. Fit of φ-distribution
2. Moments method in zero-order approximation
3. Moments method accounting for N=20 harmonics of CLAS acceptance

Higher harmonics are important in the extraction of φ–even observables from CLAS data

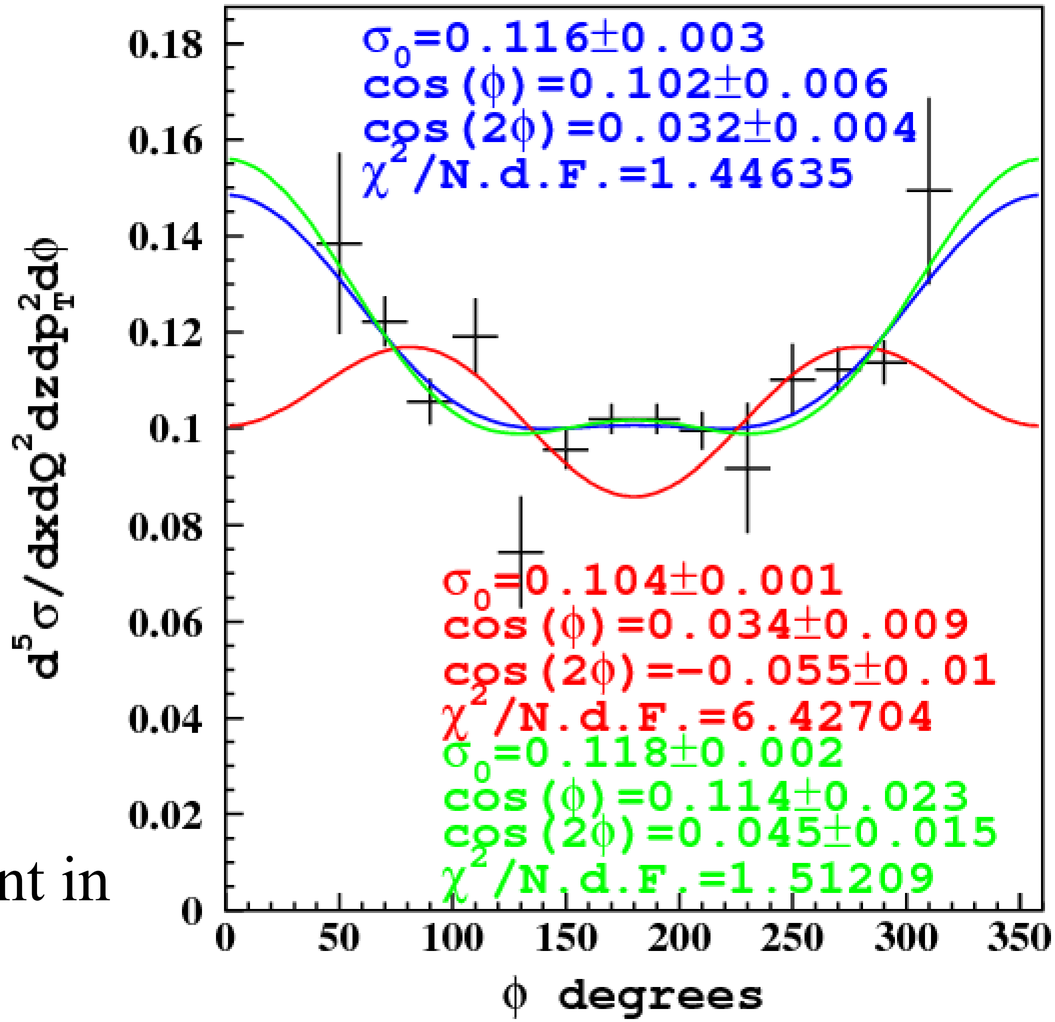

Pseudo-data Cross Check

Pseudo-data generated in a limited kinematical area from a known model (different from that used in the reconstruction) were used to check that the two extraction procedures are able to extract correct φ-moments.

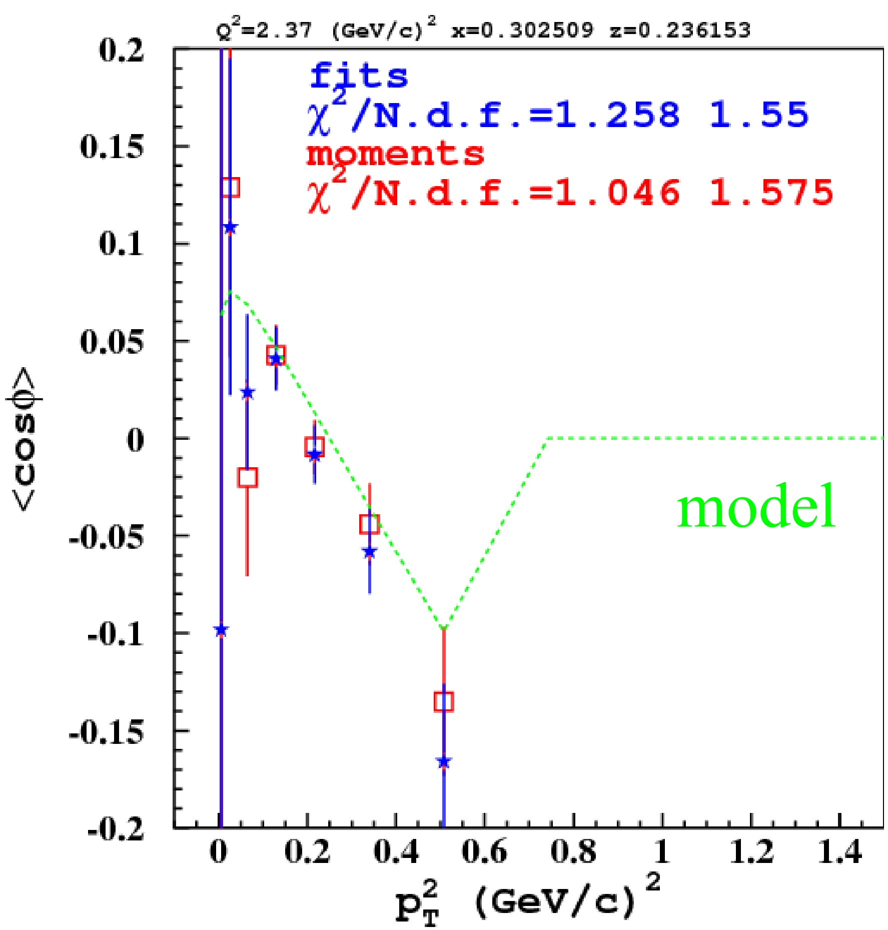

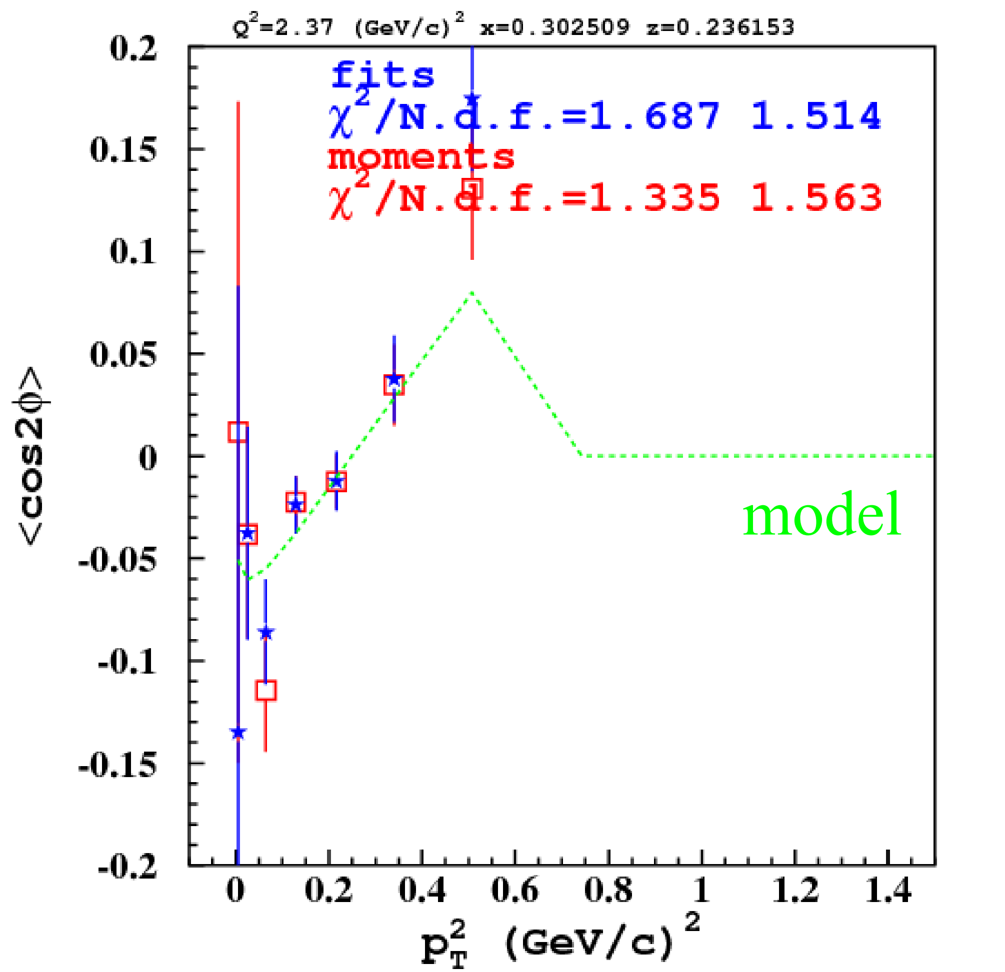

Results of Integration

Different assumptions yield slightly different results in low-z region.

Correct expression for low energy: $H_2^{DIS} = \pi E_h \int_0^{p_T^{2\,\max}} dp_T^2 \frac{H_2\left(p_T^2\right)}{\sqrt{E_h^2 - m_h^2 - p_T^2}}$

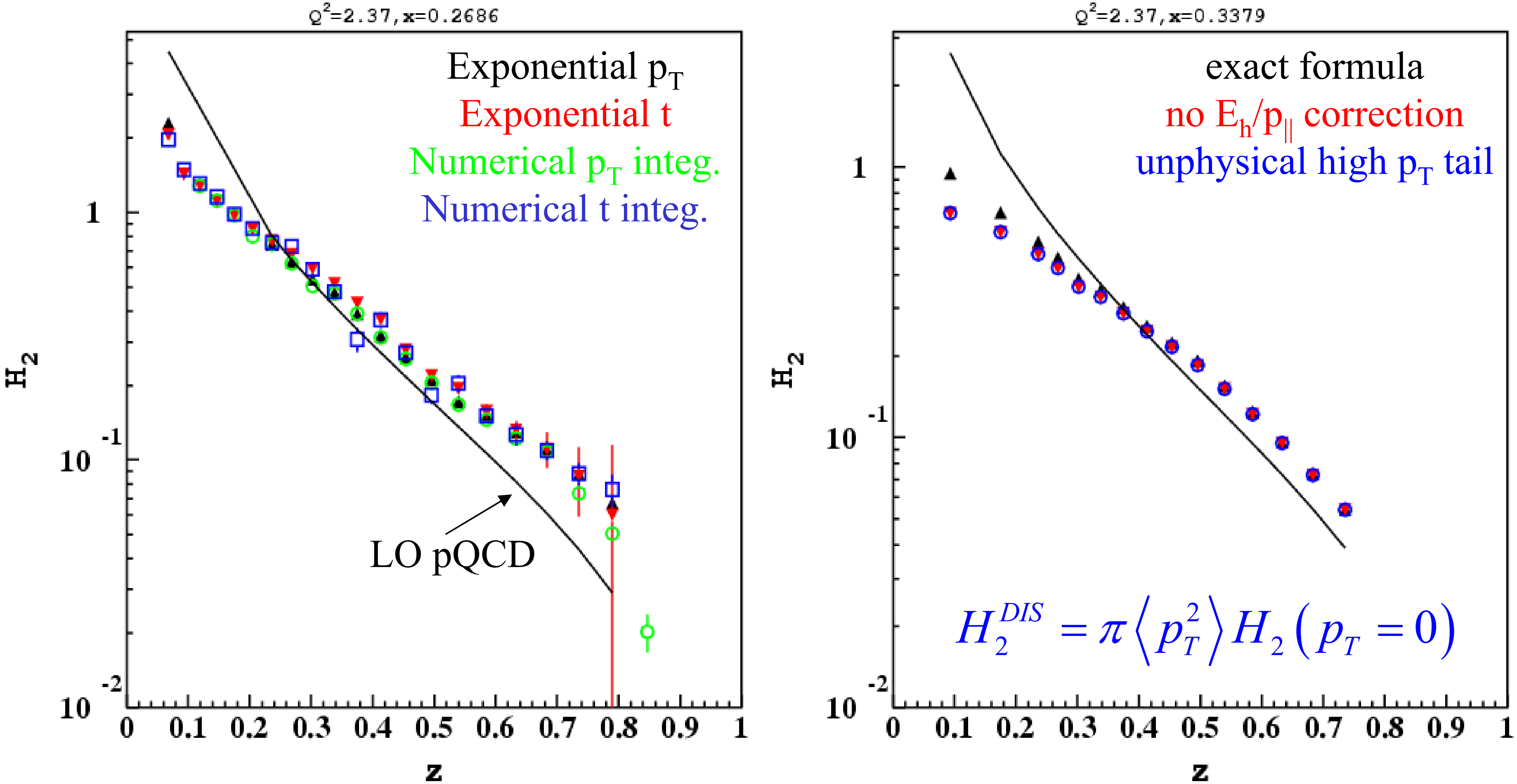

Leading Protons at HERA

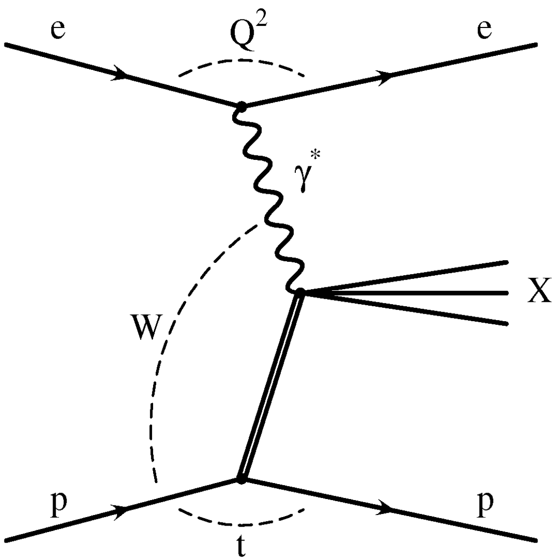

DIS on a Pomeron target

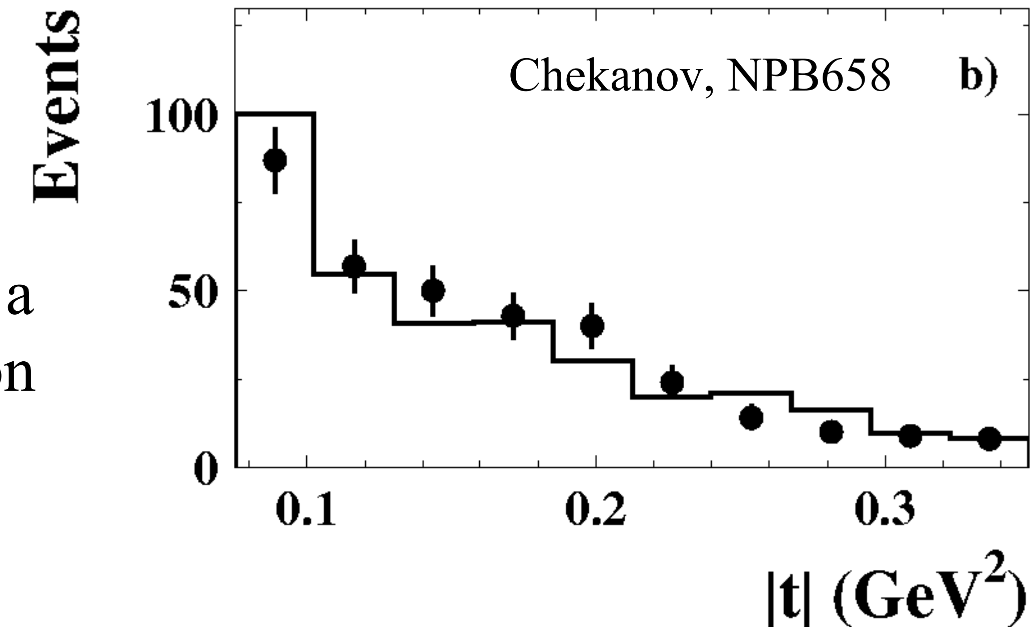

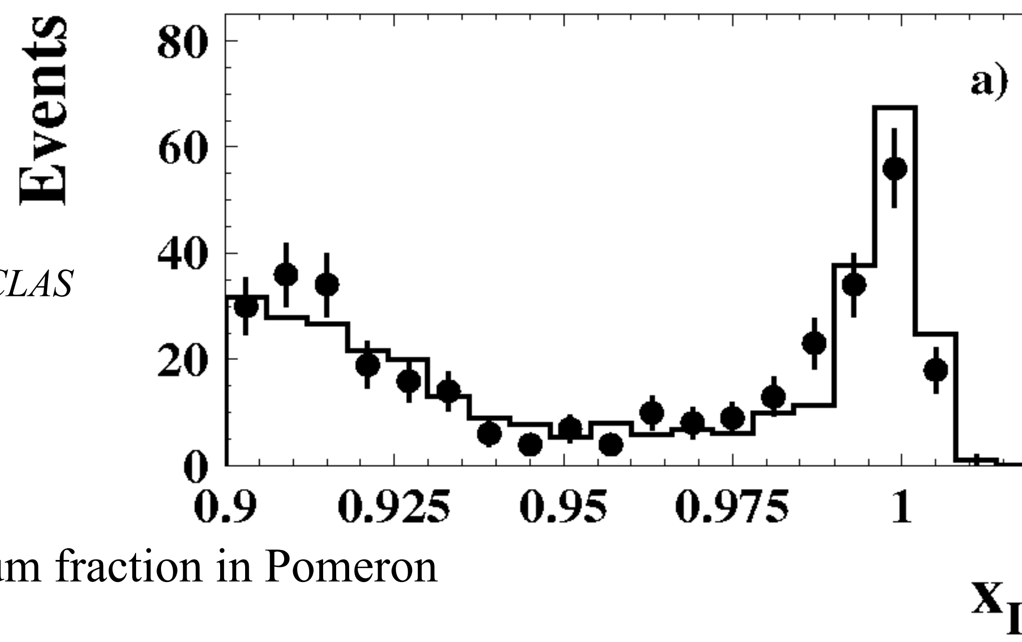

$$x_L = \frac{P'k}{Pk} \approx x_F \equiv \frac{2p_{\parallel}^{CM}}{W} \approx 1 - x_P$$

$$t_{HERA} = (P - P')^2 = \sum M_i^2 - s - t_{CLAS}$$

$$F_2^D(x_P, t, \beta, Q^2) = f_P(x_P, t) F_2^P(\beta, Q^2)$$

$$\beta = \frac{x}{x_P}$$ parton momentum fraction in Pomeron

Leading Particle Effect

Leading particle is defined as the particle carrying most of the specific jet (current or target) momentum in CM reference frame.

Systematic study of different reactions with hadron and lepton beams showed:

1. only particles present in the initial state can be leading particles in the final state,
2. more valence quarks from initial state particles are present in the particle measured in the final state then more likely particle to be leading.

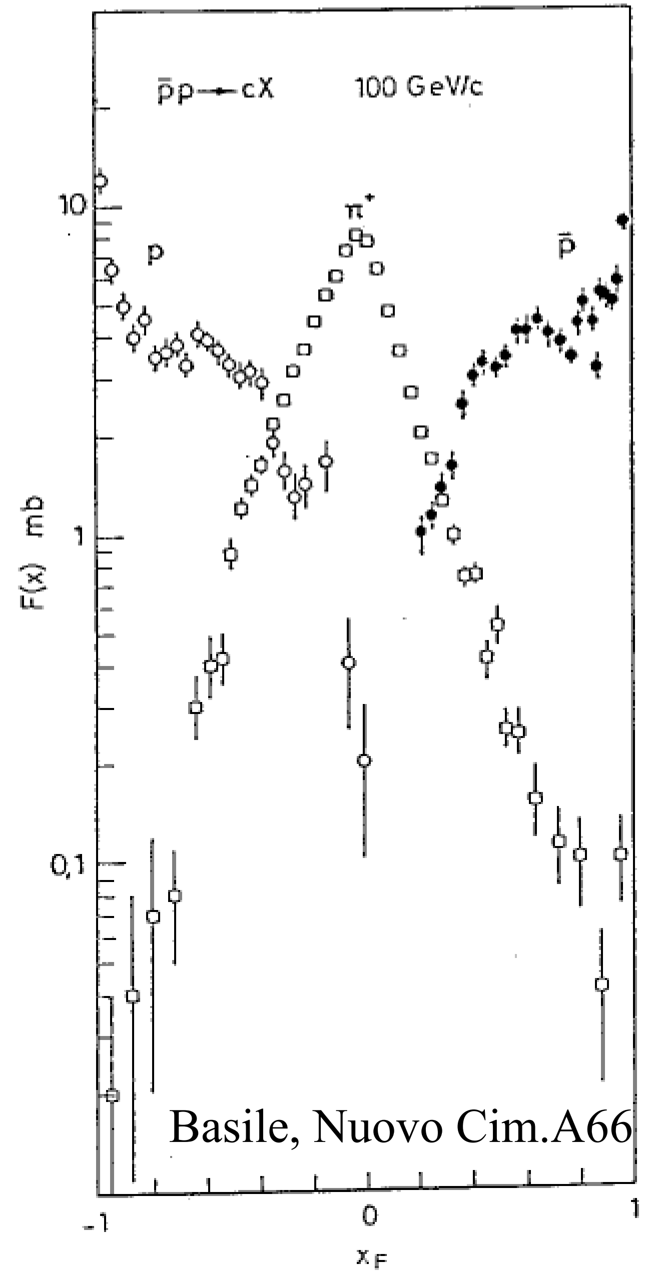

Basile, Nuovo Cim.A66

Data vs. Monte Carlo

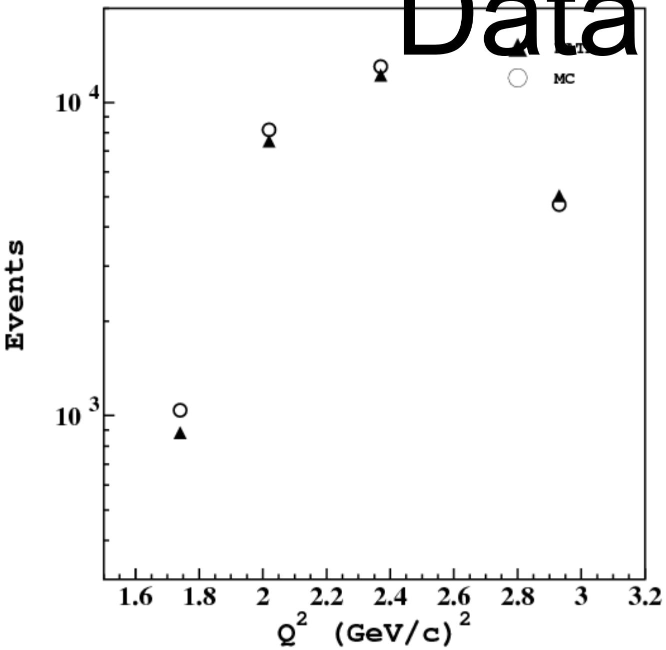

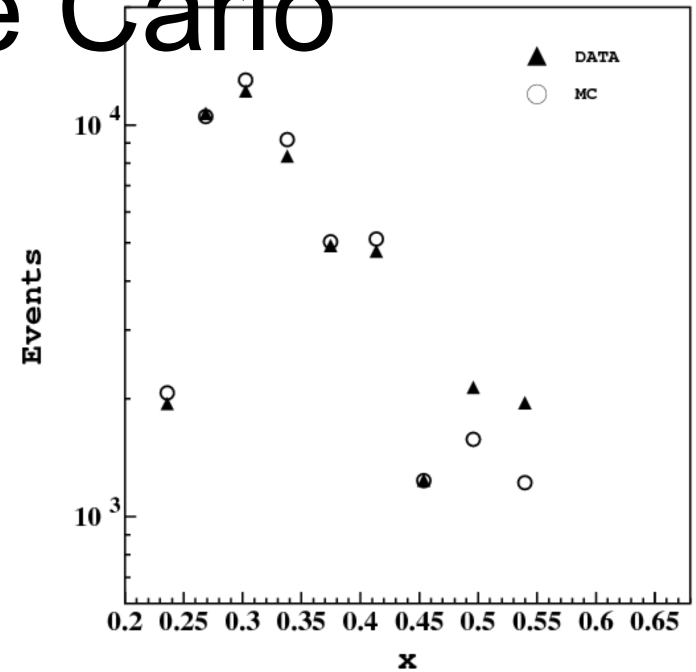

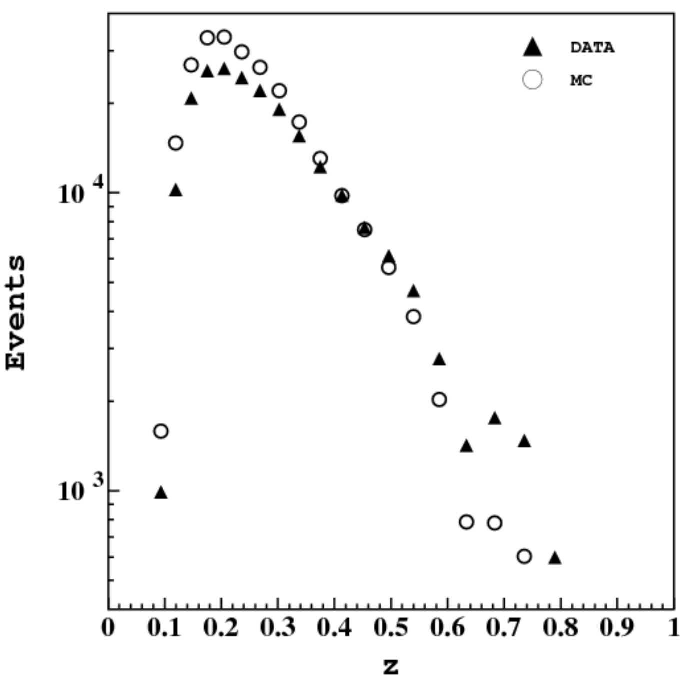

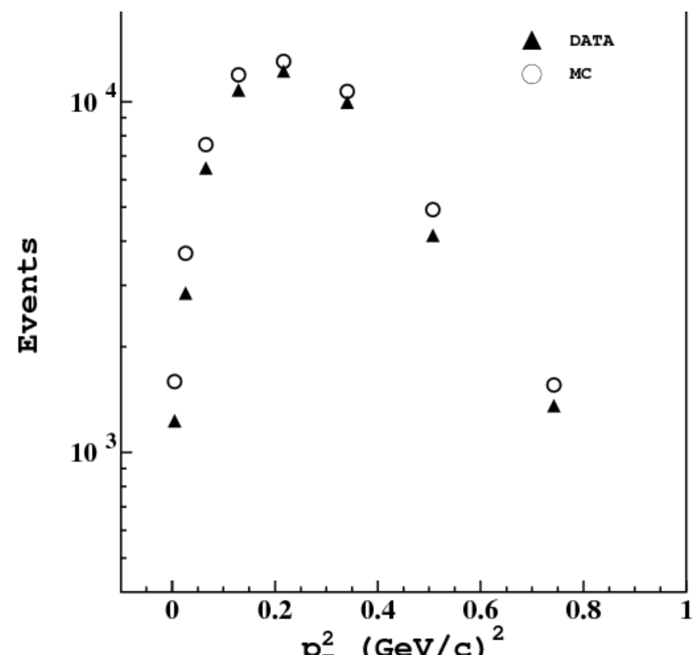

Electromagnetic Probe

Lepton scattering off a nucleon is the cleanest probe of nucleon internal structure.

detected electron
at angle θ with momentum E′

electron beam
with energy E

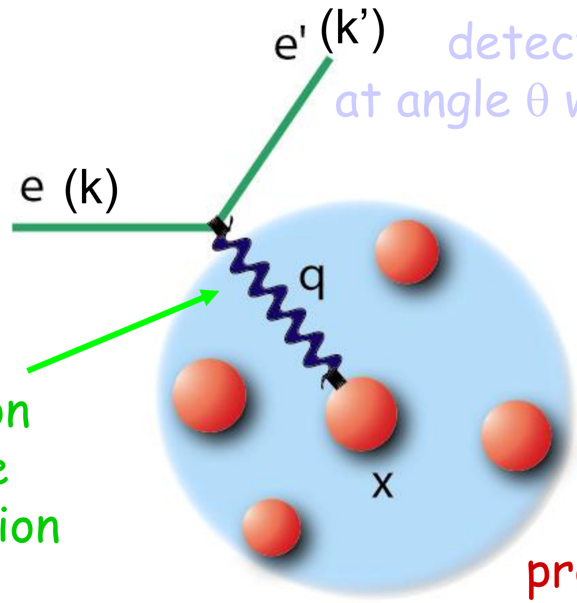

One Photon
Exchange
approximation

produced
hadronic system
of mass squared

virtual photon and target four-momenta:

$$q = (k - k') = (\nu, \vec{q}) \qquad P = (M, 0)$$

Lorentz invariants:

$$Q^2 = -q^2 \qquad x = \frac{-q^2}{2qP} = \frac{Q^2}{2M\nu}$$

$$W^2 = (P+q)^2 = M^2 + Q^2 \left\{ \frac{1}{x} - 1 \right\}$$

Electromagnetic current inclusive cross section:

$$\frac{d^2\sigma^{\pm}}{d\Omega dE'} = \frac{d\sigma}{d\Omega}_{Mott} \left\{ \left[W_2(x,Q^2) + 2\tan^2\frac{\theta}{2} W_1(x,Q^2) \right] \mp \frac{1}{2}\mathrm{ctg}^2\frac{\theta}{2} \left[(E + E'\cos\theta) G_1(x,Q^2) - \frac{Q^2}{M} G_2(x,Q^2) \right] \right\}$$

$\pm$ refers to aligned (anti-aligned) spins of incident electron and target nucleon

Inclusive Kinematical Domains

Unpolarized electron-proton scattering

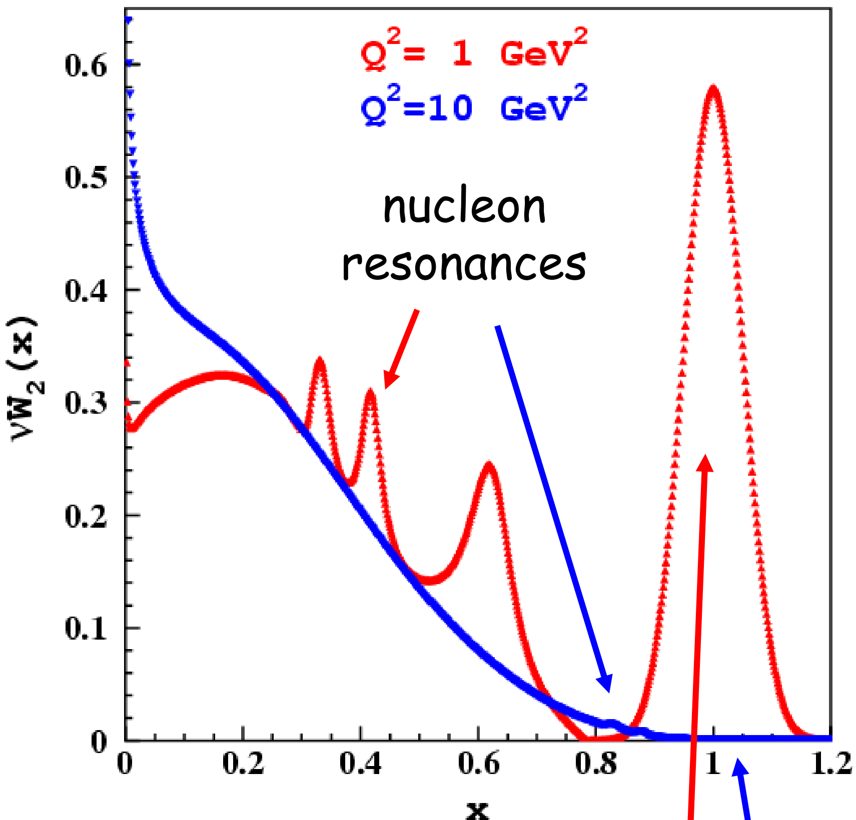

- Elastic scattering
- Inelastic scattering:
  - W<2 GeV * - Resonance region
  - W>2 GeV * - Deep Inelastic Scattering (DIS)
    - Q^2<1 GeV^2 † - Non-perturbative
    - Q^2>1 GeV^2 † - Perturbative

*Elastic and resonance peaks are due to formation of intermediate particles with a given mass M<2 GeV.

†Running coupling constant of the strong interaction $\alpha_S(Q^2)$ becomes ~0.3 at Q^2=1 GeV^2. Furthermore, higher twists are suppressed by powers M^2/Q^2.

Perturbative DIS

Bjorken limit: $Q^2 \to \infty, \nu \to \infty$ and x-fixed

- Incoherent elastic scattering of partons
- Fraction of proton momentum carried by struck parton

$$x_B = \frac{p^+}{P^+} = x$$

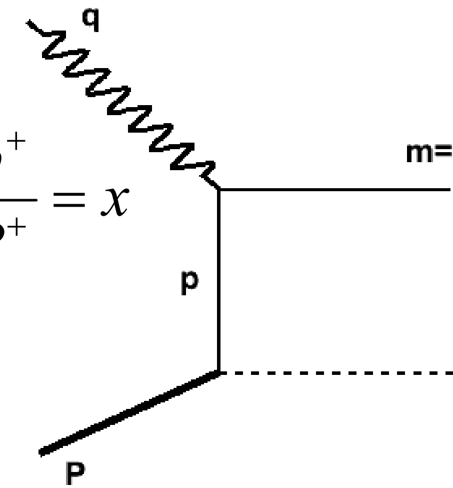

- Scaling:

$$MW_1(\nu, Q^2) \to F_1(x) \qquad M\nu G_1(\nu, Q^2) \to g_1(x)$$

$$\nu W_2(\nu, Q^2) \to F_2(x) \qquad \nu^2 G_2(\nu, Q^2) \to g_2(x)$$

- Parton spin flipping contributions vanish:

Neglect parton and target masses.

Callan-Gross

$$F_1(x) = \frac{1}{2x} F_2(x)$$

Wandzura-Wilczek

$$g_2(x) = -g_1(x) + \int_x^1 g_1(y) \frac{dy}{y}$$

- Parton distribution functions

$$F_2(x) = x \sum_i e_i^2 q_i(x) \qquad g_1(x) = \frac{1}{2} \sum_i e_i^2 \Delta q_i(x)$$

- Valence and sea partons and flavor Singlet and Non-Singlet combinations

$$\Sigma(x) = \sum_i q_i(x) + \bar{q}_i(x) \qquad \Delta_{ij}(x) = q_i(x) - q_j(x)$$

$$F_2^{NS} = F_2^p - F_2^n = \frac{1}{3} x \Delta_{ud}(x)$$

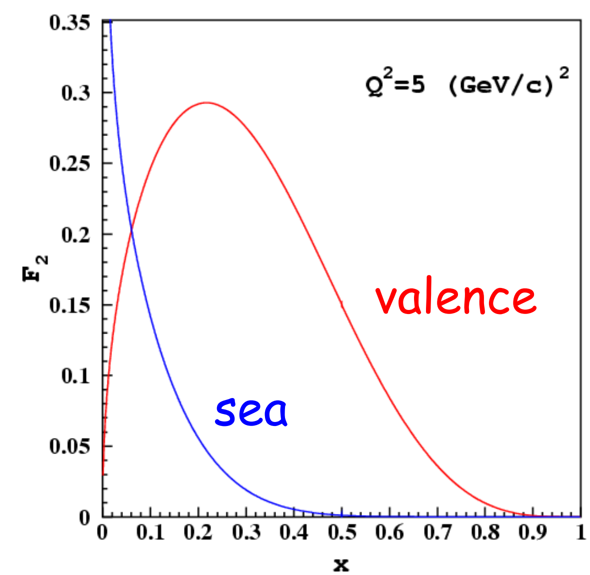

Semi-Inclusive Kinematical Domains

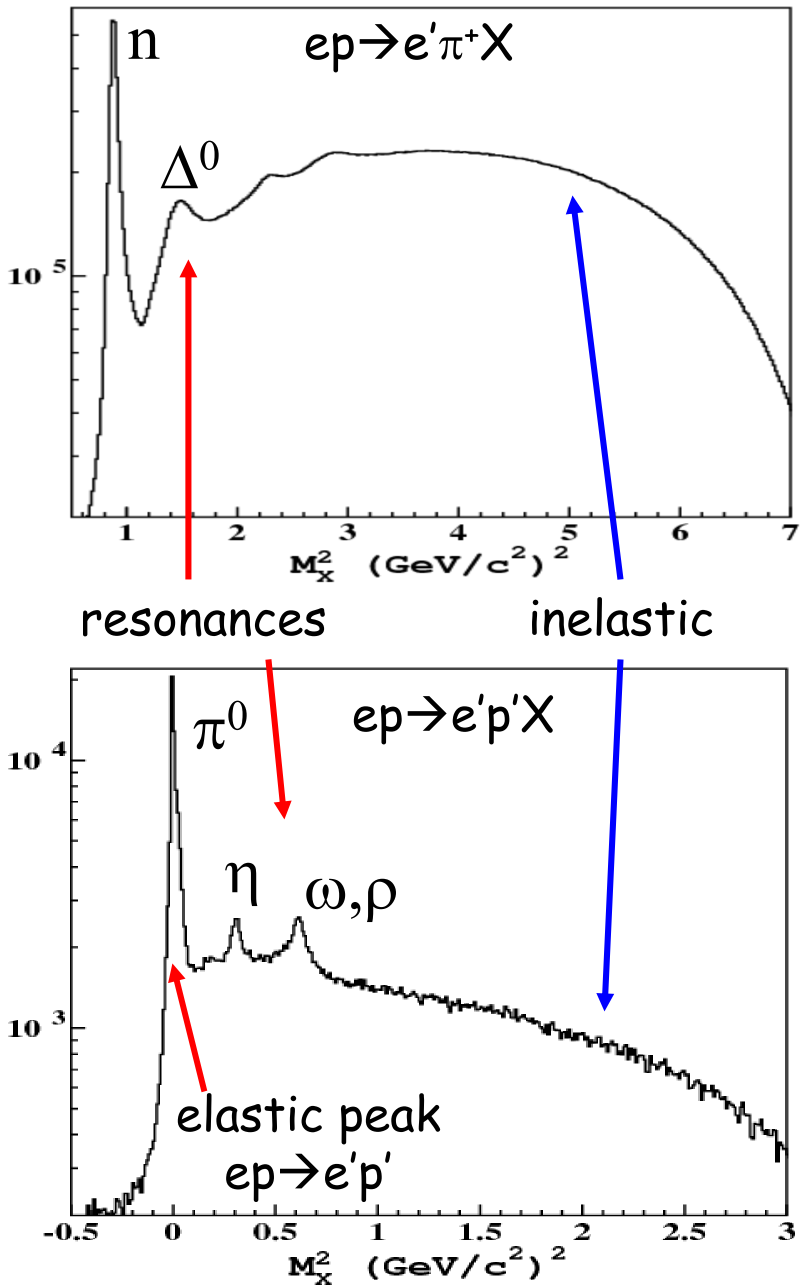

- Exclusive production
- Inclusive production:
  - M_X<1÷2 GeV * - Resonance region
  - M_X>1÷2 GeV * - Deep Inelastic Scattering (DIS)
    - Q^2<1 GeV^2 † - Non-perturbative
    - Q^2>1 GeV^2 † - Perturbative
      - Current fragmentation
      - Target fragmentation

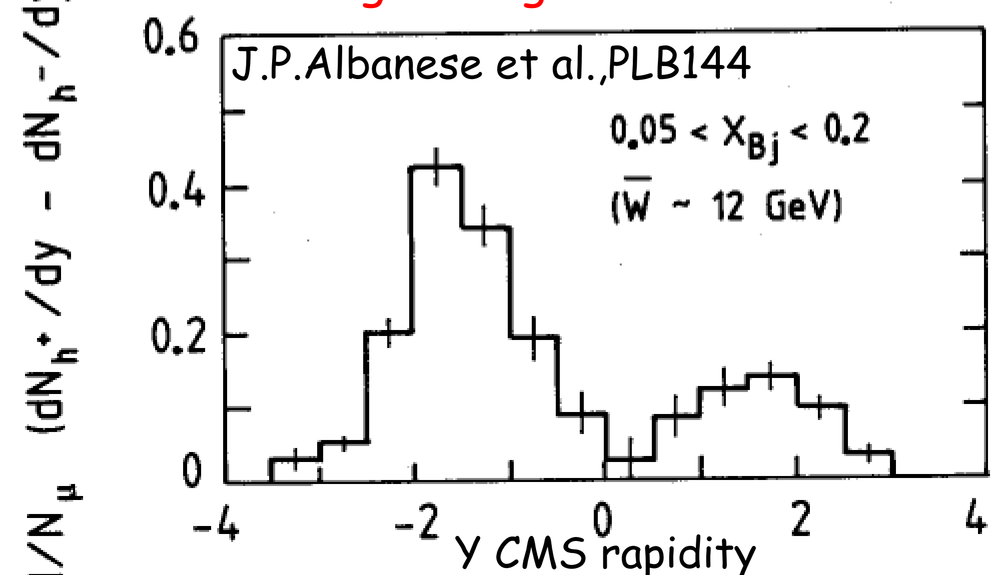

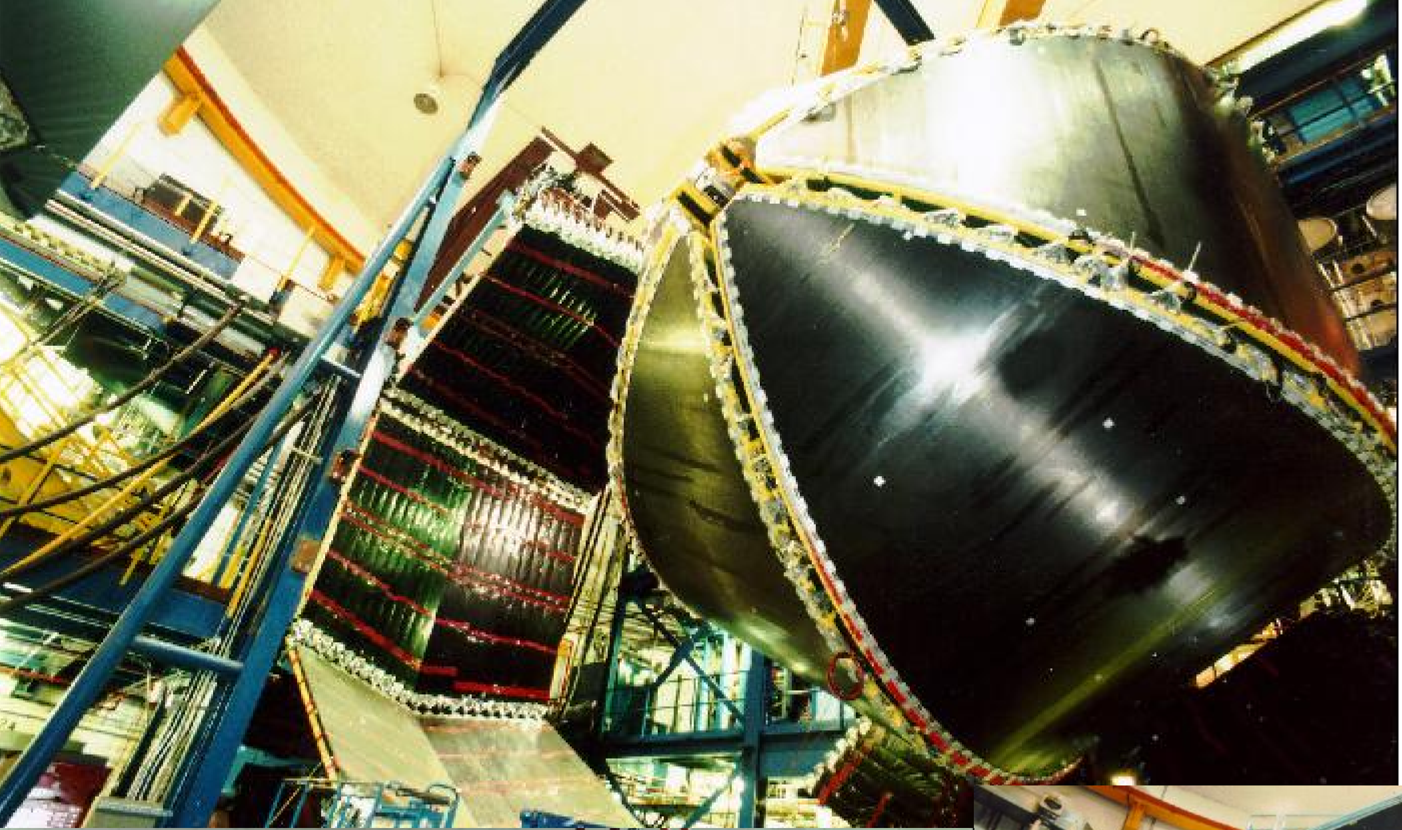

Detector CLAS

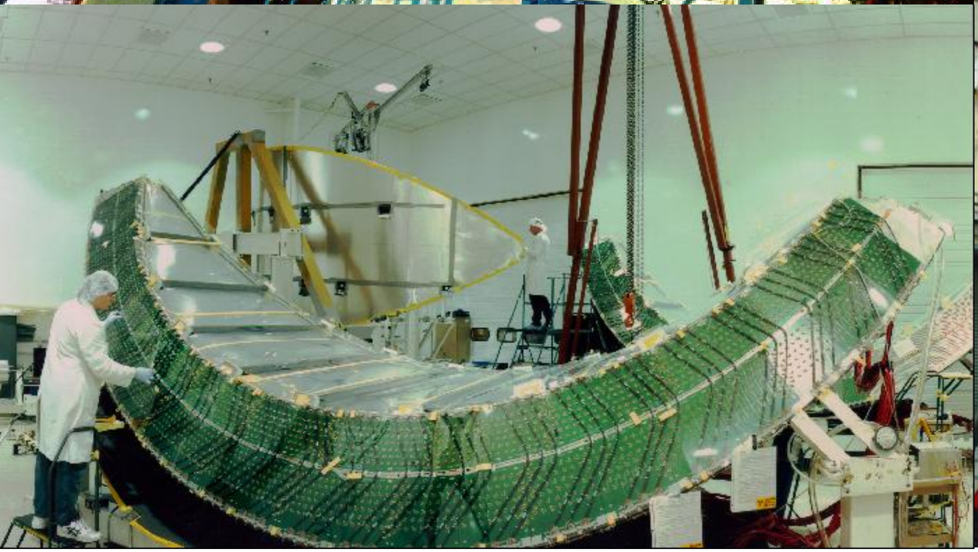

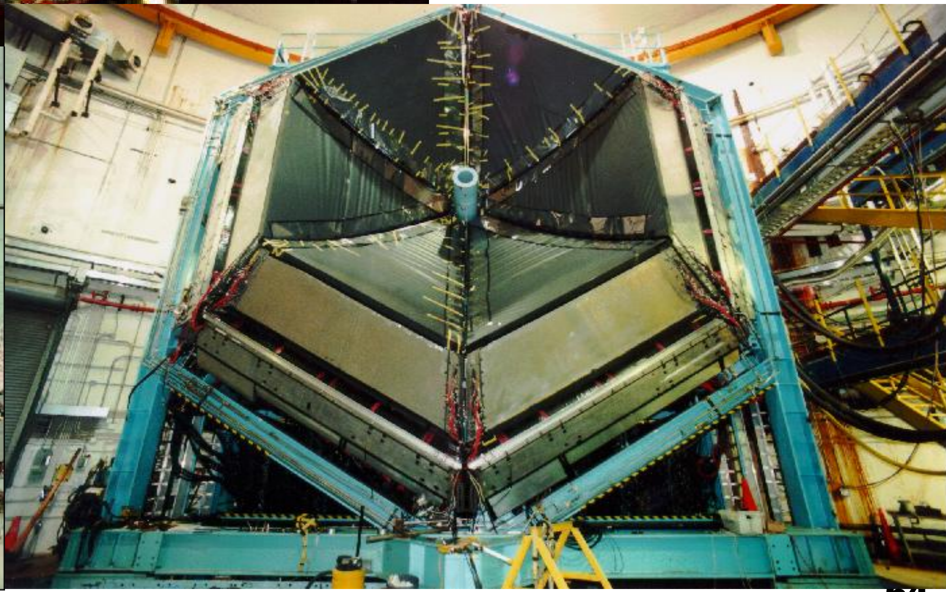

Kinematical Coverage of E1-6a run

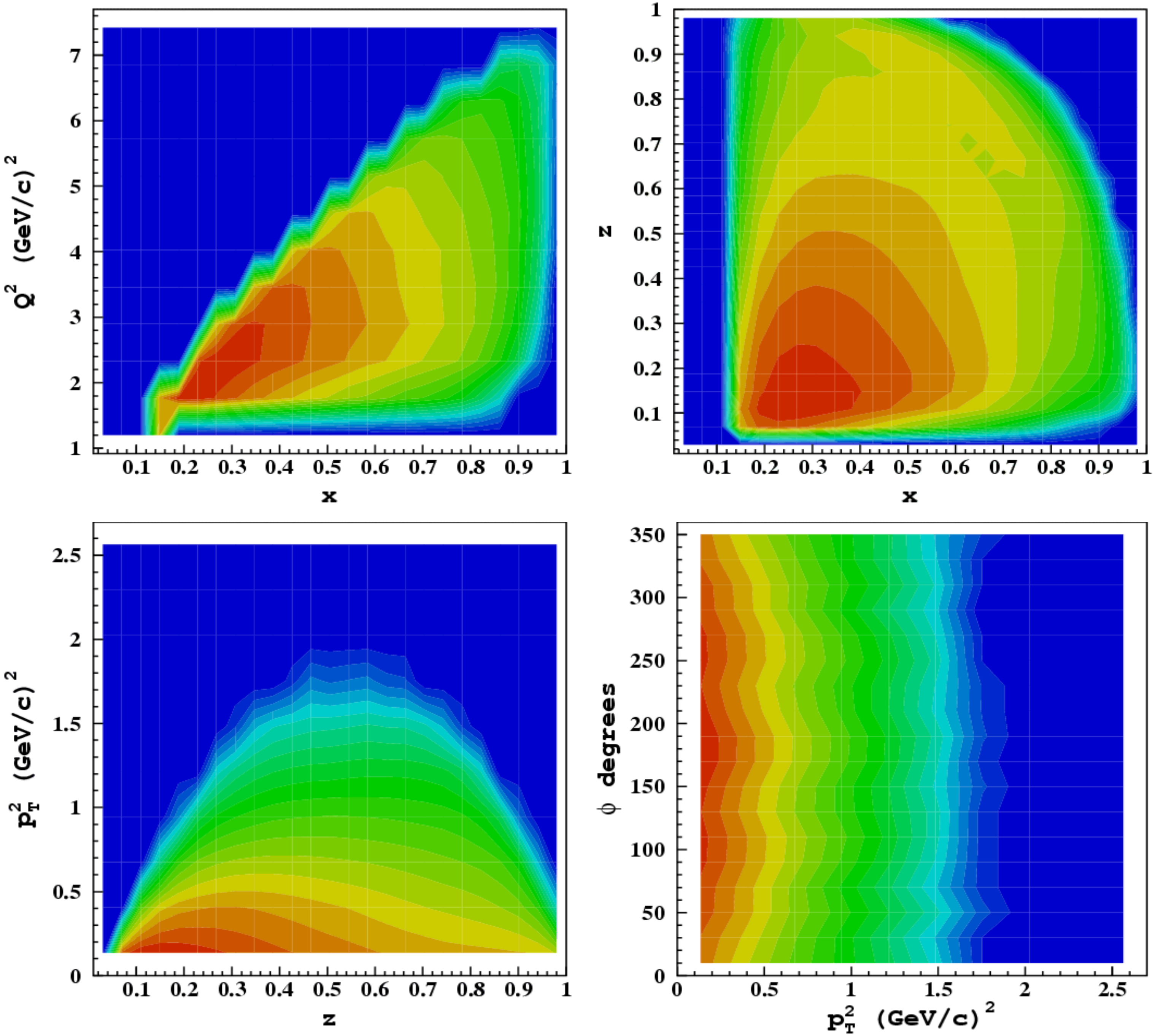

Structure Function Separation

Two methods of separation:

1. fit of ϕ-dependence
2. event-by-event moments

$$\frac{\sigma}{N\frac{E_h}{|p_{\parallel}|}\zeta} = (\varepsilon H_1 + H_2)\{1 + 2\langle\cos\varphi\rangle\cos\varphi + 2\langle\cos 2\varphi\rangle\cos 2\varphi\}$$

$$\langle\cos\varphi\rangle = \frac{\int \sigma\cos\varphi d\varphi}{\int \sigma d\varphi} \quad \langle\cos 2\varphi\rangle = \frac{\int \sigma\cos 2\varphi d\varphi}{\int \sigma d\varphi}$$

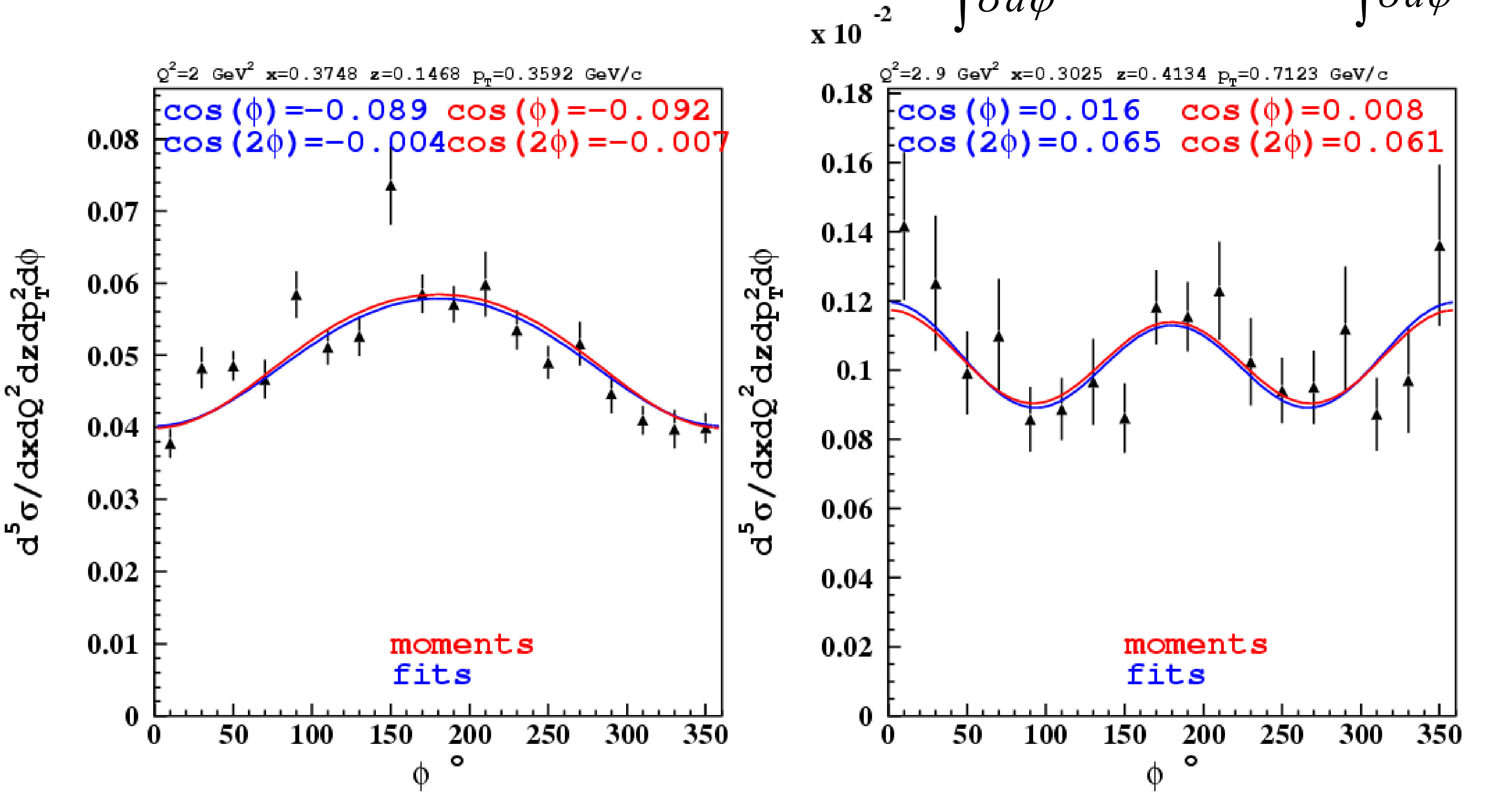

p_T and t dependences

p_T dependence cannot be calculated by ordinary pQCD, only TMD-based approach will permit for a complete description of the measurement. One has to integrate the data in p_T^2:

$$H_2^{DIS} = \pi \int_0^\infty H_2\left(p_T^2\right) dp_T^2$$

$$H_2\left(p_T^2\right) = H_2(0) e^{-\frac{p_T^2}{\langle p_T^2 \rangle}}$$

$$H_2\left(p_T^2\right) = H_2\left(t_{\min}\right) e^{-\frac{t}{\langle t \rangle}}$$

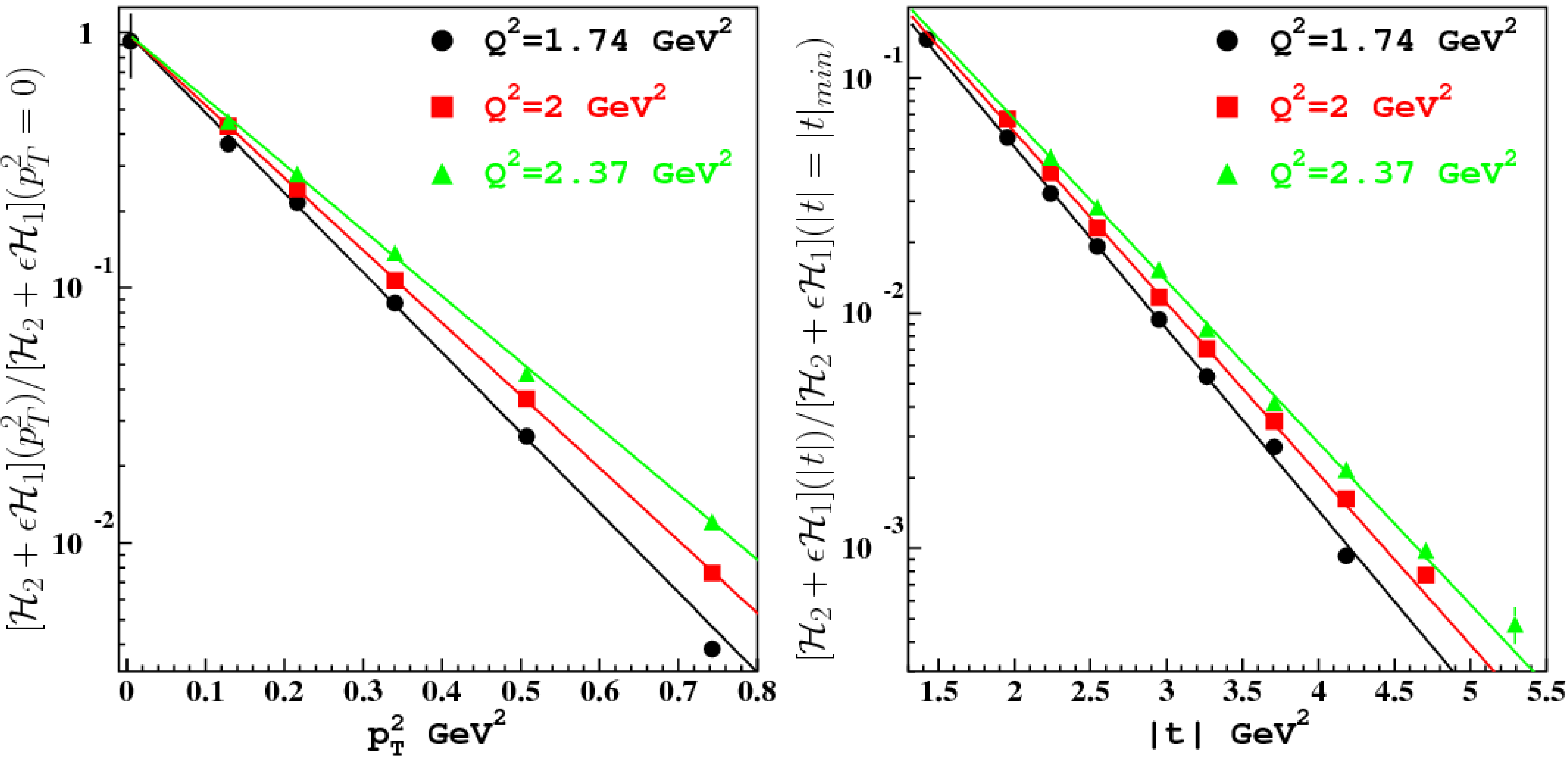

Mean transverse momentum

Parton model predicts simple z-dependence of measured mean transverse momentum:

$$\left\langle p_T^2 \right\rangle = \left\langle p_\perp^2 \right\rangle + \left\langle k_\perp^2 \right\rangle z^2$$

Kinematical constraints cut transverse momentum distributions at low-z:

$$\left\langle p_T^2 \right\rangle < p_T^{2\max} \approx \left(z\nu \right)^2$$

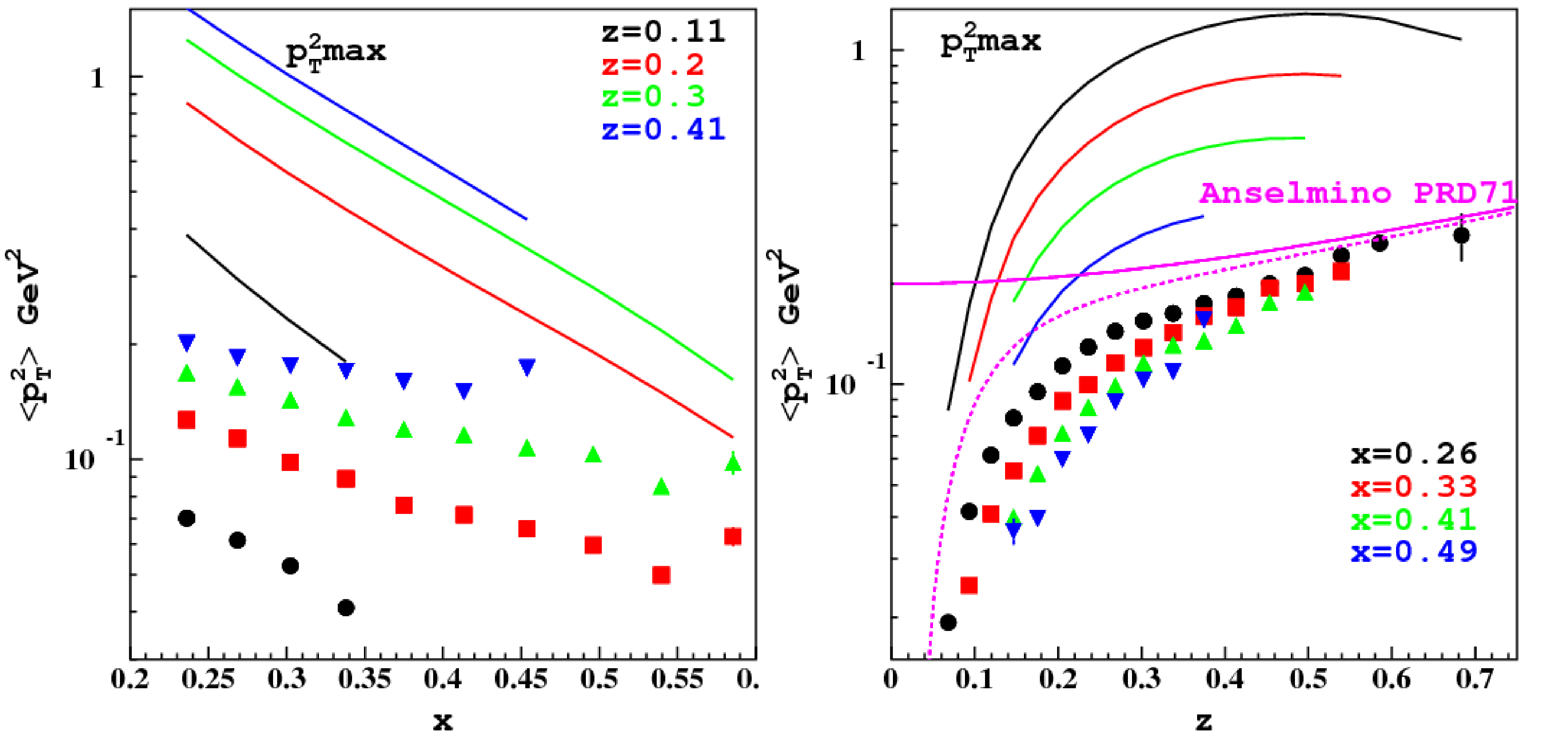

Q^2-dependence at z=0.5

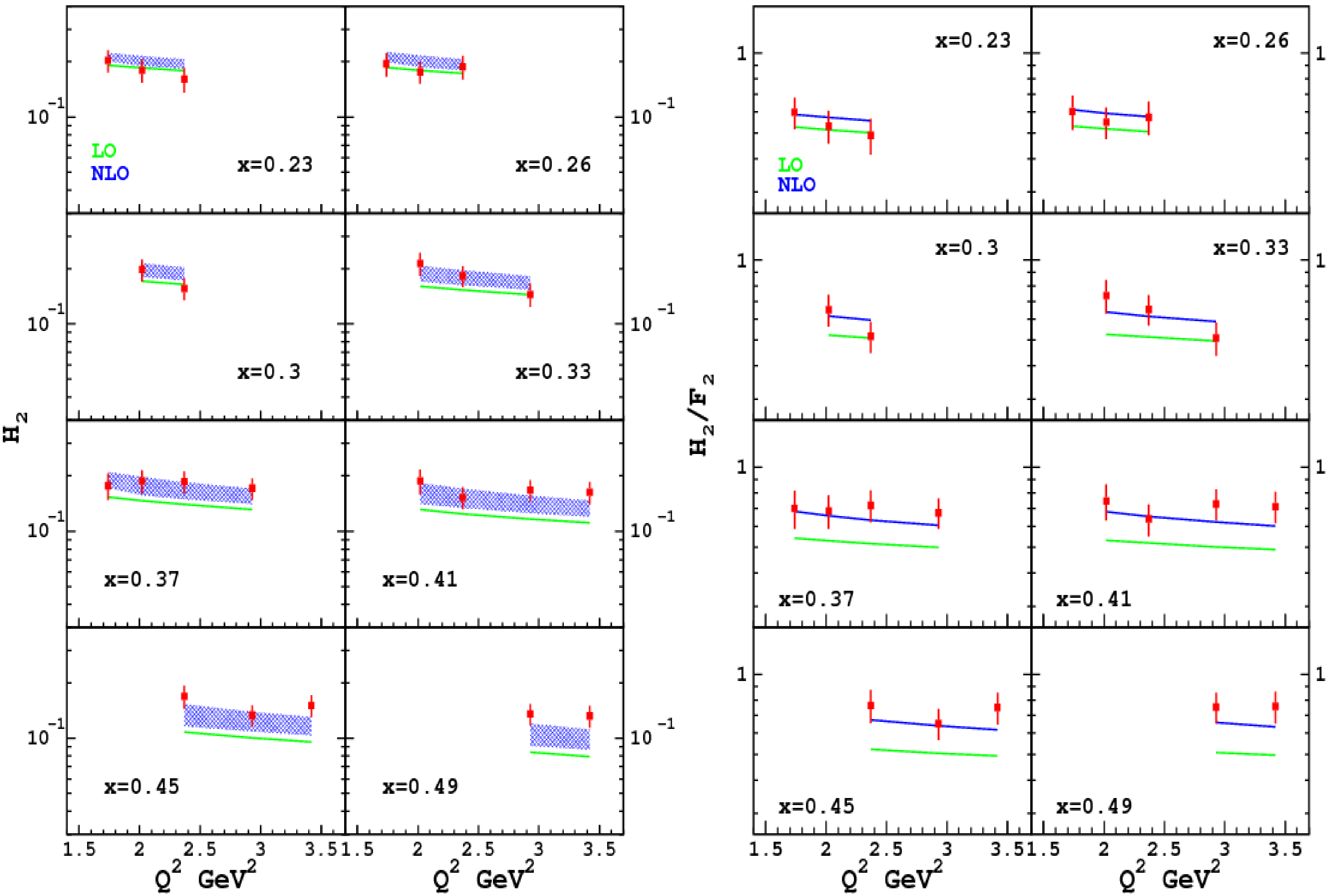

Leading Particle Effect

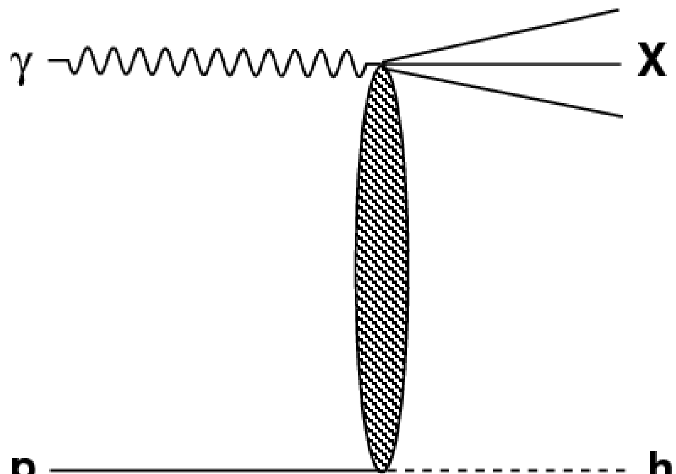

$$t = (q - p_h)^2$$

Approximate integration:

$$H_2 \approx \pi \left\langle p_T^2 \right\rangle H_2(|t|_{\max})$$

Upper limit of 5% on the leading target fragmentation contribution was estimated at lowest z=0.07 where $|t|=|t|_{max}$ is kinematically allowed.

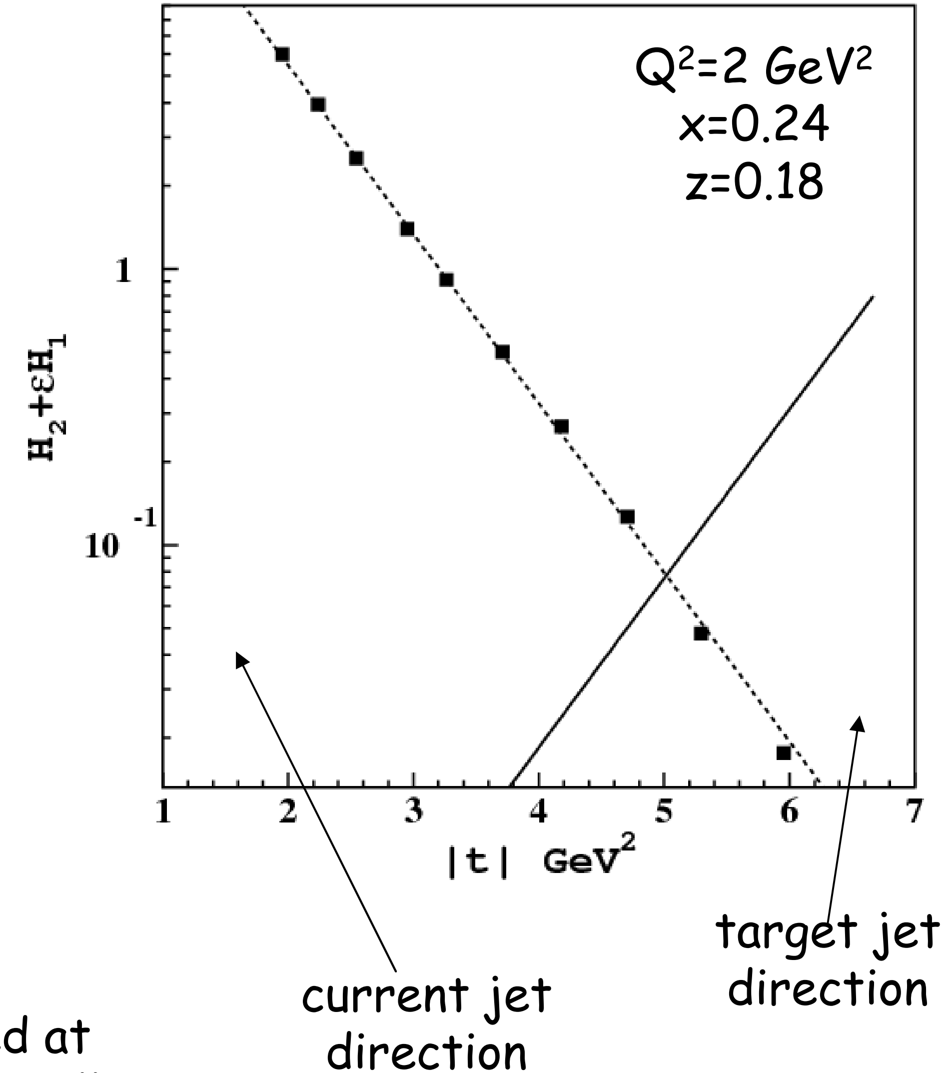

Soft Target Fragmentation

1. Most of hadrons have $x_F \sim 0$ regardless energy of the experiment. No separate peaks for target or current fragmentation.
2. Current fragmentation pQCD fails at backward CM angles

CLAS, E_e=6 GeV

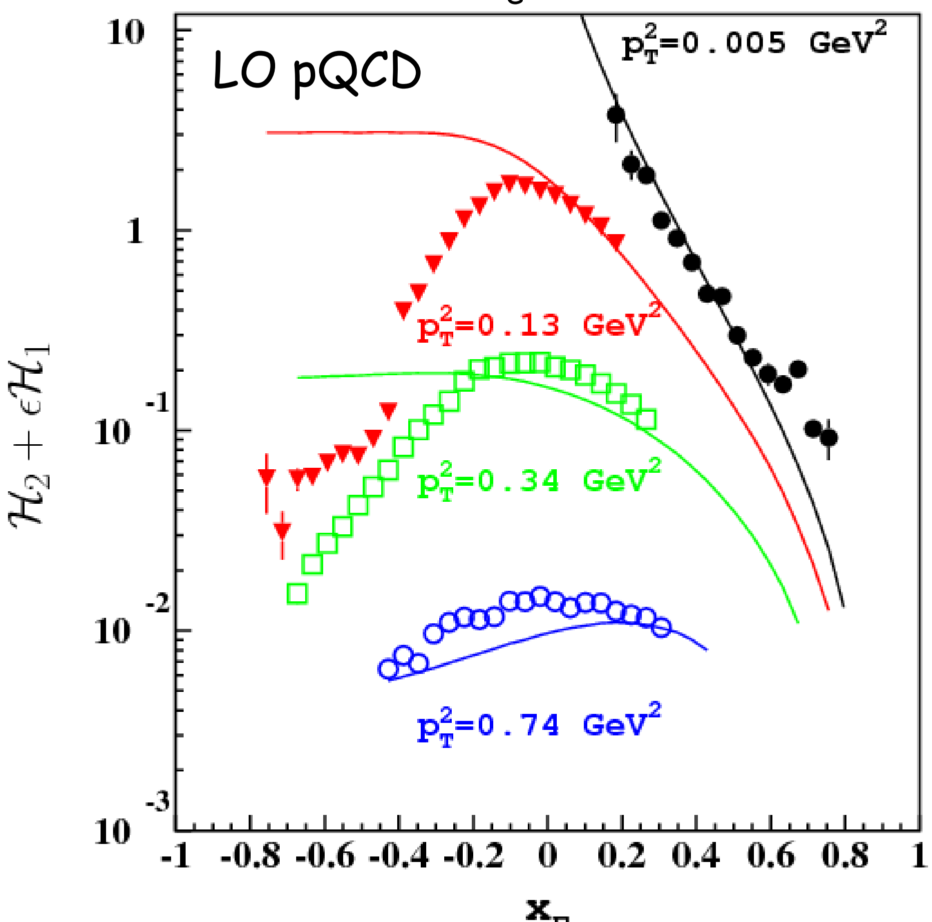

$$x_F = \frac{2 p_{\parallel}^{CM}}{W}$$

EMC, E_μ=280 GeV

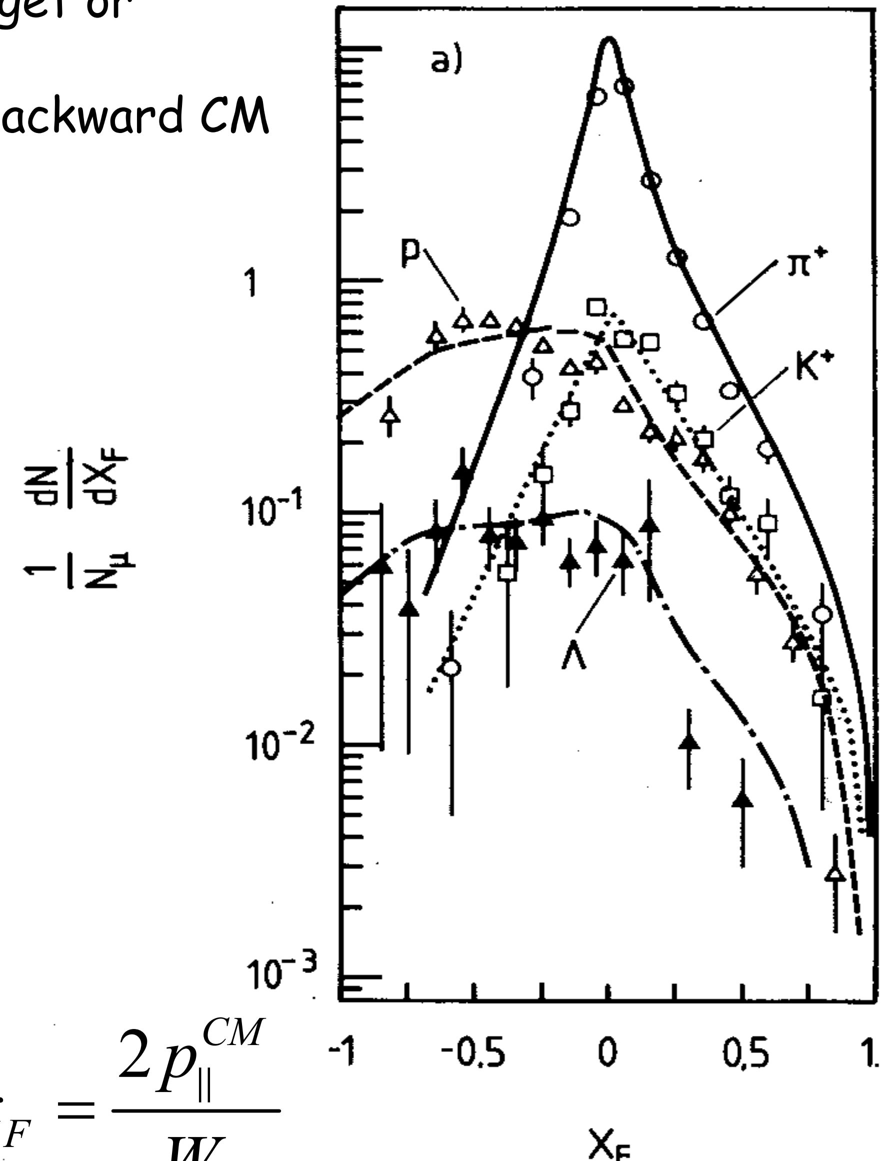

Interplay between variables

Standard SIDIS variable squeezes backward going hadrons into the very low-z region, where $z \to 0$ divergence dominates the total cross section:

$$z_H \approx \frac{1}{2}\left\{\sqrt{x_F^2 + 4\frac{p_T^2}{W^2}} + x_F\right\} \approx \frac{|x_F| + x_F}{2}$$

$$z_H(x_F < 0) \approx 0 \qquad z_H(x_F > 0) \approx x_F$$

1. Commonly used z_H variable is not suitable for target fragmentation analysis,
2. Definition of the hadron direction with respect to virtual photon is frame dependent.